Interinstitutional Master of Science Degree Programme

“Hydrocarbon Exploration and Exploitation”

“Technical and Economic Evaluation of Drill Bits”

M.Sc. Thesis

by

Stylianos N. Spyridakis

Supervisor

Sofia Stamataki

Thessaloniki, December 2018

Interinstitutional Master of Science Degree Programme

“Hydrocarbon Exploration and Exploitation”

“Technical and Economic Evaluation of Drill Bits”

M.Sc. Thesis

by

Stylianos N. Spyridakis

Supervisor: Sofia Stamataki, NTUA Professor

Scientific committee approval on 12/19/2018

Sofia Stamataki, NTUA Professor	…………………
Andreas Georgakopoulos, AUTH Professor	…………………
Konstantinos Voudouris, AUTH Professor	…………………

Thessaloniki, December 2018

Abstract

The objective of this study is the technical and economic evaluation of the drill bits used in three wells, based on the available drilling data (bit records). The three wells are located in Northern Hellas: the two neighboring wells of Nestos 1 and Nestos 2 are located close to the Nestos Delta (Kavala Prefecture) while the third well of Komotini is located nearby the Vistonida Lake (Rhodope Prefecture).

Specific energy, a non-intrinsic rock property defined as the energy required for removing a unit volume of rock, is used to technically assess bit performance. Specific energy determinations are based on the drilling parameters used for each interval (bit type and size, the weight applied on bit and rotary speed), along on the penetration rate achieved. Moreover, based on the computed specific energy, the intrinsic rock property of drillability, which shows how easily a formation is drilled by a specific bit, is determined. Based on drillability in each interval, a technical evaluation of the drill bits used is performed for the three wells, by juxtaposing the diagrams of drillability over depth with the related lithostratigraphic columns. In addition, a comparative analysis of the drillability between the neighboring wells of Nestos 1 and Nestos 2 is conducted.

One of the most basic aspects in drilling a new well with safe manner, especially in a frontier area as in this case, is the pressure regime of the formations to be drilled, which is also estimated in this study. For this purpose, the indirect method of d-exponent is used for estimating the formation pore pressure, based on in situ drilling data. Then, based on the estimated values of d-exponent, the modified d-exponent is determined (d_{mod}-exponent). Subsequently, the plot of d_{mod}-exponent over the depth is constructed for each well in order to identify zones of abnormal pressure. The linear trendline for computing the normal values (d_{mod-n}) of d_{mod}-exponents are drafted. On the basis of d_{mod}, d_{mod-n} and the normal pressure gradient, the formation pore pressure for each well under study is determined. Subsequently, the differential pressure is computed. The plots of differential pressure and penetration rate over depth for each well are juxtaposed in order to evaluate their relation.

The economic evaluation of drill bits is based on cost per foot computed for each interval of the three wells under study. Plots of cost per foot over depth for the three

wells under study are constructed in order to be assessed. Again, cost per foot of Nestos 1 and its neighboring well of Nestos 2 is compared.

Under the assumption that optimum hydraulics have been achieved, the methods and empirical equations used in this study for evaluating the above-mentioned parameters indicate that drillability generally decreases over depth for the three wells examined due to the increase of compaction at higher depths. All wells are characterized by the complete absence of abnormal pressure zones where the computed differential pressure is inversely proportional to the penetration rate achieved for most of the drilled intervals.

On the other hand, the economic assessment of drill bits based on cost per foot results in a linearly increasing trend for both wells of Nestos 1 and Komotini.

Acknowledgments

I would like to express my gratitude to Dr. Sofia Stamataki, Professor of Petroleum Engineering in the Scholl of Mining and Metallurgical Engineering at the National Technical University of Athens, for the continuous support and guidance throughout this M.Sc. thesis.

I would also thank Dr. Andreas Georgakopoulos, Professor in the Department of Geology at the Aristotle University of Thessaloniki, as well as Dr. Konstantinos Voudouris, Professor in the Department of Geology at the same University, for their participation in the scientific committee.

Special thanks to Mrs. Irene Dimitrellou, Mining & Metallurgical Engineer, Specialized Technical Laboratory Staff in the School of Mining and Metallurgical Engineering at the National Technical University of Athens, for providing me with valuable help and information in each phase of this study.

Last but not least, I would like to thank my family for standing beside me all these years and supporting all my dreams.

Stylianos N. Spyridakis

Dedicated to my beloved grandfather,

Markos G. Droumpetakis

Contents

List of Figures

List of Tables

1. Introduction

After the discovery of the Prinos oilfield in 1971, a consortium between the Hellenic oil company, (Public Petroleum Corporation S.A. (DEP)), and the Romanian oil company (Rompetrol S.A.) conducted the drilling of three exploratory wells, in the surrounding area of the Prinos oilfield. These three wells that were drilled in 1977 comprise the first attempt to discover new potential accumulations of hydrocarbons. The first of these wells, named Komotini, is located in the Prefecture of Rhodope, while the other two wells, the Nestos 1 and Nestos 2 wells, are located in the Prefecture of Kavala.

The aim of this study was to examine the drill bit performance based on the drilling data available for each well. In this context, each interval drilled by a specific drill bit (or bit) was technically and economically assessed.

The currently used methods for assessing the drill bit performance and for selecting the most appropriate bit type for a particular formation are the followings (Rabia, 1985):

a) Specific energy
b) Cost per foot
c) Bit dullness
d) Well bit records and geological information

Herein, the methods through which the drill bit technical and economic evaluation was performed are specific energy, formation drillability, and cost per drilled foot.

During the drilling of a well, the aim is to accomplish a sufficient penetration rate to reach the final planned depth with a safe manner for the drilling personnel, keeping simultaneously the environment uncontaminated. The penetration rate is directly affected by the drilling parameters as well as by the formation properties, especially the formation pore pressure. In exploratory wells, the drilling must be in overbalanced condition to avoid the entering of pore fluids into the wellbore. Thus, the pore pressure of each formation drilled by a particular bit size was determined according to the d-exponent method.

In Chapter 2, a comprehensive description of drill bits used today in rotary drilling is provided.

In Chapter 3, the available raw data (drill bit records) from the wells of Nestos 1, Nestos 2 and Komotini as well as the relevant geological and lithostratigraphic information, are presented.

Chapter 4 examines the performance of the drill bit used in each interval by computing the drillability through a series of proposed equations. Thus, the changes of drillability over depth are evaluated for each well under study and a comparative analysis of the drill bits used for the neighboring wells of Nestos 1 and Nestos 2 is also presented.

In Chapter 5, the formation pressure is determined on the basis of the indirect method of d-exponent. Additionally, the relationship between the differential pressure and the rate of penetration in each interval for the three wells under study is also examined.

In Chapter 6, the bit performance is economically evaluated through the cost per foot criterion which is computed for each drilled interval for each one of the three wells under study. Moreover, on the basis of cost per foot, a comparative analysis of the bits used for drilling the two neighboring wells of Nestos 1 and Nestos 2.

Finally, in Chapter 7 the conclusions and future research work are provided.

2. Drill Bits

One of the fundamental tasks performed by the drilling engineer is to select the most appropriate bit for a particular geological formation and to evaluate its performance.

A drill bit, which is located at the end of the drill string, is the major tool that crushes the rock under the combined action of the weight on bit and rotary speed. The bit cutting action can be described by scraping, chipping, gouging or grinding the rock. The resulting cuttings are carried by the drilling fluid out of the wellbore which is pumped through the drill string and through the nozzles to the bit front for cleaning the bottom hole in order a new surface of the rock to be continuously drilled by the bit (Rabia, 1985; Mitchell & Miska, 2011).

Over the past years, the technological advancements of rotary drilling bits are significant compared with other types of drilling equipment. These advancements that contributed to the improvement of the effectiveness of the drilling process are related to (Adams, 1985):

- roller-cone bit development
- multiple cones and jet arrangements in the roller bits
- cone lubrication methods
- diamond bit drilling and coring
- polycrystalline diamond compact (PDC) bits

In rotary oilfield-drilling, the bits are usually categorized according to their design features into two main categories (Bourgoyne et al., 1991):

- fixed-cutter bits
- roller-cone bits

The major difference between the two bit categories is that the fixed-cutter bit consists of blades that are integral with the body of the bit and rotate as a unit with the drill string, implying that no bearings are present, whereas a roller-cone bit has two or more cones containing cutting elements, which rotate about the axis of the cone as the bit is rotated with the drill string (Bourgoyne et al., 1991).

2.1 Drag Bits

In the early 1900s, the drag bit (Figure 2.1) was introduced in the drilling industry. Like an early version of today's fixed-cutter bits, a drag bit consists of blades that are integral with the body of the bit and drills the formation by physically plowing the cuttings from the bottom hole like a farmer's plow cuts a furrow in the soil (Bourgoyne et al., 1991).

Figure 2.1: Drag bits (Torquato Drilling Accessories, 2011).

Its design features include the number and shape of cutting blades, the size and location of watercourses, and the metallurgy of the bit and the cutting elements. The drag bit is further divided into the following bit types (Bourgoyne et al., 1991):

- steel-cutter bit
- diamond bit
- polycrystalline diamond compact (PDC) bit

A significant advantage of the drag bits over the roller-cone bits is the absence of rolling parts which require strong and clean bearing surfaces. This fact is important in drilling wells of small hole size where space is not available for the cone/bearing systems with the proper teeth structure (Mitchell & Miska, 2011). Since the drag bits can be manufactured by one solid piece of steel there is less chance of having bit breakage that would leave steel fragments in the bottom hole.

Drag bits with steel-cutter elements, such as two-blade fishtail bit, are suitable for drilling soft, uniform and unconsolidated formations because in hard and abrasive formations the bit wear resistance is rapidly decreased along with the penetration rate.

In addition, in soft formations that tend to be ‘gummy’, the drag bit performance is attained in conjunction with the proper jet velocity of the drilling mud so that impinges the upper surface of blades for removing the stuck cuttings (Bourgoyne et al., 1991).

The performance of drag bits was greatly improved by the introduction of hardfacing to the surface of the blades and the design of fluid passageways. High rotary speed and low weight on bit are applied owing to the dragging/scraping action of the drag bits (Mitchell & Miska, 2011).

Nevertheless, drag bits with steel-cutter elements are no longer in common use and have been displaced by other types of bits.

2.2 Diamond Bits

A diamond bit (Figure 2.2) is characterized by cutting elements that contain a large number of small-sized diamonds geometrically distributed across a tungsten carbide matrix (Rabia, 1985; Bourgoyne et al., 1991).

Figure 2.2: Diamond bit (Mensa-Wilmot et al., 2003)

Diamond bits are normally used for drilling hard and abrasive formations and when longer bit runs are required in order to reduce the trip time, e.g. in offshore drilling, where the rig costs are extremely high. The diamond bit is designed to break the rock in shear or by a ploughing/grinding action resulting in fewer energy requirements than in compression, as is the case with roller-cone bits (Rabia, 1985).

An important design feature of a diamond bit is its shape or crown profile. A bit with a long taper is suitable for drilling straight holes, allowing the use of higher bit weights while a short taper is easier to be cleaned due to less surface area. In directional drilling, a more concave bit face is normally used to assist in increasing the deviation angle of the wellbore from the vertical direction (Bourgoyne et al., 1991).

The size and number of diamonds used in a diamond bit depend on the rock to be drilled. A few large (0.75 to 2-carat) diamonds are used in soft formations that can be easily penetrated, while bits for hard formations have many small (0.07 to 0.12-carat) diamonds since diamonds cannot penetrate very far in such rocks (Rabia, 1985; Bourgoyne et al., 1991). Furthermore, the design of the fluid-course pattern and junk slots cut in the bit face and in the side of the bit face, respectively, controls the cuttings removal and prevents the overheating of diamonds and matrix material (Bourgoyne et al., 1991; Mitchell & Miska, 2011).

Diamond bits are usually operated at a given flow rate and pressure drop across the face of the bit. Several bit manufacturers have conducted experiments indicating the need of operating with approximately 2.0 to 2.5 hhp/in^2 of bottom hole and 500 to 1000 psi pressure drop across the face of the bit for efficient cleaning and cooling of diamonds (Bourgoyne et al., 1991).

Although the diamond bits are manufactured as either drilling or coring bits, the introduction of PDC bits has led to the replacement of diamond bits in drilling operations, which are currently manufactured as coring bits (Rabia, 1985).

2.3 Polycrystalline Diamond Compact (PDC) Bits

In the mid-1970s, the polycrystalline diamond compact (PDC) bit was introduced, as a new generation of the old drag or fishtail bit, employing no moving parts (Figure 2.3). A PDC bit breaks the rock in shear or by ploughing/grinding action. Breakage of rock in shear implies fewer energy requirements than in compression, resulting in less wear and tear on the rig and drill string (Rabia, 1985). Due to shear failure of rock, a PDC bit is needed to be self-sharpened for efficient drilling. PDC bits are also known as ‘stratapax’ bits (Adams, 1985).

Figure 2.3: PDC bit (Mensa-Wilmot et al., 2003)

A PDC bit employs a large number of cutting elements, also known as drill blanks. A drill blank consists of a synthetic polycrystalline diamond layer with an approximate thickness of 1/64 in. that is bonded to a cemented tungsten carbide substrate in a high pressure/high-temperature process (Bourgoyne et al., 1991). A drill blank produced by this process has the hardness and wear resistance of natural diamond complemented by the strength and impact resistance of the cemented tungsten carbide layer. The diamond layer is composed of many small diamond crystals bonded together at a random orientation that prevent any breakage of an individual diamond crystal to be propagated into the entire cutter element (Bourgoyne et al., 1991). The drill blank is bonded either to a tungsten carbide bit body matrix or to a specially shaped tungsten carbide stud that is mounted in a steel bit body and is then attached to the bit body with a low-temperature brazing method or by interference fitting (Rabia, 1985; Bourgoyne et al., 1991). Drill blanks are used as cutting elements attached to bits for drilling and mining applications as well (Adams, 1985).

PDC bits can efficiently drill a wide range of soft, firm, and medium to hard, non-abrasive formations that do not tend to be ‘gummy’. In some cases, PDC bits have also performed good results in drilling uniform sections of carbonates or evaporites that are not broken up with hard shale stringers, as well as in sandstones, siltstones, and shales (Bourgoyne et al., 1991).

2.3.1 Design Features

The design features of a PDC bit are based on nine variables (Rabia, 1985):

1) bit body material
2) bit profile
3) gauge protection
4) cutter shape
5) number or concentration of cutters
6) locations of cutters
7) cutter exposure
8) cutter orientation
9) hydraulics

Each design feature reinforces the PDC bits resulting in greater bit performance and wear resistance.

2.3.1.1 Bit Body Material

There are two types of body materials in use (Rabia, 1985):

a) heat-treated alloy steel
b) tungsten carbide matrix

Steel body bits use stud-type cutters which are attached to the bit body by interference or shrink fitting and are also provided with three or more jet nozzles for fluid passage. On the other hand, the tungsten carbide matrix body bits are manufactured in a mold like the manufacturing process of diamond bits, resulting in more complex profiles. The process of casting a matrix body requires high temperatures to be obtained that prevent to insert drill blanks until after furnacing of the body, as the compact diamond will be destroyed. It should be pointed out that the bonding between the small diamond crystals is destroyed at about 750^{o}C.

Unlike with the steel body PDC bits, the matrix body bits are more resistant to erosion by drilling fluid and use watercourses for hydraulic cleaning action (Bourgoyne et al., 1991). Thus, matrix body bits are preferred over the steel body bits in environments where body erosion is likely to be caused.

2.3.1.2 Bit Profile

There are two types of bit profiles in common use affecting hole cleaning, hole stability and gauge protection (Rabia, 1985):

a) double-cone profile
b) shallow-cone profile

The cutters in the double-cone profile are placed near the gauge controlling the hole deviation. As for the shallow-cone profile which has less area to be cleaned, this bit type drills faster than the bit of double-cone profile due to the more direct loading of the cutters by the weight applied by the drill collars.

2.3.1.3 Gauge Protection

The gauge protection for a steel body bit is achieved by tungsten carbide inserts which are set near the edges, while the gauge protection for a matrix body bit is based on the utilization of natural diamonds (Rabia, 1985).

2.3.1.4 Cutter Shape

The shapes of the manufactured drill blanks are basically three (Rabia, 1985):

a) standard cylindrical shape
b) chisel (or parabolic) shape
c) convex shape

2.3.1.5 Number of Cutters

The greater the number of cutters the longer the bit life, although the penetration rate decreases as the number or concentration of cutters increases, owing to the difficulty of efficient cleaning the spaces between the cutters (Rabia, 1985).

2.3.1.6 Location of Cutters

Several experiments and models have been conducted in order to determine the best location of cutters for maximum penetration rate and minimum wear and torque applied (Rabia, 1985).

2.3.1.7 Cutter Exposure

Cutter exposure defines the amount by which the cutter protrudes from the bit body. Penetration rate decreases with increasing cutter exposure. However, the cutter is less resistant to breakage as the exposure becomes greater (Mitchell & Miska, 2011; Rabia, 1985).

2.3.1.8 Cutter Orientation

Cutter orientation is described by two angles, the back rake, and side rake angles. Back rake angle is formed by the deviation of the face of the cutter from the vertical and varies between 0° and 25° (Mitchell & Miska, 2011; Rabia, 1985). The side rake angle is defined as the measure of the orientation of the cutter from left to right and assists in removal of the cuttings by mechanically directing them towards the annulus. The penetration rate decreases as the rake angle increases, but the resistance to cutter failure also increases as a result of spreading the load over a larger area (Rabia, 1985).

2.3.1.9 Hydraulics

A PDC bit used for drilling a wellbore requires optimum hydraulics where the maximum jet velocity of the drilling fluid is provided to flow through the nozzles in order to achieve efficient hole cleaning and high penetration rates. Also, a PDC bit may employ more than three nozzles which may not be round, as with the roller-cone bit (Rabia, 1985).

2.3.2 Thermally Stable Polycrystalline Diamond (TSP) Bits

A PDC bit fails when the temperatures developed by the interaction between the bit and the formation exceed 750℃. The introduction of Thermally Stable Polycrystalline Diamond (or TSP) bits in the oil industry was crucial in facing such temperatures, with the result of a potential increase of the penetration rate and bit wear resistance in hard and abrasive rocks (Radtke, Riedel & Hanaway, 2004). A TSP bit is manufactured similarly to the PDC bit but employs cutters which have been processed in order to resist in higher operating temperatures than the regular cutting elements inserted on a PDC bit. In addition, the TSP bits fail the rock through a grinding process (Mitchell & Miska, 2011).

2.3.3 Impregnated Bits

The impregnated bit (Figure 2.4) is only manufactured by a PDC matrix material where the natural or synthetic diamonds are embedded in the bit body to minimize any breakage from impact. These bit types operate in conjunction with turbo drills at rotary speeds varying from 500 to 1500 rpm for drilling small intervals, achieving sufficient penetration rate. Several drilling reports indicate that better bit performances have been achieved in abrasive and heterogeneous formations when impregnated bits with turbines are used instead of roller-cone bits and PDC bits (Mitchell & Miska, 2011).

Figure 2.4: Impregnated bit (Mitchell & Miska, 2011)

2.4 Roller-Cone Bits

A roller-cone bit comprises cones which rotate about their own axis as the bit is rotated at the bottom of the hole. This type of bit can be manufactured with various tooth designs and bearing types, making it suitable for drilling a wide range of formations. The three-cone bit constitutes the most common bit type among roller-cone bits that are currently used in oilfield rotary drilling (Bourgoyne et al., 1991).

There are four types of roller-cone bit depending on the number of cones (Rabia, 1985; Mitchell & Miska, 2011):

1) The mono-cone bit (Figure 2.5a) is capable of drilling small-hole sizes in which bearing sizing faces serious engineering problems.
2) The two-cone bit (Figure 2.5b) is used in soft formations and is only manufactured as milled tooth bit.
3) The three-cone or tricone bit is the most used type in oilfield drilling, employing either milled teeth or tungsten carbide inserts.
4) The four-cone bit is currently only manufactured as milled tooth bit and is proper for drilling large-hole sizes, e.g. 26 in and larger.

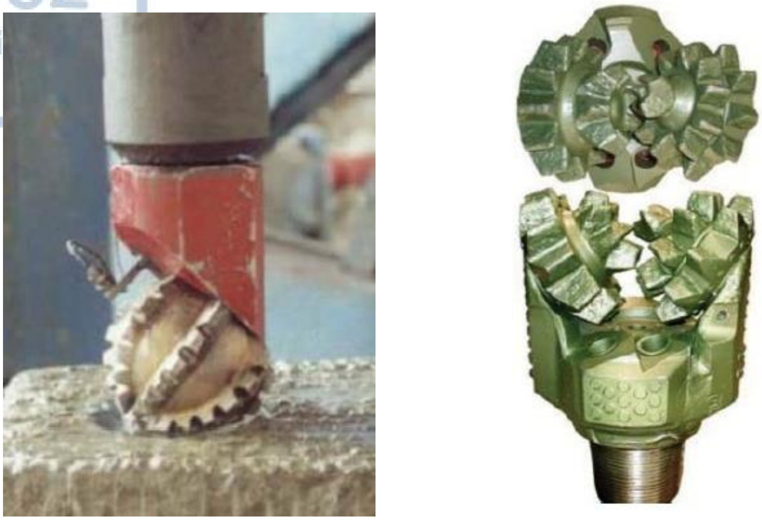

(a) (b)

Figure 2.5: (a) A mono-cone bit (Hu & Qingyou, 2006); (b) A two-cone bit (Centala et al., 2006)

2.4.1 Three-Cone Bit

The three-cone (or tricone) bit (Figure 2.6) is the most common bit type currently used in rotary drilling operations. A three-cone bit consists of three equal-sized cones and three identical welded legs, where each cone is mounted on a bearing pin forming an integral part of the bit leg. Each leg has fluid passageways through which the drilling fluid flows and their size can be reduced by placing nozzles in order to obtain the appropriate jetting velocity for efficient hole cleaning. In addition, the bit leg comprises a lubricant reservoir containing a lubricant supply for bearings. A threaded connection (or shank) is also provided for the attachment of the bit body with the drill string (Rabia, 1985; Adams 1985; Mitchell & Miska, 2011).

Figure 2.6: Three-cone bit (Mitchell & Miska, 2011)

The design factors of a roller-cone bit are directly affected by the type and hardness of formation as well as the borehole size to be drilled. According to Rabia (1985), the factors affecting the designing and manufacturing of a three-cone bit are the following: (a) journal angle, (b) amount of offset, (c) teeth geometry, (d) bearings types and (e) interrelationship between teeth and bearings.

2.4.1.1 Journal Angle

Each bit leg employs a journal (Figure 2.7a) which is a bearing system for supporting the loads applied. The journal angle is the angle formed by a line perpendicular to the axis of the bit and the axis of the journal (Figure 2.7b). Journal angle is the most significant element in designing a roller-cone bit. Its magnitude is inversely related to the cone size, since any increase in journal angle will result in a decrease in the basic angle of the cone and, in turn, in cone size (Mitchell & Miska, 2011; Rabia, 1985). In addition, the weight on bit is also determined by the journal angle, where an increase in journal angle will result in an increase in the weight on bit applied (Rabia, 2002). Furthermore, the gouging and scraping actions of the bit cones decrease, as the journal angle increases. It has been also found that journal angle directly influences the size and shape of the cutters. Since the journal angle depends on the hardness of the formation being drilled, the optimum journal angles for drilling soft and hard formations are 33^{o} and 36^{o}, respectively (Rabia, 1985).

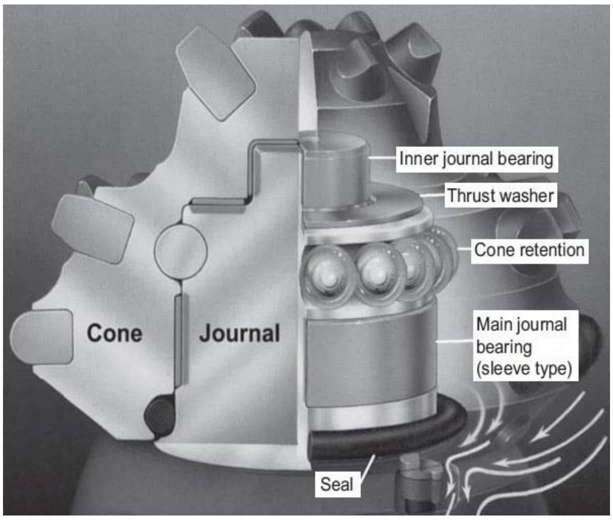

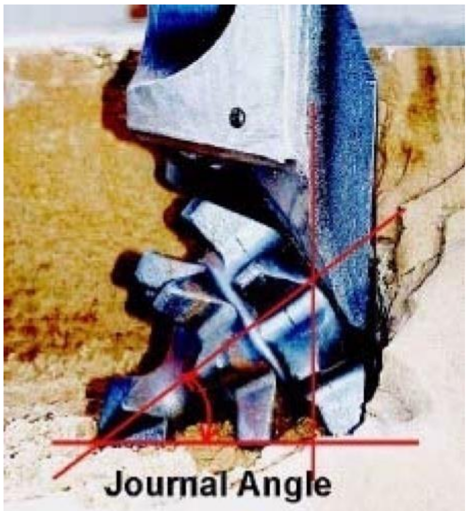

(a) **(b)**

Figure 2.7: (a) Bit journal (Wamsley & Ford, 2007); (b) Journal angle (Rabia, 2002).

2.4.1.2 Cone Offset

Cone offset is the measure of how much the cones are shifted, resulting in their axes do not intersect at the centerline of the bit. Cone offset is defined as the horizontal distance between the axis of the bit and a vertical plane through the axis of the journal, as shown in Figure 2.8. A cone with zero offset rotates about its own axis in a circle centered at the axis of the bit, as the drill string rotates. This movement produces a true rolling action. When the cone is offset from the bit center, it rotates around a circle which is now not centered at the axis of the bit, but the drill string rotation forces the cone to rotate in a circle around the centerline of the bit. As a result, cone starts to slip and act as a drag bit producing tearing and gouging actions which are preferable in drilling soft formations. These actions tend to increase penetration rate in most formation types, but induce faster tooth wear in abrasive formations (Bourgoyne et al., 1991; Rabia, 2002).

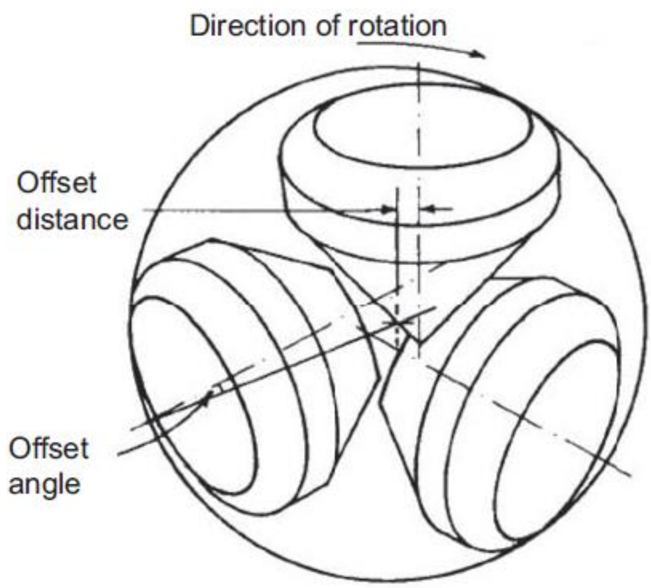

Figure 2.8: Cone offset (Bourgoyne et al., 1991)

The magnitude of the cone offset is directly influenced by the hardness of the formation to be drilled. The breakage of soft formations is performed by gouging and scraping actions provided by a three-cone bit made with a large offset so that the cones slip while rolling on the bottom of the hole. On the other hand, hard and abrasive formations can be efficiently drilled by crushing and chipping actions which are provided by a three-cone bit with zero offset in order to overcome the compressive strength of the rock, creating fines and chips. The cone offset of a roller-cone bit can vary from 1/2 to 3/8 in. for soft formations and usually approaches zero, typically 0.0325 to 0.0 in., for hard formations (Mitchell & Miska, 2011).

In some cases, the cone offset is expressed as the angle of the cone axis would have to be rotated in order to intersect and rotate around the centerline of the bit. Cone offset angle, also known as skew angle, varies from about 4^o for soft formation bits to zero for bits used in extremely hard formations (Mitchell & Miska, 2011).

2.4.1.3 Teeth Geometry

The geometry of the bit teeth directly affects the drilling action of a roller-cone bit and depends on the hardness of the formation being drilled. Long, slim, widely spaced, steel teeth are used for drilling soft formations. The use of longer teeth leads to greater volumes of rock removed at any contact between bit and rock. The long teeth penetrate deep into the soft rocks and cut them by scraping/twisting action provided by both the alternated rotation and plowing actions of an offset bit (Borgoyne et al., 1991). The widely spaced teeth permit the efficient removal of the resultant drill cuttings and self-cleaning of the bit. For soft formation bits, the included angle of teeth fluctuates between 39^o and 42^o (Rabia, 1985).

The teeth suited for drilling hard formations are manufactured shorter, heavier and more closely spaced to withstand the high compressive loads required to break the rock since these rock types fail under crushing and chipping actions provided by a roller-cone bit with zero offset. The included angle of teeth for hard formation bits is 45^o to 50^o. In formations of medium hardness, a moderate number of teeth is used with included angles ranging between 43^o and 45^o (Rabia, 1985).

There are two primary types of bit teeth used in oilfield rotary drilling, as shown in Figure 2.9 (Bourgoyne et al., 1991):

1) Milled tooth cutters
2) Tungsten carbide insert (TCI) cutters

In milled-tooth bits, the cutters are produced by milling the teeth out of a steel cone, while in insert bits the cutters, mostly tungsten-carbide-inserts, are pressed into accurately machined holes in the cone (Bourgoyne et al., 1991; Mitchell & Miska, 2011).

(a) **(b)**

Figure 2.9: (a) Milled-tooth bit (www.fasterdrilling.com); (b) TCI bit (www.horizontaltech.com)

The cutters of a milled-tooth bit designed for soft formation have been processed by hardfacing with a wear resistant material, such as tungsten carbide, on the one side of the teeth, leaving the other side to be sharpened as wears faster, a procedure known as self-sharpening hardfacing (Rabia, 2002). Moreover, the cutters of a milled-tooth bit designed to drill harder formations are usually case hardened by special processing and heat treated during the stage of manufacturing (Bourgoyne et al., 1991).

On the other hand, the tungsten carbide insert bits designed for drilling soft formations employ long and with chisel-shaped end inserts, while the inserts used for drilling hard formations are short and have a round or hemispherical end (Figure 2.10). The later bits are also called button bits. As a result, milled-tooth bits are typically best suited for drilling relatively soft formations, whilst tungsten-carbide-insert (TCI) bits (or button bits) perform best in the drilling of medium to hard formations.

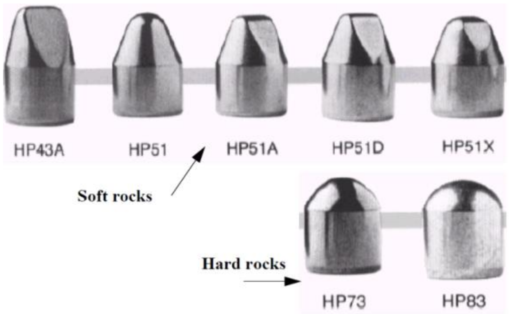

Figure 2.10: Insert types (Rabia, 2002)

2.4.1.4 Bearings Types

There are three types of bearings used in roller-cone bits (Mitchell & Miska, 2011):

1) roller bearings
2) ball bearings
3) friction bearing

The roller bearings support the radial loads (or weight on bit) forming the outer assembly. The ball bearings are suited to resist thrust loads and also help to secure the cones on the journals. Except for the resistance to radial loads supported by the roller bearings, the friction bearing in the nose assembly helps in supporting of radial loads as well (Mitchell & Miska, 2011).

Furthermore, the bearings are classified as non-sealed or sealed. The lubrication of the non-sealed bearings is performed by the drilling mud entering through the surface between the cone and the journal. The sealed bearings consist of a closed system containing a grease seal placed at the contact between the cone and the bearing lowermost point, a reservoir for grease supply and, a compensator plug for equalizing the grease pressure with the hydrostatic fluid pressure at the bottom of the hole. Hence, the sealed bearings are protected by the abrasive solids (sand, barite, etc.) which are included in the drilling mud and directly affect the working life of the bit (Rabia, 1985). In addition, sealed bearings can handle high temperatures. Most bits employ sealed bearings with a variety of designs included, ‘O’ ring and radial, V-ramp, wave (shaped seal pushing pockets of grease around the sealing area) and metal face seals (Rabia, 2002).

A recent advance over the bearing assembly is the journal bearing bit. In journal bearing bits, each cone rotates in contact with its journal bearing pin by eliminating the roller bearings. As a result, a larger area is provided through which the weight on bit is transmitted to the cone. Due to the absence of the roller bearings, there is more available space for strengthening the remaining components. There are some requirements that should be met in manufacturing journal bearing bits, such as effective grease seals, special metallurgy and extremely close tolerances. Silver inlays are also provided in the journal for minimizing friction and preventing galling (Bourgoyne et al., 1991).

2.5 IADC Bit Classification

The International Association of Drilling Contractors (IADC) has established a system of comparison charts for classifying the large variety of drill bits based on their design characteristics and their applications. There exists one comparison chart for roller-cone bits and one for fixed-cutter bits (Mitchell & Miska, 2011).

2.5.1 Roller-Cone Bit Classification

According to the IADC classification system introduced in 1992, each roller-cone bit is distinguished by a four-character code system. The first three characters are always numeric, and the last character is always alphabetic (Mitchell & Miska, 2011).

The *first character* refers to bit series and subsequently defines the general formation characteristics. Eight series or categories are used to describe the roller-cone bits. Series with numbers ranging from 1 to 3 apply to milled-tooth bits, while series between 4 and 8 apply to insert-type bits. As the number of the series increases, the rock hardness and abrasivity are also increased.

The *second character* is a further subdivision within each series related to the degree of formation hardness. Formation types range from 1 through 4, implying from the softest to hardest within each series.

The *third character* defines both bearing design and gauge protection. These features are classified into the nine following categories:

1. non-sealed roller bearing (also known as open-bearing bits)
2. air-cooled roller bearing (apply for air-, foam-, or mist-drilling)
3. non-sealed roller bearing, gauge protected
4. sealed roller bearing
5. sealed roller bearing, gauge protected
6. sealed friction bearing
7. sealed friction bearing, gauge protected
8. directional
9. other

The *last character* defines features available. According to IADC rules, only one alphabetic character can be used for defining the available bit features, as shown in

Table 2.1. However, in the case of a bit employing more than one feature, then only the most significant feature is usually listed.

Table 2.1: Additional features available for roller-cone bit classification (McGehee et al., 1992)

A	Air application
B	Special bearing seal
C	Center jet
D	Deviation control
E	Extended Reach
G	Extra gauge/body protection
H	Horizontal/steering application
J	Jet deflection
L	Lug pads
M	Motor application
S	Standard steel tooth model
T	Two-cone bits
W	Enhanced cuttings structure
X	Chisel insert
Y	Conical insert
Z	Other insert shape

2.5.2 Fixed-Cutter Bit Classification

The distinguishing of the large variety of the available fixed-cutter bits is based on a four-character coding system which was introduced by the IADC for clarifying the various bit features (Mitchell & Miska, 2011). This classification system has been modified for producing another four-character coding system describing seven-bit features (Winters & Doiron, 1987). The first character is always alphabetic, and the last three characters are always numeric.

The *first character* describes both primary cutter type and body material. There are currently five letters available (Winters & Doiron, 1987):

1. D-natural diamond/matrix body
2. M-PDC/matrix body
3. S-PDC/steel body

4. T-TSP/matrix body
5. O-other type

It should be noted that one type of diamond is used as the primary cutting element whereas the function of the other type is to provide support as backup material.

The *second character* refers to the cross-sectional profile of the bit and carries the numbers between 1 and 9. The bit profile is defined by the arrangement of the outer taper (gauge height) and the inner concavity (cone height). Gauge height and cone height are both normalized to the bit diameter for drill bits. Figure 2.11 shows the arrangement of both gauge height and cone height. A 3×3 matrix contains the nine-bit profiles where the gauge height and cone height systematically decrease from top to bottom and from left to right, respectively (Table 2.2). The number 0 is assigned for indicating unusual bit profiles that cannot be described by the 3×3 matrix.

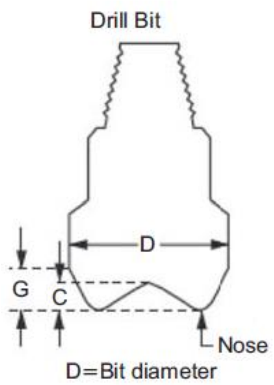

Figure 2.11: Demonstration of the gauge height (G) and cone height (C) (Mitchell & Miska, 2011)

Table 2.2: Bit profile codes (Winters & Doiron, 1987)

G-gauge height	C-cone height		
	High $C > 1/4\,D$	Medium $1/8 \le C \le 1/4\,D$	Low $C < 1/8\,D$
High $G > 3/8\,D$	1	2	3
Med $1/8 \le G \le 3/8\,D$	4	5	6
Low $G < 1/8\,D$	7	8	9

The *third character* indicates the hydraulic design of the bit and ranges from 1 through 9. The hydraulic design is described by the type of fluid orifice and the flow distribution. A 3×3 matrix includes nine hydraulic-design codes for identifying the orifice types and flow distributions. The orifice type ranges from changeable jets to fixed ports to open throat from left to right in the matrix, while the flow distribution varies from bladed to ribbed to open-faced from top to bottom, as shown in Table 2.3. The bladed and ribbed types of flow distribution define restricted flow arrangements whereas the flow in the open-faced type is non-restricted. In the special case of the open throat bits, radial flow or crossflow or another type of flow may occur and the letters R, X and O are used for indicating such flow types, respectively.

Table 2.3: Bit hydraulic design codes (Winters & Doiron, 1987)

	Changeable jets	Fixed Ports	Open throat
Bladed	1	2	3
Ribbed	4	5	6
Open faced	7	8	9

The *fourth character* refers to the cutter size and placement density on the bit and varies from 1 to 9. A 3×3 matrix includes the nine codes that indicate both cutter sizes and placement densities available. The cutter size varies from large to medium to small from top to bottom in the matrix, while the placement density ranges from light to medium to heavy from left to right, as shown in Table 2.4. The special case of the combination of small cutters placed on the bit with high-density pattern is denoted by the number 0, implying the type of impregnated bits. It should be noted that cutter size is defined for natural diamonds as the number of the stones per carat, while in the PDC and TSP bits is defined as the amount of usable cutter height or exposure of cutting element.

Table 2.4: Bit cutter size and density codes (Winters & Doiron, 1987)

		Density	
Size	Light	Medium	Heavy
Large	1	2	3
Medium	4	5	6
Small	7	8	9

0-Impregnated bit

3. Drilling Data

In 1977, three exploratory wells were drilled for discovering new potential accumulations of hydrocarbons by the consortium of the new founded Hellenic Public Petroleum Corporation (DEP) and the Romanian oil company, named ROM-PETROL, in the NE region of Hellas. These wells are called Nestos 1, Nestos 2 and Komotini. The first two are located in the Prefecture of Kavala, nearby the Nestos Delta, and the latter is located in the Prefecture of Rhodope, nearby the Vistonida Lake. The following map demonstrates the locations of Nestos 1, Nestos 2 and Komotini wells denoted by the characters N1, N2 and K, respectively (Figure 3.1).

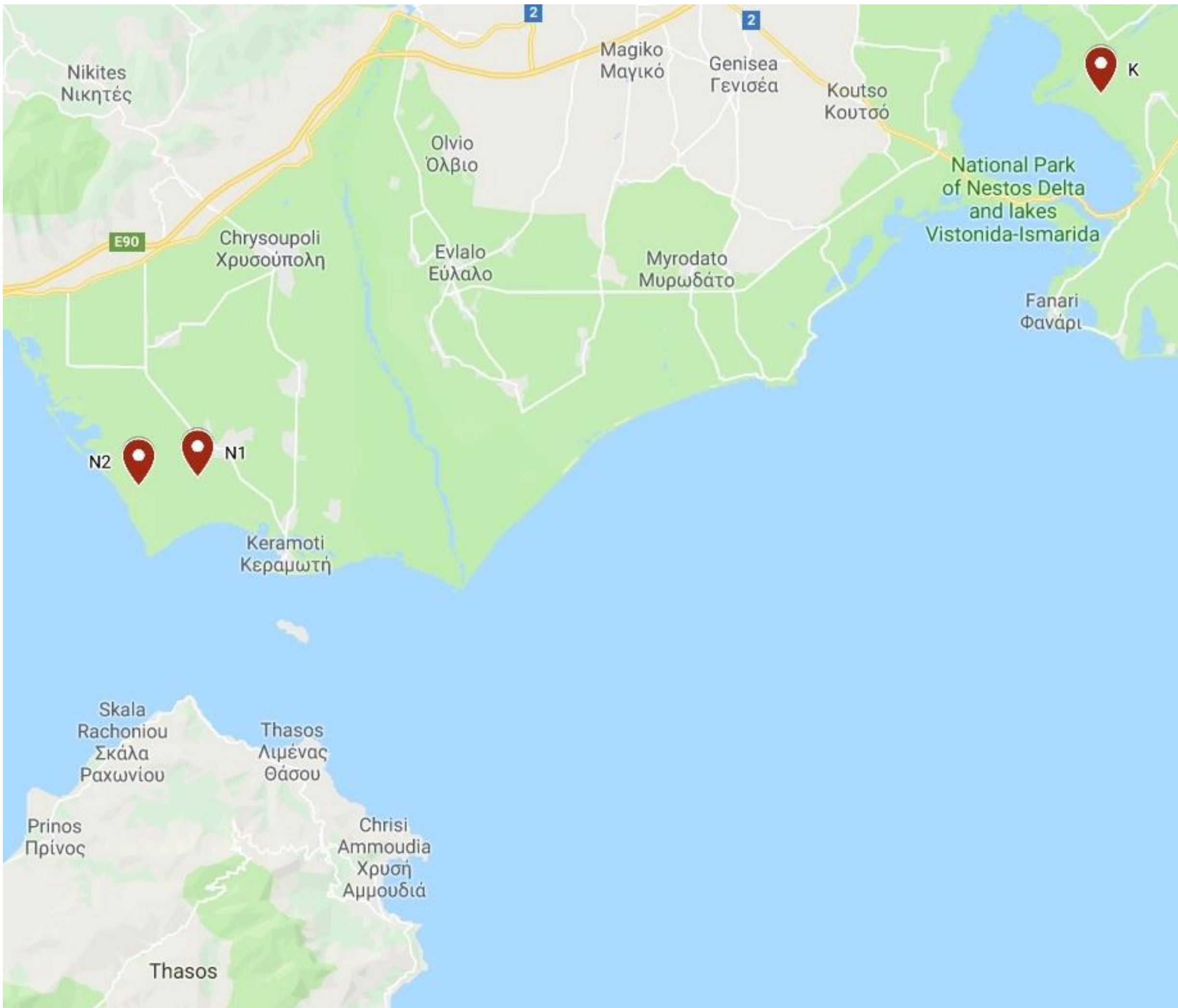

Figure 3.1: Political map demonstrating the location of N1, N2 and K wells (Google maps)

3.1 Drilling Program for the Nestos 1 Well

Nestos 1 well, which is located about 1 km SW of the Piges village, was drilled for the exploration of Nestos Delta stratigraphy (Figure 3.2). The drilling operation was conducted by an onshore rig (F-2002DH type) and lasted from September 29, 1976 up to March 9, 1977, reaching a total depth of 10,364 ft (Adam, Maleas & Misirlis, 1978).

Figure 3.2: Geological map demonstrating the location of N1 and N2 wells (I.G.M.E., 1982)

The drilling workflow can be separated into four stages based on hole geometry. These stages are the following:

a) <u>First stage (from surface up to 994 ft):</u> A Romanian bit of RS type (for soft formations) was used for drilling the first 994 ft, having a size of 17½". Afterward, a reamer bit with a size of 26" diameter was run into the same interval to enlarge the wellbore size for placing the conductor casing consisting of API J-

55 casing pipes of 18⅝" in size. An amount of 73 tons cement of type D was used for cementing the conductor casing up to the surface. The drill string used in this interval consisted of 5" drill pipes and 8" drill collars. The total length of the bottom hole assembly was 433 ft.

b) Second stage (from 994 up to 3,599 ft): At this stage, six RS bits (for soft formations) and one RMTA bit (for medium to abrasive formations) were used, all manufactured in Romany and with the same diameter of 17½". The drill string configuration remained the same as in the previous stage. At this stage, surface casing was placed, consisting of API-P 110 casing pipes of 13⅜" in diameter. For the cementing process 40 tons of type D cement and 2.5 tons of type G cement, were used.

c) Third stage (from 3,599 up to 7,841 ft): This interval was drilled by using Romanian bits with a diameter of 12¼". More specifically, ten bits of type S (for soft formations), nine bits of type M (for medium hard formations) and two bits of type MTA (for medium to abrasive formations) were used. The drill string used in this interval consisted of 5" drill pipes and 8" drill collars, while the total length of the bottom hole assembly was 518 ft. At this stage the first intermediate casing was placed in the well, consisting of API C-75 casing pipes of 9⅝" in diameter. At this stage, 76.5 tons cement of type G were used for cementing the annulus between the wellbore and the casing string from the bottom up to 3,599 ft. During this interval, two coring bits were also used to retrieve core samples from depth intervals of 5,843-5,862 ft and 6,365-6,394 ft, respectively.

d) Fourth stage (from 7,841 up to 10,364 ft): At this stage, drilling was performed by using bits of 8½" in diameter. In general, 12 bits of SM type (for soft to medium hard formations), 12 bits of MTA type (for medium to abrasive formations), 11 bits of A-type (for abrasive formations), 7 bits of SLJ type and 2 bits of T2HJ type were used in total for drilling this interval. The drill string consisted of 5" drill pipes and 6¼" drill collars. Bottom hole assembly had a total length of 702 ft. As for the casing string (second intermediate casing), two types of 7" casing pipes were placed into the wellbore: 7,798 ft of API C-75 pipes and 2,490 ft of EL C-75. During drilling, a thief zone was observed at 10,170 ft imposing the borehole to be cased off and cemented. For the cementing process, 62.5 tons of type G cement and 410 lbs of type CH-50 cement were used. The small amount of CH-50 cement was added for reducing the specific weight of the cement mixture. Finally, two DST tests were conducted at the intervals from 8,756 to 8,940 ft and from 9,425 to 9,544 ft, in which there was no observation of oil flow to the surface, while medium to high flow rates of natural gas were found.

Unfortunately, only the drilling data of the upper section of Nestos 1 well (up to the depth of 5,964 ft) was available and used in this study (Table 3.3).

3.2 Drilling Program for Nestos 2 Well

Nestos 2 well is an exploratory well in the region of Nestos Delta and is located about 2.5 km SW of the Agiasma village (Figure 3.2). Drilling was performed with the same onshore rig of F-2002DH type, as the case of Nestos 1 well, and lasted from March, 23 up to August 14, 1977, reaching a total depth of 13,025 ft (Adam, Maleas & Misirlis, 1978).

The drilling workflow comprised of 5 stages which are described below:

a) First stage (from surface up to 515 ft): A bit of RS type (manufactured in Romany for soft formations) was used for drilling this interval, having a size of 17½". The drill string used in this interval consisted of 5" drill pipes and drill collars of 9½" and 8" in diameter, having a length of 187 ft and 230 ft, respectively. After drilling the first 515 ft, a reamer bit of 26" in diameter was run to enlarge the hole size. The casing setting depth of the 18⅝" conductor pipe used in this interval was 487 ft. Conductor pipe comprised of API J-55 casing pipes and after proper placement was cemented using 34 tons of type G cement.

b) Second stage (from 515 up to 3,461 ft): For drilling this interval six bits type of RS type were used having a diameter of 17½". For the upper section, the same bit as in the previous stage was used. Additionally, the drill string was exactly the same as in the first stage. The casing string for this interval consisted of the 13⅜" API P-110 casing pipes, set to a depth of 3,461 ft. Finally, this casing string was cemented in place using an amount of 80 tons of type D cement.

c) Third stage (from 3,461 up to 7,775 ft): For drilling this interval 14 bits type of RS (for soft formations) and 5 bits of RM type (for medium hard formations) were used in total, all manufactured in Romany and with the same diameter of 12¼". The drill string was composed of 5" drill pipes and 9½" drill collars (total length of bottom hole assembly was 426 ft). The wellbore was cased of using API C-75 casing pipes set to a depth of 7,775 ft. The casing string was then cemented by using an amount of 59 tons of type G cement.

d) Fourth stage (from 7,775 up to 11,634 ft): This interval was drilled using 44 Romanian bits (1 of S type, 11 of SM type, 24 of SLJ type and 8 of MTA type), as well as 7 bits manufactured by Hughes (1 of J33 type, 3 of J44 type and 3 of X1G type), all with the same diameter of 8½". The drill string consisted of 5" drill pipes and 6¼" drill collars, having a length of 525 ft. At this stage, a 7" liner of 4,163 ft in length was placed into the wellbore for ensuring the smooth and safe drilling up to the 11,634 ft. Drilling operations were delayed by the installation of the liner causing serious economic problems as well. For cementing the liner 34 tons of type G cement were used.

e) Fifth stage (from 11,634 up to 13,025 ft): The lower interval of the well was drilled by bits of 5⅞" in diameter. Seven Hughes bits (6 of J55 type and 1 of OWV type) and one Romanian bit of MTA type were used in total. The configurations of the drill string were as below:
   - 5" of drill pipes (from surface up to 7,185 ft)
   - 3½" of drill pipes (from 7,185 up to 12,310 ft)
   - 4" of drill collars (from 12,310 up to 13,025 ft)

Finally, five DST tests took place at the interval between 9,842 and 11,483 ft. For this reason, the 7" liner was perforated by balls of ½" in diameter and density of 4 balls per foot. Unfortunately, the DST tests showed the existence of natural gas of low flow rate due to the extremely low permeability of the reservoir rocks which led to the abandonment of the well.

The availability of the drilling data for Nestos 2 well was also limited (up to the depth of 5,643 ft), as in the case of the Nestos 1 well (Table 3.4).

3.3 Drilling Program for Komotini Well

The exploratory well of Komotini was drilled near the village of Salpi in the Prefecture of Rhodope. Drilling started on October, 23 and lasted until November 19, 1977, reaching a total depth of 5,623 ft. Drilling was conducted using the same onshore rig of F-2002DH type, manufactured in Romany, as in the other two wells.

Based on the hole geometry, the drilling program can be classified into three stages, as follows (Adam, Maleas & Misirlis, 1978):

a) First stage (from surface up to 997 ft): Drilling started with a Romanian 17½" bit of S type (for soft formations) up to 997 ft. The drill string consisted of 5" drill pipes and drill collars of 9½" and 8" with a length of 150 ft and 180 ft, respectively. Casing string consisted of 13⅜" API J33 casing pipes was set to 968 ft from the surface. 43 tons of D type cement was used for cementing the casing string.
b) Second stage (from 997 up to 4,236 ft): At this stage, drilling was performed by using seven 12¼" bits from which five came from Romania, two S type for soft formations and three M type for medium hard formations, and the other two bits (X3A) were manufactured by Hughes for drilling soft formations (Table 3.1). As for the casing, wellbore was cased using 9⅝" API J55 casing pipes, set to a depth of 4,236 ft. Since the installation of casing was completed, cementing took place by using 39.3 tons of type D cement.
c) Third stage (from 4,236 up to 5,623 ft): Seven bits of 8½" were used in drilling this interval. Four of them were of type X1G bits (Table 3.1) for soft formations, two of them were of type J22 bits and one was J44 bit. The last three bits are both suitable for medium hard formations, as shown in Table 3.2. The performance of the drill bits was not the expected due to the successive alternations of soft and abrasive formations which resulted in the increase of the tripping time. The drill string consisted of 5" drill pipes and 6¼" drill collars with a length of 540 ft. Three core samples were taken for analysis at depths between 4,265 and 5,623 ft as well. The well did not show any evidence of hydrocarbons accumulation. As a result, the well was cemented with 5 tons of D type cement up to the surface and abandoned.

In this case, the whole of the drilling data of Komotini well was available (Table 3.5).

The following Tables 3.1-3.2 present the characteristics of the Hughes' bits which were used, classified according to the IADC three-code bit classification system.

Table 3.1: IADC three-code for Hughes' milled tooth bits (Rabia, 1985)

IADC Code		Standard Roller Bearings 1	Sealed Roller Bearings 4	Sealed Journal Bearings 6
1	1	R1	X3A	J1
	2	R2		J2
	3	R3	X1G	J3
2	1	R4		J4
3	1	R7		J7
	2	R8		

Table 3.2: IADC three-code for Hughes' insert bits (Rabia, 1985)

IADC Code		Roller Bearing Air 2	Sealed Roller Bearing 5	Sealed Journal Bearing 7
4	3			J11
5	1			J22
	3	HH33	X33	J33
6	2	HH44	X44	J44 J44C
	3			J55R
	4	HH55		J55
7	3	HH77		J77
8	1	HH88		
	3	HH99		J99

3.4 Bit Records of Nestos 1, Nestos 2 and Komotini Wells

The bit records provide crucial information concerning the drilling program that took place. Herein, the information contained in the bit records for each interval of the three wells under study include, the bit type and size used, the depth where a bit ran in and pulled out of the wellbore, the operation hours of a specific bit or the rotating time, the weight applied on the bit, the rotary speed, the penetration rate, etc. Furthermore, regarding the hydraulic program, duplex pumps of the same type (2PN630) were used for drilling all the three wells, and the data concerning the mud properties, such as the mud density, can also be found in the bit records.

In addition, it should be noticed that all the bits used in the three wells of Nestos 1, Nestos 2 and Komotini, were three-cone bits regardless if they came from the Romanian oil company or Hughes.

Unfortunately, only in Komotini well, the whole set of bit data is available, whereas the bit records for the neighboring wells of Nestos 1 and Nestos 2 provided contain information only for the upper section.

Table 3.3: Bit records of Nestos 1 well (Adam, Maleas & Misirlis, 1978)

Bit Record of Nestos 1 Well																																		
																		Hydraulic Program							Mud Properties					Vert.	Drilling speed			
Date	Run No.	Size		Type	Serial No.	Nozzles			Drilled		Meters	Hours	Cumul. Hours	Weight	R.P.M.	Flow Rate	Pump Press.	Pump Type	Pump 1		Pump 2		Velocity		M.W.	V	W.L.	F.C.	Ph	Dev.	V.D.	V.M.	V.T.	V.C.
						1	2	3	From	To									Liner	SPM	Liner	SPM	Jet	Annular										
		in	*mm*			*mm*	*mm*	*mm*	*m*	*m*	*m*	*h*	*h*	*ton*	*h /min*	*l/s*	*kgf/cm²*		*inc*		*inc*		*m/s*	*m/s*	*kg/dm³*	*sec*	*cm³*	*mm*			*m/h*	*m/h*	*m/h*	*m/h*
	1	17 1/2	444.5	**RS**	666	14	14	14	0	329	329	31.00	31.00	4-18	100		20-30	2PN630	8	65	-	-			1.19	60	-				10.61			
	2	"	"	"	671	"	"	"	329	693	364	25.40	56.40	18	"		60-70	"	"	60	8	55			1.22	50	-				14.18			
	3	"	"	"	664	"	"	"	693	730	37	3.45	60.25	"	120		70	"	"	"	"	53			1.23	45	-				9.86			
	4	"	"	"	659	"	"	"	730	823	93	14.45	75.10	"	130		60	"	6 3/4	65	6 3/4	65			"	50	10				6.30			
	5	"	"	"	668	"	"	"	823	883	60	15.45	90.55	14	120		80	"	"	45	"	55			1.27	"	7				3.80			
	6	"	"	**RMTA**	337	16	16	16	883	914	31	13.05	104.00	8-18	100		75-80	"	"	64	"	50			"	48	"				2.36			
	7	"	"	**RS**	672	14	14	14	914	983	69	28.00	132.00	10-16	"		85	"	"	55	"	55			1.28	55	7.5				2.46			
	8	"	"	"	675	"	"	"	983	1,097	114	30.35	162.35	8-15	100-110		"	"	"	"	"	"			"	48	5				3.79			
	9	12 1/4	331.2	**RM**	771	"	"	"	1,060	1,191	131	10.35	173.10	14-16	120		75-80	"	"	"	"	"			1.27	43	8				12.46			
	10	"	"	**RS**	1043	13	13	13	1,191	1,401	210	21.00	194.10	14	110		85-90	"	"	"	"	"			1.23	50	7				10.00			
	11	"	"	"	426	"	"	"	1,401	1,521	120	16.20	210.30	10-14	"		90	"	"	"	"	"			1.32	55	6				7.34			
	12	"	"	"	338	"	"	"	1,521	1,613	92	17.40	228.10	8-14	90-100		85-90	"	"	"	"	"			1.24	58	7				5.20			
	13	"	"	"	352	"	"	"	1,613	1,696	83	18.40	246.50	10-14	100		90	"	"	"	"	50			1.29	50	6.5				4.44			
	14	"	"	"	317	"	"	"	1,696	1,781	85	16.05	262.55	"	90		100	"	"	"	"	"			1.34	58	5.5				5.07			

Table 3.4: Bit records of Nestos 2 well (Adam, Maleas & Misirlis, 1978)

Bit Record of Nestos 2 Well

Date	Run No.	Size		Type	Serial No.	Nozzles			Drilled		Meters	Hours	Cumul. Hours	Weight	R.P.M.	Flow Rate	Pump Press.	Hydraulic Program							Mud Properties					Vert. Dev.	Drilling speed			
						1	2	3	From	To								Pump Type	Pump 1 Liner	Pump 1 SPM	Pump 2 Liner	Pump 2 SPM	Velocity Jet	Velocity Annular	M.W.	V	W.L.	F.C.	Ph		V.D.	V.M.	V.T.	V.C.
		in	*mm*			*mm*	*mm*	*mm*	*m*	*m*	*m*	*h*	*h*	*ton*	*h /min*	*l/s*	*kgf/cm²*		*inc*		*inc*		*m/s*	*m/s*	*kg/dm³*	*sec*	*cm³*	*mm*			*m/h*	*m/h*	*m/h*	*m/h*
21.3.77	1	17 1/2	444.5	**RS**	648	12	12	12	0	157	157	14.00	14.00	3-10	100	47	45	2PN630	8	65	-	-	78	0.35	1.27	50	13	2	7.0		11.21	9.10	2.62	2.62
22.3.77		26	660.4	"	**Roler reamer**				0	"	"	13.00	-	2-6	70-80	-	40	"	"	"	-	-	-	-	"	"	10	"	"		-	-	-	-
24.3.77	1	17 1/2	444.5	"	648	16	16	16	157	565	408	15.45	29.45	10	120	47	45	"	"	"	-	-	78	0.35	1.25	"	"	"	"		26.40	-	-	-
TOTAL BIT	"	"	"	"	"				0	565	565	29.45	"																		19.18	-	-	-
26.3.77	2	"	"	"	673	16	16	16	565	660	95	22.15	52.00	15	130	47	55	"	"	"	-	-	"	"	"	53	9	2	7.5		4.28	-	-	-
28.3.77	3	"	"	"	653	"	"	"	660	957	297	30.30	82.30	18	140	"	75	"	"	"	-	-	"	"	1.23	60	7	"	"		9.80	-	-	-
30.3.77	4	"	"	"	654	"	"	"	957	982	25	3.45	86.15	"	130	"	"	"	"	"	-	-	"	"	1.21	70	6.8	"	"		7.24	-	-	-
8.4.77		9 5/8	244.5	"	1085	—	—	—	954	"	28	**DRILL A NEW HOLE**				42	80	"	-	-	7 1/4	65	-	-	1.23	47	9	1.5	10.5					
9.4.77		"	"	"	"	—	—	—	982	996	14	2.30	88.45			"	"	"	-	-	"	"	-	-	1.20	"	8	"	11.5					
10.4.77	5	17 1/2	444.5	"	658	—	—	—	954	996	42	10.30		35	70	47	65	"	8	40	"	40	-	-	"	48	8.5	"	"					
10.4.77	6	"	"	"	725	16	16	16	996	1,055	59	11.30	100.15	18	130	"	70	"	"	65	-	-	78	0.35	"	"	8	"	11.0		5.22			
STAGE 2		"	"	"					157	1,055		123.45																			7.29	5.46	3.66	1.99
14.4.77	7	12 1/4	311.2	"	327	16	16	16	1,055	1,121	66	5.15	105.30	9	130	47	65	"	8	65	-	-	78	0.74	1.20	50	10	2	11.5		12.81			
15.4.77	8	"	"	"	288	"	"	"	1,121	1,270	149	17.30	123.00	15	"	"	75	"	"	"	-	-	"	"	"	45	9	"	"		8.61			
16.4.77	9	"	"	"	257	15	15	15	1,270	1,351	81	14.45	137.45	"	"	"	"	"	"	"	-	-	88	"	"	"	"	"	"		5.6			
17.4.77	1 0	"	"	**RM**	777	"	"	"	1,351	1,405	54	12	149.45	"	"	35	"	"	-	-	7 1/4	60	68	0.50	1.23	55	8	1.5	"		4.5			
18.4.77	1 1	"	"	**RS**	278	"	"	"	1,405	1,482	77	15	164.45	16	140	47	90	"	6 3/4	55	6 3/4	35	88	0.74	1.26	60	"	"	"		5.13			
19.4.77	12	"	"	"	267	"	"	"	1,482	1,631	149	18	182.45	15	"	50	100	"	"	"	"	40	94	0.78	"	"	"	"	"		8.27			
20.4.77	13	"	"	"	247	"	"	"	1,631	1,734	103	17.30	200.15	11	"	"	"	"	"	"	"	"	"	"	1.28	"	7.5	"	"		5.95			

Table 3.5: Bit records of Komotini well (Adam, Maleas & Misirlis, 1978)

Bit Record of Komotini Well

Date	Run No.	Size		Type	Serial No.	Nozzles			Drilled		Meters	Hours	Cumul. Hours	Weight	R.P.M.	Flow Rate	Pump Press.	Hydraulic Program							Mud Properties					Vert. Dev.	Drilling speed			
						1	2	3	From	To								Pump Type	Pump 1		Pump 2		Velocity		M.W.	V	W.L.	F.C.	Ph		V.D.	V.M.	V.T.	V.C.
																			Liner	SPM	Liner	SPM	Jet	Annular										
		in	mm			mm	mm	mm	m	m	m	h	h	ton	h /min	l/s	kgf/cm²		inc		inc		m/s	m/s	kg/dm³	sec	cm³	mm			m/h	m/h	m/h	m/h
23.10.77	1	17 1/2	444.5	**RS**	734	16	16	1 6	0	304	304	19.15	19.15	2-6	80	44	50-60	2PN630	8	65	-	-	73	0,3-0,4	1.20	50	2	—	—		15.79	7.37	2.79	2.79
27.10.7 7	2	12 1/4	311.2	"	748	15	15	15	304	485	181	13.45	33.00	4-8	120	52	60-75	"	6 3/4	54	6 3/4	60	98	0.8-1.2	1.18	"	"	—	—		13.16	9.52	9.05	8.62
28.10.77	3	"	"	"	799	13	13	13	485	622	137	16.00	49.00	6-8	"	40	70-90	"	"	44	"	44	100	0,6-1,3	1.19	48	"	9	—		8.56	6.08	6.08	6.08
29.10.77	4	"	"	**RM**	633	"	"	"	622	801	179	16.30	65.30	4-8	110	42	75-100	"	"	45	"	45	106	0,6-1 ,4	1 ,18	47	"	8	—		10.84	7.53	7.53	7.53
30.10.77	5	"	"	"	610	16	16	16	801	960	159	15.15	80.45	5-10	"	45	70-80	"	"	"	"	50	75	0,7-1,5	1.16	"	1.5	7.5	—		10.42	7.06	7.06	7.06
31.10.77	6	"	"	"	650	"	"	"	960	1046	86	12.30	93.15	8-10	100	"	80-90	"	"	"	"	"	"	"	"	45	"	7	—		6.88	4.35	4.35	4.35
1.11.77	7	"	"	**X3A**	775SL	13	13	13	1046	1207	161	21.45	115.00	8-12	120	38	100-105	"	"	37	"	43	95	0,6-1,5	1.17	47	"	7.5	—		7.40	4.99	4.99	4.99
2.11.77	8	"	"	"	776"	"	"	"	1207	1287	80	12.45		8-15	"	36	105	"	"	36	"	42	91	0,55-1,2	"	45	"	7	—		—	—	—	—
3.11.77	**Core ∅ 188,9**								1287	1296	9	5.00	120.00	5	70	—	70	"	"	35	—	—	—	—	—	—	—	—	—		—	—	—	—
4.11.77	8	12 1/4	311.2	**X3A**	776SL	13	13	13	1296	1300	4	3.00		12-14	120	35	100	"	"	36	"	40	88	—	1.18	47	1.5	7	—		—	—	—	—
		TOTAL		"	"				1207	1300	84	13.45	133.45																		6.11	2.82	2.82	2.82
		STAGE 2							304	1300	996		114.30																		8.69			
7.11.77	9	8 1/2	215.9	**X1G**	984 AL	12	12	12	1300	1301	1	1.15	135.00	8-10	100	33	110	"	5 3/4	44	5 3/4	56	97	1.2	1.18	47	1.5	6	—		0.80	0.16	0.12	0.11
8.11.77	10	"	"	"	985 "	11	11	11	1301	1360	59	11.15	146.15	12-15	120	32	120	"	"	45	"	52	112	"	"	48	"	"	—		5.24	3.27	3.27	3.19
9.11.77	11	"	"	**J22**	915 RL	"	"	"	1360	1497	137	28.45	175.00	10-12	80-90	27	110	"	"	42	"	41	95	>1	1.20	50	"	5	—		4.76	3.63	3.63	3.56
10.11.77	12	"	"	"	926 "	"	"	"	1497	1509	12	10.15	185.15	10-14	70-80	28	120	"	"	44	"	"	98	"	1.19	48	"	"	—		1.17	0.75	0.75	0.75
11.11.77	13	"	"	**J44**	FS385	"	"	"	1509	1516	7	6.15	191.30	12-15	60-70	"	"	"	"	46	"	39	"	"	1.20	50	"	"	—		1.12	0.61	0.61	0.61
11.11.77	14	"	"	**X1G**	768 AL	"	"	"	1516	1550	34	6.00	197.30	12-15	100	"	"	"	"	48	"	37	"	"	1.21	48	"	"	—		5.66	2.83	2.83	2.83
12.11.77	**Core ∅ 188,9**					—	—	—	1550	1553	3	2.00	199.30	4-6	70	13	90	"	"	35	—	—	—	—	—	—	—	—	—		—	—	—	—
13.11.77	14	8 1/2	215.9	**X1G**	768 AL	11	11	11	1553	1578	25	7.30	207.00	12-14	100	28	120	"	"	37	"	48	98	>1	1.19	50	1.5	5	—		3.33	1.75	1.315	1.30
		TOTAL		"	"				1516	1578	59	13.30																			4.37	2.24	1.90	1.88
14.11.77	12	8 1/2	215.9	**J22**	926 PL	11	11	11	1578	1600	22	12.00	219.00	15-17	60-90	28	130	"	"	"	"	"	"	"	1.20	48	"	"	—		1.83	1.15	1.15	1.11
		TOTAL		"	"				1497	1600	34	22.15																			1.53	0.97	0.97	0.95
14.11.77	15	8 1/2	215.9	**X1G**	776 AL	11	11	11	1600	1638	38	8.00	227.00	12-14	120	28	130	"	"	38	"	46	"	"	1.19	47	"	"	—		4.75	2.45	2.45	2.45
15.11.77	**Core ∅ 188,9**					—	—	—	1638	1643	5	3.15	230.15	4-6	70	13	60	"	"	35	-	-	—	—	—	—	—	—	—		—	—	—	—
16.11.77	13	8 1/2	215.9	**J44**	FS385	9	9	9	1643	1731	88	27.45	258.00	12-14	80	26	135	"	"	"	5 3/4	45	120	"	1.21	48	"	"	—		3.17	2.38	2.38	2.36
17.11.77	**Core ∅ 188,9**					—	—	—	1731	1736	5	3.00	261.00	4-6	70	13	50	"	"	"	-	-												
		TOTAL		**J44**	FS385				1509	1737	96	35.30	264.30																		2.82	1.98	1.98	1.97
		STAGE 3							1300	1737	437		128.75																		3.39			
GENERAL TOTAL									0	1737	1737	264.30	264.30																		6.56			

3.5 Geology-Stratigraphy of Nestos Region

The surrounding area of Nestos Delta belongs geologically to the Rhodope Massif and constitutes an extension of the tectonic graben of Prinos, extending from the West of Thassos Island to the Nestos River. The Nestos basin is separated into two sub-basins: the West and the East. Among these two the West sub-basin appears to have greater potentiality in finding hydrocarbons, as it is located in the southeastern section of the oil-bearing graben of Prinos (Adam, Maleas & Misirlis, 1978).

The basis of the basin is filled with the onshore sediments which are underlain by lacustrine (VARVES Zone) and offshore deposits (Evaporites Zone). Above this set of sedimentary rocks, Pliocene offshore sediments and Quaternary deposits (loose sand and sand and gravel) of deltaic origin were deposited. The sedimentary rocks overlie the metamorphic basement (Rhodope Schist), which lies in depth of greater than 10,000 ft.

In addition, the sedimentation process has been interrupted many times, as indicated by the occurrence of unconformity layers.

3.5.1 Stratigraphy of Nestos 1 Well

The cuttings analysis and core samples as well as the assessment of loggings conducted in the Nestos 1 well, were performed by Institute of Petroleum ICPPG of Bucharest resulting in the following lithostratigraphic column (Adam, Maleas & Misirlis, 1978):

1) <u>Quaternary 0-557 ft:</u> It consists of loose sand and sand and gravel formations, poorly sorted with a large number of shells at the upper part. It is mainly composed of quartz and metamorphic fragments. Interbeds of plastic clay and soft fine-grained silt are absent. The entire shape and the origin of the sedimentary material suggest that circular deltaic sedimentation took place in the region.
2) <u>Pliocene 557-2,555 ft:</u>

   <u>557-984 ft:</u> The same Quaternary formations, with the upper section, appear here also but more compact.

   <u>984-1,853 ft:</u> A continuous series is present with alternations (thickness up to 16 ft) of sandstone, conglomerate, and clay.

1,853-2,335 ft: The sandy and silty clay are predominant. At the lower part of this zone, soft siltstone occurs. The claystone is also alternated with interbeds of clayey sandstone and conglomerate.

2,335-2,555 ft: It is mainly composed by grey-sandstone with a clay cement material and interbeds of grey-limestone.

3) Miocene 2,555-10,167 ft: In the section between 2,555 and 3,772 ft a series of evaporite is observed, which is characterized by the presence of white anhydrite and brownish limestone.

   2,555-2,919: The dominant formation is conglomerate with metamorphic material and concentrations of pyrite, through which brownish limestone and grey-marly and sandy clay are interbedded.

   2,919-3,349: Comprises the main zone of anhydrides, which are white in color, compacted and alternated with limestones, conglomerates, and clays.

   3,349-3,772 ft: The lower part of the evaporite series consists of claystone, mostly marly, and alternations of anhydrite, limestone, and conglomerate.

   3,772-4,232 ft: The grey clay, plastic, sandy and silty, interbedded with sandstone is dominant.

   4,232-7,776 ft: An extended zone of peculiar sedimentation, called VARVES, is present. This zone consists of alternations of thin layers (thickness of some mm) of hard clay, siltstone, sandy siltstone, fine-grained sandstone (locally carbonaceous), hard marl, limestone and rarely anhydrite.

   7,776-10,167 ft: It is mainly composed of sandstone layers. The cement material through these formations is siliceous and calcareous. At the lower part of this zone, these formations are more compacted. These formations are also interbedded with hard grey clays and marls of lower thickness, black bituminous clays, and coal layers. At the base of this series, the presence of coal is rare. In addition, poor hydrocarbon shows have been observed through these layers. This series is characterized by high values of electrical resistivity owing to the presence of bituminous clays.

4) Metamorphic basement from 10,167 ft: Consists of metamorphic rocks of Rhodope schist, mostly schist, and aplite.

The stratigraphy that was encountered during the drilling of Nestos 1 well, as well as the borehole profile, are shown in Figure 3.3.

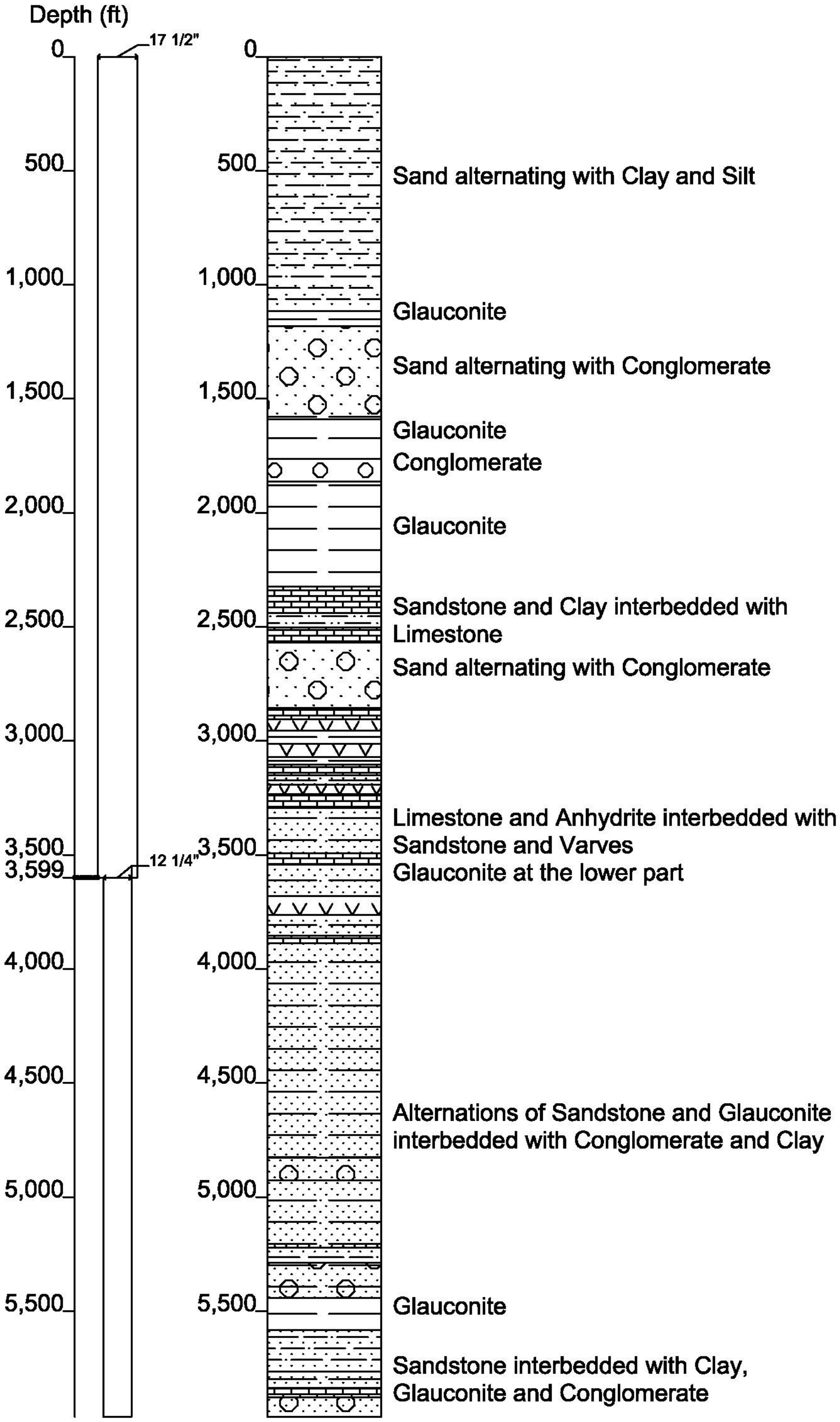

Figure 3.3: Well profile and the related lithostratigraphic column of Nestos 1 well

3.5.2 Stratigraphy of Nestos 2 Well

The laboratory analysis of the samples and the assessment of loggings conducted in the Nestos 2 well, were performed by BEICIP resulting in the following lithostratigraphic column (Adam, Maleas & Misirlis, 1978):

1) Quaternary 0-557 ft: Consists of loose sand and sand and gravel formations with plenty amount of shells up to 328 ft. It is mainly composed of poorly sorted fragments of quartz and metamorphic rocks, while the occurrence of interbeds of plastic clay and silt with some traces of lignite is also observed. The origin of these sedimentary formations is fluvial, which are alternated with saline and marine water deposits.
2) Pliocene 557-3,126 ft: The Pliocene formations are distinguished into two big series:

   557-2,542 ft: It is composed by deltaic, continental and shallow marine deposits. The upper part of this series (557-1,148 ft) consists of alternating layers of sand and plastic clay. Interbeds of loose sandstone and clay are observed in the lower part. Indications of thin marl and anhydrite layers are also rare.

   2,542-3,126 ft: This series is composed mainly of marine deposits, consisting of sandy and silty clay, more marly locally, with interbeds of loose sandstone. Thin layers of marl and anhydrite are rarely observed.
3) Miocene 3,126-12,979 ft: It is characterized by marine, lagoonal and less by lacustrine deposits.

   3,126-4,593 ft: The zone of evaporites is present, which consists of fine- to coarse-grained sandstone and conglomerate with alternations of clay, anhydrite and dolomitic limestone.

   4,593-4,954 ft: This section comprises the sedimentary zone of VARVES, alternating with marly and silty clay and fine-grained sandstone with concentrations of pyrite.

   4,954-8,055 ft: It is mainly composed of continental and lacustrine deposits. At this depth, the presence of VARVES alternated by fine-grained sandstone and microconglomerate is observed.

   8,055-9,186 ft: A series of mostly continental sediments are present. It is composed by interbeds of hard sandstone and conglomerate, formations of relatively low porosity and permeability, alternating with compacted marl and clay with concentrations of pyrite. At the lower part of this series, thin coal layers also appear.

9,186-12,979 ft: This zone is characterized by the occurrence of formations that came from continental and lacustrine deposits, containing organic matter with a high degree of coalification. The section between 9,842 and 11,482 ft has been proven as the most interesting due to hydrocarbon shows. In this zone, alternations of sandstone, where the porosity reduces downwards, along with layers of marl and marly clay are present. At depth greater than 11,647 ft, a continuous, compacted series of sandstone appear, containing interbeds of hard clay and coal. The largest coal layer is beyond the depth of 12,795 ft.

4) Metamorphic basement from 12,979 ft: Comprises the metamorphic Rhodope schist, mostly chlorite schist.

The following Figure 3.4 shows the upper section of the Nestos 2 well profile along with the lithostratigraphic column described above.

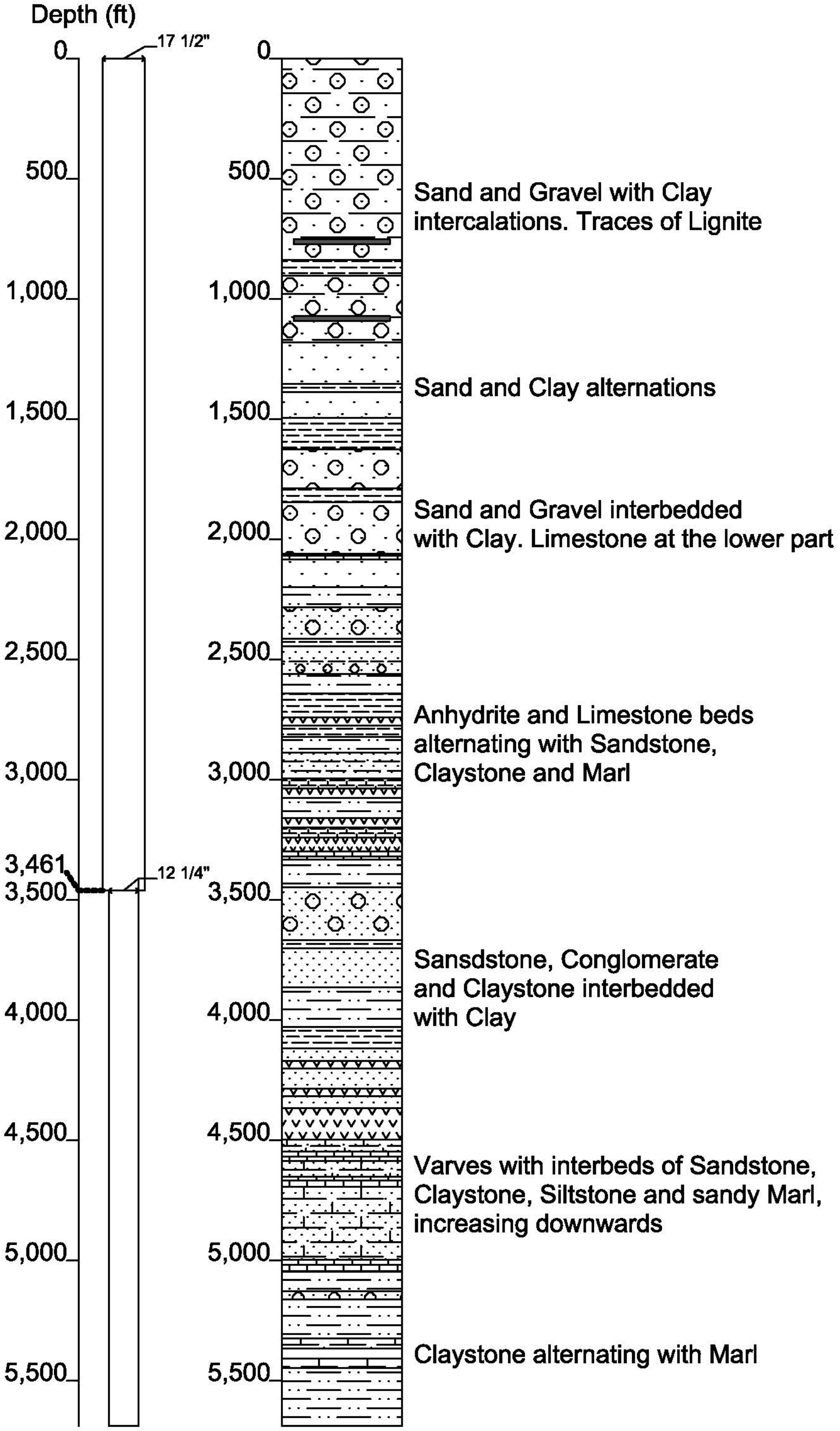

Figure 3.4: Well profile and the related lithostratigraphic column of Nestos 2 well

3.6 Geology-Stratigraphy of Komotini Region

The surrounding area of Xanthi-Komotini basin belongs geologically to the Rhodope Massif. The Komotini well is located in the tectonic graben of Komotini which constitutes the northeastern extension of Prinos-Nestos graben and is distinguished by the tectonic horst of Abdera. Before the implementation of drilling in the area of interest, the photogeological recognition, as well as an extended geological cartography, had been conducted. The total coverage of the area is 13,993 ft^2, while the Vistonida Lake, which is in communication with the sea, is also situated in the center.

The central part of Xanthi-Komotini basin, near the Vistonida Lake, is occupied by Quaternary deposits that contain clay and sandy clay of red color. The South part of the basin comprises sand and gravel of fluvial origin, while thick layers of scree are extended along the limits of the Northern part. In addition, the Tertiary deposits cover a significant area of Xanthi-Komotini basin and are mostly present in the southwestern part either as Neogene deposits containing conglomerate, marl, and sandstone or as Paleogene deposits (Oligocene-Eocene) comprising of sandstone, marl, conglomerate, claystone and clayey and marly schist. The total thickness of the deposits exceeds the 6,560 ft.

The metamorphic basement of Rhodope schist appears in the periphery of the Xanthi-Komotini basin and towards its Northwestern part and consists of marble, gneiss, and schist. Finally, the area hosts formations such as andesite and granite.

3.6.1 Stratigraphy of Komotini Well

The laboratory analysis of cuttings and core samples as well as the assessment of loggings conducted in the Komotini well were performed by Institute of Geology and Mineral Exploration (I.G.M.E.) resulting in the following lithostratigraphic column (Adam, Maleas & Misirlis, 1978):

1) Quaternary 0-997 ft: Consists of loose sand and sand and gravel formations which present to be slightly compacted at the lower part. These formations are mainly composed of poorly sorted fragments of metamorphic rocks and quartz. Plastic clay is also alternated through these formations. This geological setting comes from fluvial and saline water deposits.

2) Mio-Pliocene 997-3,871 ft: The Mio-Pliocene formations are characterized by alternations of plastic clay and slightly compacted sandstone, with interbeds of conglomerate and clay. Often, beds of limestone with a thickness of approximately 3.28 ft occur.
3) Eocene-Oligocene 3,871-5,679 ft:

   3,871-4,265 ft: Consists of plastic clay interbedded with well-compacted sandstone and alternations of microconglomerate with compacted clay.

   4,265-4,593 ft: The sandstone is the dominant formation, which is alternated with clay or marl.

   4,593-4,921 ft: The same sandstone, as in the above section, is present, which is now more microconglomeratic and often argillaceous. Interbeds of limestone also occur through the sandstone.

   4,921-5,679 ft: This zone is predominantly characterized by alternations of sandstone with plastic clay and conglomerate. Occasionally, there are lignite interbeds.
4) Metamorphic basement from 5,679 ft: Consists of the metamorphic Rhodope schist, mainly argillaceous and sericite schist.

The whole well profile and the related lithostratigraphic column of the Komotini well are presented in the following Figure 3.5, since it is the only well where the full set of drilling data was available, until the depth of 5,623 ft where the basement of argillaceous schist lies.

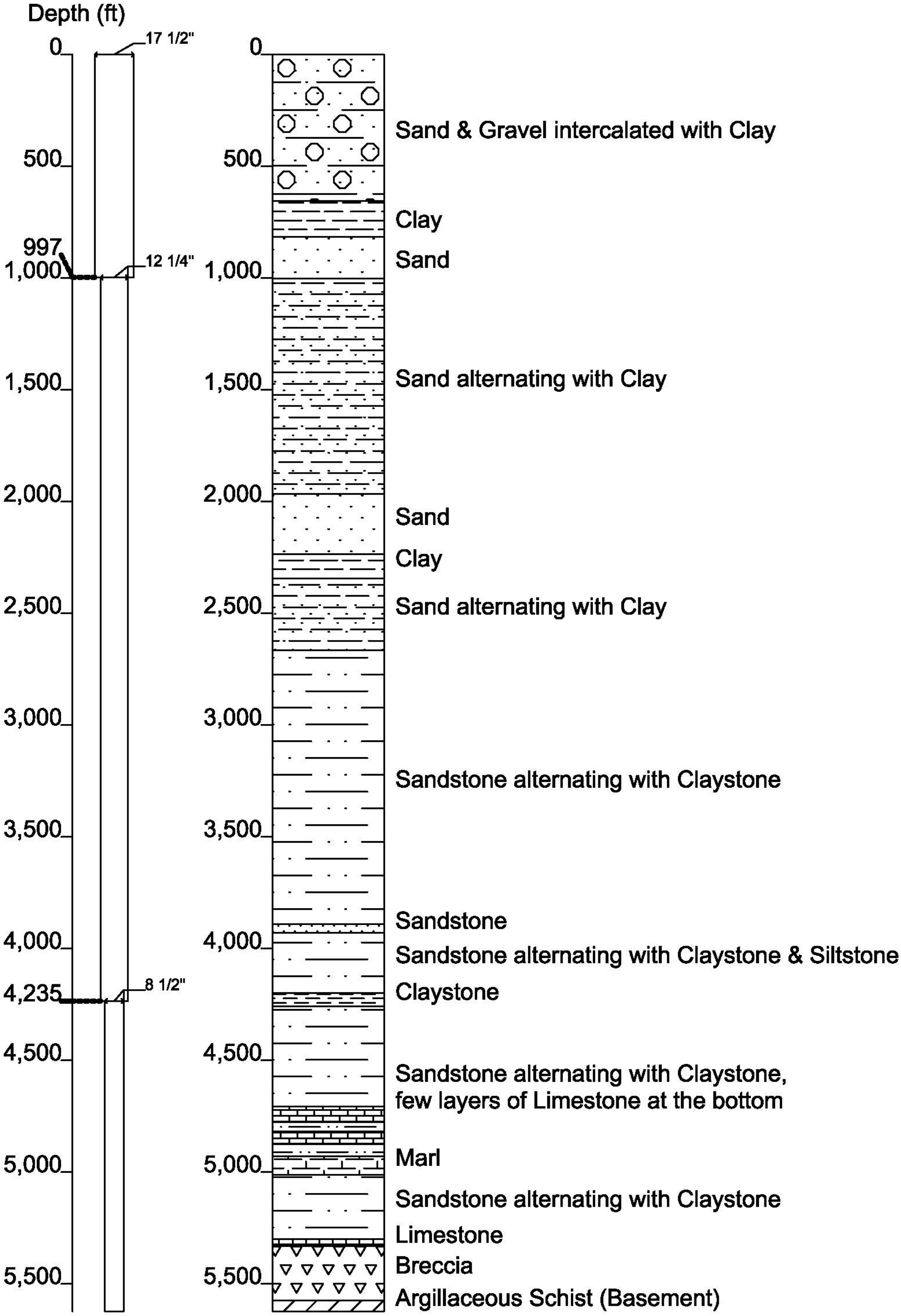

Figure 3.5: Well profile and the related lithostratigraphic column of Komotini well

4. Specific Energy

Specific energy (E_S) or mechanical specific energy (MSE) is defined as the energy required to excavate a unit volume of rock and may have any set of consistent units (Teale, 1965). The concept of specific energy was introduced by Teale (1965) as a convenient tool and practical method of assessing the rock drillability.

There are two different definitions regarding the specific energy (Rabia, 1982):

1. The energy required to remove a unit volume of rock.
2. The energy required to create a new surface area.

In this study, only the specific energy related to the energy required to remove a unit volume of rock will be evaluated for the three wells Komotini, Nestos 1 and Nestos 2 drilled in 1977.

Theoretically, the bit requires a certain minimum quantity of energy to be provided in order to break a specific volume of rock. The minimum value of specific energy will depend entirely on the nature of the rock and is suggested as a fundamental rock property (Teale, 1965). Unfortunately, there are losses during energy transfer from the power system to the bit due to friction, the undesirable further breaking of the rock already excavated into smaller fragments than necessary, etc. Further breaking of the cuttings produced by the bit into smaller fragments may have a disproportionate effect on the energy needed to excavate a given volume of rock. Not only the bottom hole fills with more fragments which block the bit face area, but field and laboratory measurements have shown that the specific energy increases as the fragment size is reduced. This fact implies that optimum drilling and hydraulic conditions should be sought, where the weight-on-bit, the applied torque, the specific gravity and the quantity of the drilling fluid being injected by the jet nozzles are suitable for carrying the cuttings up to the surface.

Several measurements have also indicated that the value of specific energy is systematically reduced approaching to a minimum quantity as the fragment size is continuously increased (Walker & Shaw, 1954). That constant minimum quantity of specific energy defines the unconfined compressive strength (UCS) of the excavated formation, irrespective to the drilling conditions (Teale, 1965). Hence, mechanical efficiency is a maximum when the specific energy is a minimum.

4.1 Mathematical Expression of the Specific Energy

The specific energy equation can be derived by considering the mechanical energy input expended at the bit in one minute. Thus:

$$E = W \times 2\pi R \times N \quad (in - lb) \tag{4.1}$$

where:

W: weight on bit (lb)

N: rotary speed (rpm)

R: radius of the bit (in)

The volume of rock being excavated by the bit in one minute is

$$V = (\pi R^2) \times R_p \quad (in^3) \tag{4.2}$$

where:

R_p: rate of penetration (ft/hr)

Hence, dividing equation (4.1) by equation (4.2) results in the specific energy in terms of volume, as:

$$E_s = \frac{E}{V} = \frac{W \times 2\pi R \times N}{\pi R^2 \times R_p} \quad \frac{lb \times in \times \frac{1}{min}}{in^2 \times \frac{ft}{hr} \times \frac{hr}{60\ min} \times \frac{12\ in}{ft}} \rightarrow$$

$$E_s = 10 \frac{WN}{R \times R_p} \quad (\frac{lb \times in}{in^3}) \tag{4.3}$$

Replacing the radius of the bit R by D/2, where D is the borehole diameter, the equation (4.3) becomes:

$$E_s = 20\frac{WN}{D \times R_p} \quad \left(\frac{lb \times in}{in^3}\right) \tag{4.4}$$

In metric units, the equation (4.4) becomes:

$$E_s = 2.35\frac{WN}{D \times R_p} \quad \left(\frac{MJ}{m^3}\right) \tag{4.5}$$

Since the penetration rate (R_p) is defined as the drilled footage (F) divided by the rotating time (t_r), the equation (4.5) becomes:

$$E_s = 20\frac{WN}{D \times F}t_r \tag{4.6}$$

Assuming optimum hydraulics and usage of a given bit for drilling a formation of constant strength, the specific energy can be considered constant under any combination of the weight-on-bit (W) and rotational speed (N) values (Rabia, 1985). That is because changes in the product between these drilling parameters usually result in increased penetration rate (R_p) values. A particular bit type working with variable weight-on-bit and rotational speed values would yield an infinite number of penetration rate values. Thus, specific energy which is less sensitive to changes of weight-on-bit and rotational speed constitutes a direct measure of bit performance in a particular formation as well as a practical tool for bit selection in comparison with the penetration rate.

4.2 Specific Energy as a Drilling Property

The specific energy units are actually identical to the stress or pressure units (since in-lb/in^3 is equivalent to lb/in^2 or psi). Despite the Teal's suggestion about the relation between the specific energy and the unconfined compressive strength (UCS) of the rock excavated, there is a different approach given by the following equation (Mellor, 1972):

$$E_s \cong 10^{-3} \times C_o \tag{4.7}$$

where:

C_o: Unconfined compressive strength (psi)

It should be noted that, for a particular rock type, the equation (4.7) yields too small values of specific energy in comparison with the Teale's minimum specific energy.

The fact that in many cases the specific energy is related to unconfined compressive strength has been overturned by various researchers. In the past, many attempts have been made in order to correlate or replace the specific energy with the unconfined compressive strength (UCS) or confined compressive strength (CCS) of the rock. Black et al. (2008) found that specific energy spent was much higher than the confined compressive strength (CCS) of the rock, confirming that other parameters contribute to the specific energy value. The ratio between specific energy and unconfined compressive strength for a PDC bit and a three-cone bit (WC) for a variety of rocks (schist, soft and hard sandstone, limestone and siltstone), did not remain constant and fluctuated between 0.75 and 2.90, demonstrating that only the parameter 'UCS' is not enough (Ersoy, 2003).

Hence, the specific energy is not a fundamental intrinsic property of rock but is highly dependent on the type and design features of the bit. This property affords an accurate way of selecting the appropriate bit type: the bit that yields the lowest value of specific energy in a given section is the most economical (Rabia, 1982). It is also known that for a certain bit type the value of specific energy, thus the bit performance, is controlled by the hardness of the formation being drilled (Rabia, 1982).

4.3 Parameters Affecting Rock Drillability

In general, there are several parameters that actually define the well design and affect the penetration rate which can be categorized into two major groups (Kelessidis, 2010):

- Drilling parameters, such as weight applied on bit, rotational speed, specific gravity and viscosity of the drilling fluid, bit type, mud flow rate, number and size of jet nozzles.
- Formation parameters, such as rock properties (hardness, abrasiveness, mineralogy) and well environment properties (in-situ stresses, compaction of rocks, formation pore pressure).

4.3.1 Weight on Bit

Rotary drilling depends on the weight applied on bit and the rotational speed so that with the proper combination rock breaks and the produced cuttings are carried by the drilling fluid from the bottom hole up to the surface. There are some rules of thumbs in the determination of the required weight on bit and the rotational speed of the drill string. Several researchers indicated that as the weight on bit increases the penetration rate also increases as well, assuming that the drilling fluid sufficiently cleans up the bottom hole area from cuttings. The weight applied on the bit is provided by the drill collars that consist bottom hole assembly (BHA). In Figure 4.1, control of the weight applied on bit by the driller is presented (Moore, 1986).

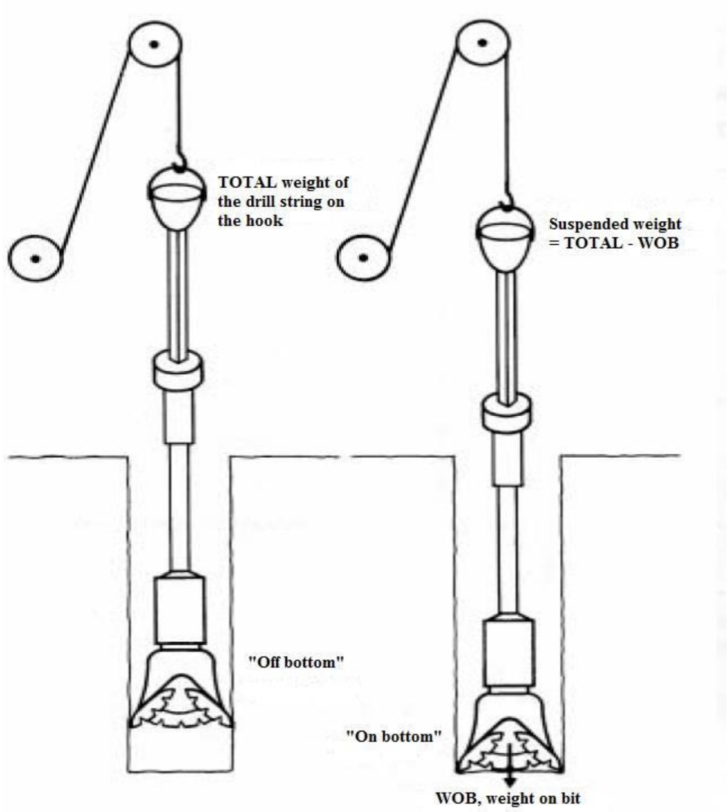

Figure 4.1: Control of the applied weight on bit (Moore, 1986).

A typical curve of how the weight on bit (WOB) influences the penetration rate is shown in Figure 4.2, considering all the other drilling parameters to be constant. In order to notice an increase in penetration speed, a threshold value of WOB, depending on rock type and bit type used, should be exceeded. Afterward, the penetration rate is increasing almost linearly by increasing the WOB (section ad). Again there is another threshold of WOB (point d) where further increase leads to a reduction of penetration rate. This reduction is due to insufficient cleaning of the cuttings which are produced at a higher rate or to the completely penetrated bit teeth into the rock formation (Kelessidis, 2012).

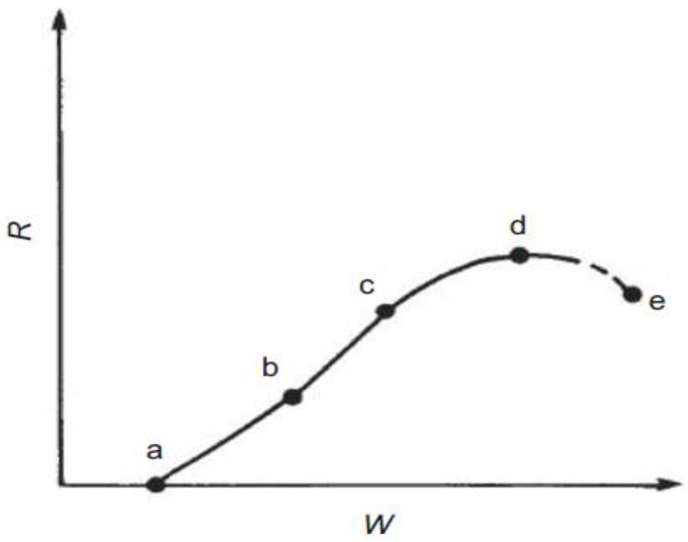

Figure 4.2: Influence of the weight on bit (W) on the penetration rate (R) (Bourgoyne et al, 1991).

4.3.2 Rotary Speed

The rotary speed is also directly linked to the weight applied on bit. Both parameters cannot be continuously increased without causing problems on the drill string and the bit. Figure 4.3 shows a typical curve of the penetration rate (R) in relation to the rotary speed (N).

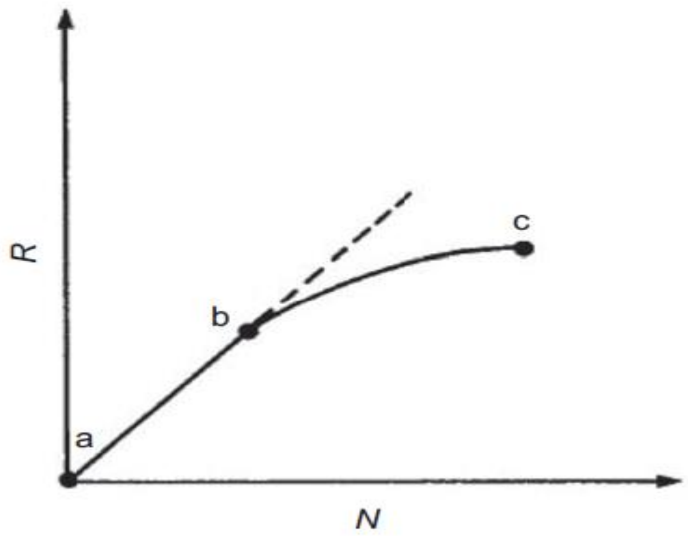

Figure 4.3: Influence of the rotary speed (N) on the penetration rate (R) (Bourgoyne et al., 1991).

The penetration rate usually increases linearly with the increase of the rotary speed, for low values of rotary speed (section ab). In higher rotary speed values the increase in penetration rate seems to be reduced. This reduction is also due to the insufficient cuttings removal from the bit surface (Kelessidis, 2012). Many studies have shown that penetration rate increases proportionally to the rotary speed for soft rocks and not for hard rocks. In hard rocks, the penetration rate does not further increase when an optimum rotary speed is reached. The rotary speed could be restricted by (Stamataki, 2003):

- Drill string shocks
- Bit type
- Friction resistance in directional wells

4.3.3 Mud Flow Rate

As mentioned above, the penetration rate increases by increasing the weight applied on bit under constant mud flow rate until a weight limit is reached. Above this weight limit, a reduction of penetration rate might be observed with the further increase of the weight on bit. Beyond this point which is known as “balling up point” the mud flow rate is no longer able to clean the bottom hole from the produced cuttings. The balling up point could be extended by increasing the mud flow rate in order to have better bottom hole cleaning. Hence, the mud flow rate directly affects the penetration rate. The computation of the mud flow rate is based on slip velocity of generated cuttings in the annular space. However, the determination of the slip velocity is complicated due to its dependence on many parameters, such as (Stamataki, 2003):

- The type, shape and equivalent diameter of cuttings
- The state of flow (laminar or turbulent)
- The mud rheological parameters

As a rule of thumb, the suggested ranges of annular velocity depending on formation hardness are 98 through 131 ft/min and 82 through 98 ft/min for soft and hard formations, respectively. In practice, annular velocities between 65 and 82 ft/min have been used with satisfactory results in essential removal of cuttings for proper bottom hole cleaning.

4.3.4 Jet nozzles

Jet nozzles contribute in bottom hole cleaning, inducing sufficient vortex of cuttings for keeping the bit teeth clean. The reduction of the size of openings, which assist the drilling mud circulation, is succeeded by fitting jet nozzles of different sizes. As a result, an increase in the jet (or mud) velocity will occur, increasing the force of the mud impinges the rock beneath the bit for fracturing the rock, and thus, the mud flow rate will be increased (Koulidis, 2014).

The minimum jet velocity is approximately considered equal to 262 ft/sec, while is generally fluctuated between 262 and 492 ft/sec (Stamataki, 2003).

4.3.5 Mud density

The increase of the mud density causes an increase of the mud hydrostatic pressure, and therefore, the differential pressure (the difference between the hydrostatic pressure in the bottom hole and formation pore pressure) will be increased. As the differential pressure becomes greater, the increase of the mud density causes rapid reduction in the penetration rate (Stamataki, 2003).

The ideal mud density is equal to the water density for optimum penetration rate and to reduce the probability of fracturing the rock. In practice, the mud density could be twice the water density, especially in wells with a high probability of facing zones of abnormal pressures. Nevertheless, the mud pressure must be greater than the formation pore pressure throughout the whole well in order to avoid an influx of pore fluids in the wellbore. In addition, the mud pressure needs to be smaller than the formation fracture pressure for preventing the drilling mud from entering into the surrounding formations. The formation pore pressures for a certain region are referred to as pressure gradients, which are basically an expression of relating the value of formation pore pressure per unit depth of interest (Koulidis, 2014).

4.4 Drillability

The drillability (K) is a formation property that describes how easy is for the formation to be drilled by a specific type of bit. From the above stated for the specific energy, it is obvious that the drillability is inversely proportional to the specific energy. Thus, the less specific energy required by a bit for drilling a formation the more drillability is achieved by the bit in this formation (the more drillable is the formation by the specific bit). This relation between these two parameters can be quantitatively expressed as follows (Perakis, 2006):

$$K \propto \frac{1}{E_s} \tag{4.8}$$

The drillability (K) of a formation can be generally computed by the following empirical equation:

$$K = \frac{R_p}{\left(\frac{W}{D}\right) \times N} = \frac{D \times R_p}{WN} \tag{4.9}$$

where:

R_p: penetration rate (ft/hr)

W: weight on bit (lb)

D: bit diameter (in)

N: rotary speed (rev./min−rpm)

The correlation between the equations (4.8) and (4.9) with the equation (4.4) results in the following equation:

$$K = \frac{20}{E_s} \tag{4.10}$$

In this study, the empirical equation (4.10) is used for the evaluation of the drillability of formations, although the determination of the drillability is only based on the parameters relating to the bit (weight on bit, bit diameter, rotary speed). This fact is acceptable because of the penetration rate (R_p) is greatly affected by the energy transfer in the bit-formation system, and thus, by the type, the composition and the properties of the formation being drilled. Furthermore, given that the wells have been drilled by three-cone bits and assuming that the most appropriate bit (teeth pattern, bearing types) for each formation was chosen, then the drillability is mostly influenced by the formation properties rather than the drilling parameters (Perakis, 2006).

4.4.1 Specific energy and Drillability for Nestos 1 well

The computation of specific energy (E_S) and drillability (K) for Nestos 1 well are based on the equations (4.4) and (4.10), respectively. The computed values for both specific energy (E_S) and drillability (K) are presented in the following Table 4.1.

Table 4.1: Computation of specific energy (E_S) and drillability (K) for Nestos 1 well

# Interval	Depth	Penetration Rate-R_p	Bit Diameter-D	Weight on Bit-W	Rotary Speed-N	E_s	K
	ft	ft/hr	in	$x10^3$ lb	rpm	$x10^3$ in·lb/in^3	$x10^{-4}$ in^3/in·lb
1	1,079	34.8	17½	24	100	80	2.513
2	2,273	47.0	17½	40	100	96	2.073
3	2,395	35.2	17½	40	120	155	1.293
4	2,700	21.1	17½	40	130	279	0.716
5	2,897	12.7	17½	31	120	332	0.602
6	2,998	7.8	17½	29	100	420	0.476
7	3,225	8.1	17½	29	100	405	0.494
8	3,599	12.3	17½	25	105	247	0.810
9	4,028	41.5	12¼	33	120	156	1.282
10	4,717	32.8	12¼	31	110	169	1.184
11	5,111	24.3	12¼	26	110	196	1.023
12	5,413	17.3	12¼	24	95	217	0.922
13	5,685	14.8	12¼	26	100	292	0.685
14	5,964	17.4	12¼	26	90	224	0.894

Based on Table 4.1, the semi-logarithmic plot of drillability over depth is presented in the following Figure 4.4a.

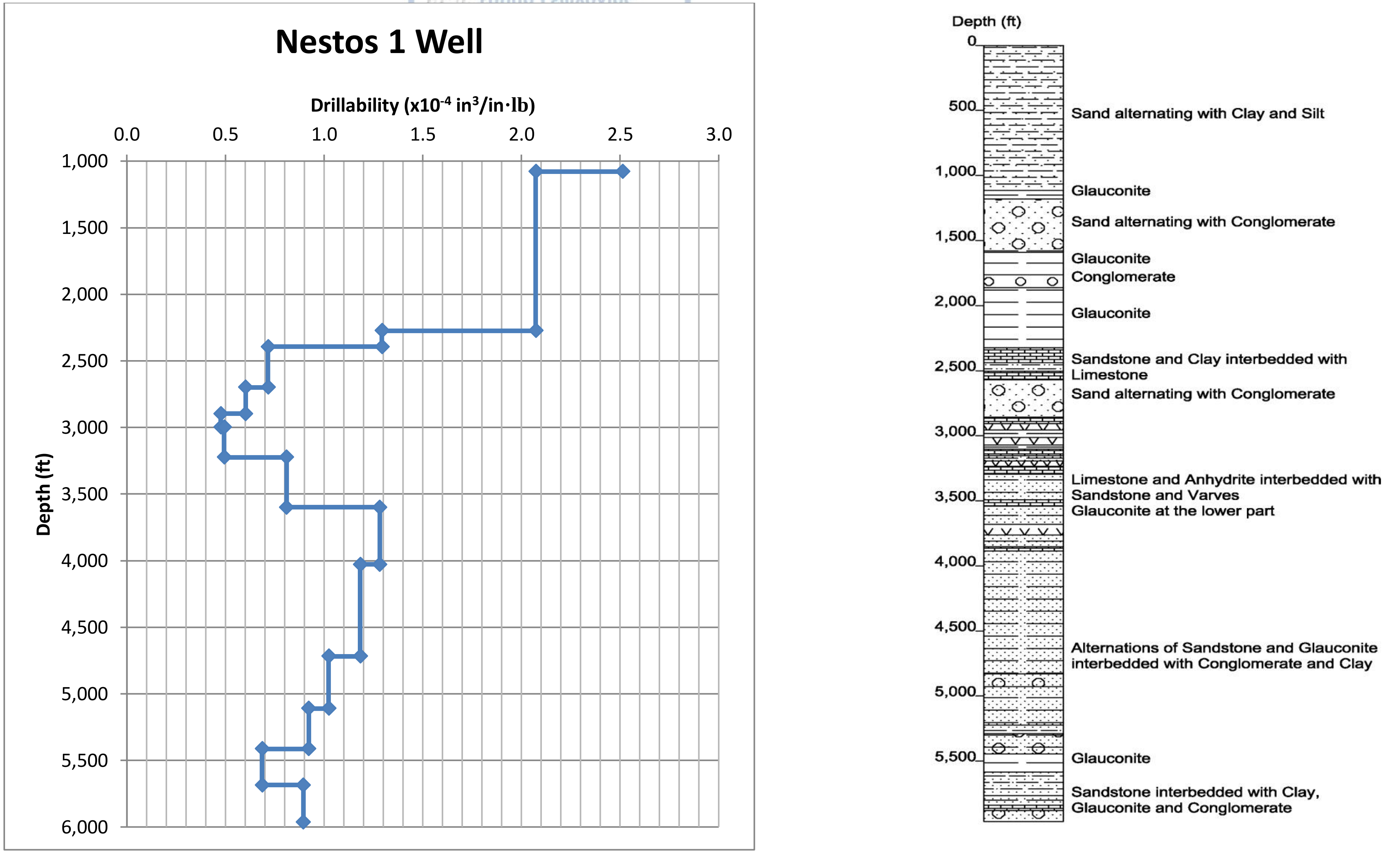

(a) **(b)**

Figure 4.4: (a) Diagram of Drillability vs. Depth; (b) Lithostratigraphic column for Nestos 1 well

The following observations regarding the variation of drillability (Figure 4.4a) are based on the assumption that mud density is constant throughout the total length of the Nestos 1 well and in accordance to the related lithostratigraphic column (Figure 4.4b). These observations are analyzed below:

From the surface up to the depth of 2,998 ft, the drillability systematically decreases over depth, owing to the higher compaction of the formations in greater depths. The upper part of this interval consists of soft formations, including alternations of sand with clay and silt, glauconite beds, etc., whereas the lower part mainly comprises medium hard formations, such as sandstone and clay interbedded with limestone. All these formations were drilled by various combinations of drilling parameters, where the applied weight on bit and rotary speed ranged from 24,000 to 40,000 lb and from 100 to 130 rpm, respectively. Two drill bit types (RS and RMTA) with a diameter of 17½" were used in this interval. Moreover, since the values of weight applied on bit and rotary speed constantly increased up to the depth of 2,700 ft, drillability was increased further.

Below the depth of 2,998 ft, the 17½" RMTA drill bit was replaced by a drill bit of RS type of the same size which operated with the same applied weight on bit (29,000 lb) and rotary speed (100 rpm), as in the last section of the previous interval (2,897-2,998 ft), causing a further decrease in drillability in the interval from 2,998 to 3,225 ft. This interval is characterized by high heterogeneity, due to the interbeds of limestone, anhydrite, and glauconite with sandstone and varves. The next interval, from 3,225 to 3,599, where formation presents the same heterogeneity as before, was drilled by the same type of bit (17½" RS drill bit) with less weight applied on bit (25,000 lb) and a slightly higher rotary speed (105 rpm). This resulted in an increase of the drillability.

Below 3,599 ft, the drilling process continued with a smaller drill bit (12¼"), for the depths below the 3,599 ft. The reduction of drill bit size from 17½" to 12¼" as well as the change of drill bit type from RS to RM, led to a significant further increase of drillability, in the interval between 3,599 and 4,028 ft. In this interval, the formation presents the same heterogeneity as before with alternations of sandstone, glauconite, and varves interbedded with limestone and anhydrite.

Below 4,028 ft, drilling was conducted using only 12¼" drill bits of RS type. In this interval, the weight applied on bit varied from 24,000 to 31,000 lb and the rotary speed ranged between 95 and 110 rpm, as well. Nevertheless, it is obvious that from this depth forward the drillability constantly declines up to 5,685 ft. The formation in this interval also presents heterogeneity, consisting mainly of alternations of sandstone and glauconite interbedded with conglomerate and clay. Therefore, the drillability decrease can be easily attributed to the higher compaction of the formation at higher depths.

Lastly, in the last interval, below 5,685 ft up to 5,694 ft, even though there is no significant change of the formations (sandstone interbedded with clay, glauconite, and conglomerate), there is a slight increase in drillability. This can possibly be associated with a slight decrease in rotary speed to 90 rpm.

4.4.2 Specific energy and drillability for Nestos 2 well

According to the equations (4.4) and (4.10), the specific energy (E_S) and drillability (K) for Nestos 2 well were also computed (Table 4.2).

Table 4.2: Computation of specific energy (E_S) and drillability (K) for Nestos 2 well

# Interval	Depth	Penetration Rate-R_p	Bit Diameter-D	Weight on Bit-W	Rotary Speed-N	E_S	K
	ft	ft/hr	in	x10^3 lb	rpm	x10^3 in·lb/in^3	x10^{-4} in^3/in·lb
1	515	36.8	17½	14.3	100	45	4.493
1a	1,854	86.6	17½	22.0	120	35	5.731
2	2,165	14.1	17½	33.1	130	349	0.573
3	3,140	32.2	17½	39.7	140	197	1.013
4	3,222	23.8	17½	39.7	130	248	0.806
6	3,415	17.1	17½	39.7	130	344	0.581
7	3,632	42.0	12¼	19.8	130	100	1.997
8	4,121	28.3	12¼	33.1	130	248	0.805
9	4,386	18.4	12¼	33.1	130	382	0.524
10	4,564	14.8	12¼	33.1	130	475	0.421
11	4,816	16.8	12¼	35.3	140	479	0.418
12	5,305	27.2	12¼	33.1	140	278	0.719
13	5,643	19.5	12¼	24.3	140	284	0.705

The plot in Figure 4.5a presents the variation of drillability over depth, based on the data of Table 4.2.

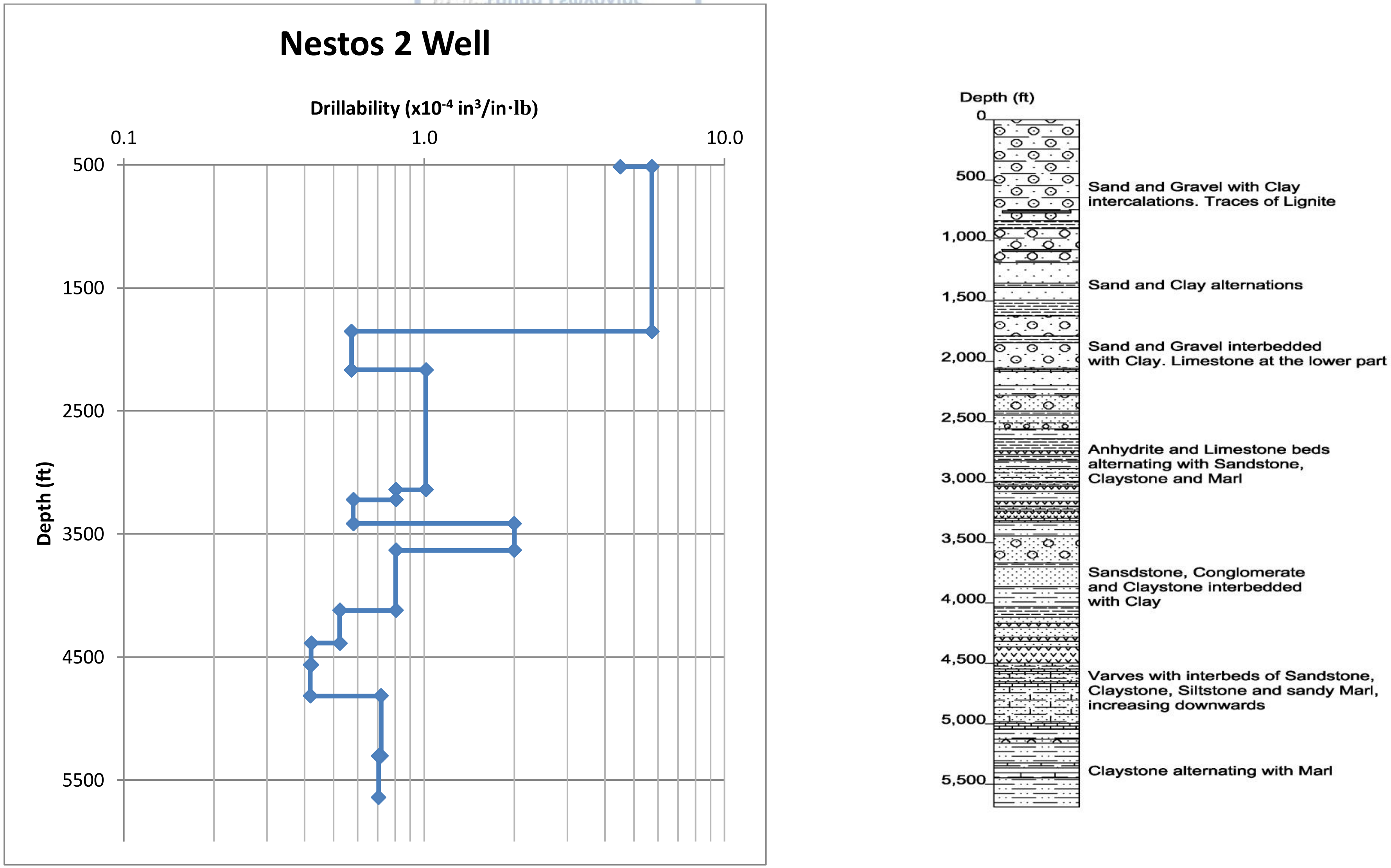

(a) (b)

Figure 4.5: (a) Diagram of Drillability vs. Depth; (b) Lithostratigraphic column for Nestos 2 well

Since the density of drilling mud used in the drilling of Nestos 2 well did not significantly change through depth, it is assumed to remain constant. Hence, on the basis of the drilling parameters and the lithology of the formation being drilled (Figure 4.5b), the variations of drillability over depth (Figure 4.5a), are evaluated as follows:

From the surface up to 3,415 ft, drilling was conducted by a drill bit of RS type and of 17½" in diameter. There is no significant change in the lithology of the formations drilled in this interval, consisting of sand and gravel with clay intercalations, in the upper part (0-515 ft) and alternations of sand and clay, in the lower part of the interval (515-1,854 ft). However, there is a slight increase of drillability in the lower part, even though both the weight applied on bit and rotary speed were increased from 14,300 to 22,000 lb and from 100 to 120 rpm, respectively.

Subsequently, the compaction of sand and gravel over depth, the thin bed of limestone as well as an increase of the weight applied on bit at 33,100 lb and the rotary speed at 130 rpm, contribute in a significant reduction of drillability, in the interval between 1,854 and 2,165 ft. Although the weight applied on bit and the rotary speed further increased below 2,165 ft at 39,700 lb and 140 rpm, respectively, drillability increased as well in this interval up to 3,140 ft.

The drillability constantly decreases further in the interval from 3,140 to 3,415 ft, while drilling with constant weight on bit at 39,700 lb, as in the previous interval, and lower rotary speed at 130 rpm. This is due to the higher compaction of the anhydrite and limestone beds alternating with sandstone, claystone, and marl.

Below the depth of 3,415 ft, drilling was performed using two types of drill bits (RS and RM), of a smaller size (12¼"). As a result, drillability significantly increases at first, in the interval between 3,415 and 3,632 ft, due to the lower volume of rock per feet of penetration. From this depth and further down drillability presents steadily lower values due to the higher compaction of drilled formations (sandstone and claystone interbedded with clay and anhydrite) over depth. Even though, there was a change in the drill bit type used, from RS to RM, in the interval between 4,386 and 4,564 ft, this did not improve drillability because of the heterogeneity of the formations drilled (alternations of soft with medium hard formations, such as varves with interbeds of sandstone, claystone, siltstone, and sandy marl).

The interval below the depth of 4,564 ft was drilled under constant rotary speed at 140 rpm while the weight applied on bit decreased downwards ranging from 35,300 to 24,300 lb. In this interval up to 4,816 ft, drillability did not change much, since the formation remained heterogeneous consisting of varves interbedded with sandstone, claystone, siltstone and sandy marl, directly affect the drillability which remains approximately constant.

Finally, in the last interval, below the depth of 4,816 ft, there is an increase in drillability. Since in this interval formation presents the same heterogeneity as above, mainly consisting of sandstone interbedded with sandy marl and alternations of claystone with marl, the increase of drillability can be attributed to the reduction of the weight applied on bit from 35,300 lb to 33,100 lb.

4.4.3 Specific energy and drillability for Komotini well

Table 4.3 presents the values of specific energy (E_S) and drillability (K) for Komotini well computed by equations (4.4) and (4.10), respectively.

Table 4.3: Computation of specific energy (E_S) and drillability (K) for Komotini well

# Interval	Depth	Penetration Rate- R_p	Bit Diameter- D	Weight on Bit- W	Rotary Speed- N	E_s	K
	ft	ft/hr	in	x10^3 lb	rpm	x10^3 in·lb/in^3	x10^{-4} in^3/in·lb
1	997	52.1	17½	9	80	15	12.919
2	1,591	44.2	12¼	13	120	59	3.407
3	2,041	28.1	12¼	15	120	108	1.858
4	2,628	36.0	12¼	13	110	66	3.033
5	3,150	34.4	12¼	17	110	86	2.319
6	3,432	22.9	12¼	20	100	141	1.416
7	3,960	24.6	12¼	22	120	175	1.140
8	4,222	21.1	12¼	25	120	236	0.849
8a	4,236	4.4	12¼	29	120	1284	0.156
9	4,239	2.9	8½	20	100	1636	0.122
10	4,432	17.4	8½	30	120	484	0.413
11	4,882	15.8	8½	24	85	307	0.651
12	4,921	3.9	8½	26	75	1204	0.166
13	4,944	3.7	8½	30	65	1219	0.164
14	5,056	18.6	8½	30	100	377	0.531
14a	5,138	11.2	8½	29	100	600	0.333
12a	5,210	6.0	8½	35	75	1035	0.193
15	5,335	15.6	8½	29	120	519	0.385
13a	5,623	10.5	8½	29	80	513	0.390

According to the data of Table 4.3, a semi-logarithmic plot demonstrating the changes of drillability over depth for Komotini well is presented in Figure 4.6a.

It should be noticed that an evaluation of the drillability variations is based on the assumption of constant mud density throughout the drilling process for Komotini well. By juxtaposing the diagram of drillability over depth (Figure 4.6a) along with the related lithostratigraphic column (Figure 4.6b), valuable information emerge about the effect of drilling parameters and the formation properties on drillability.

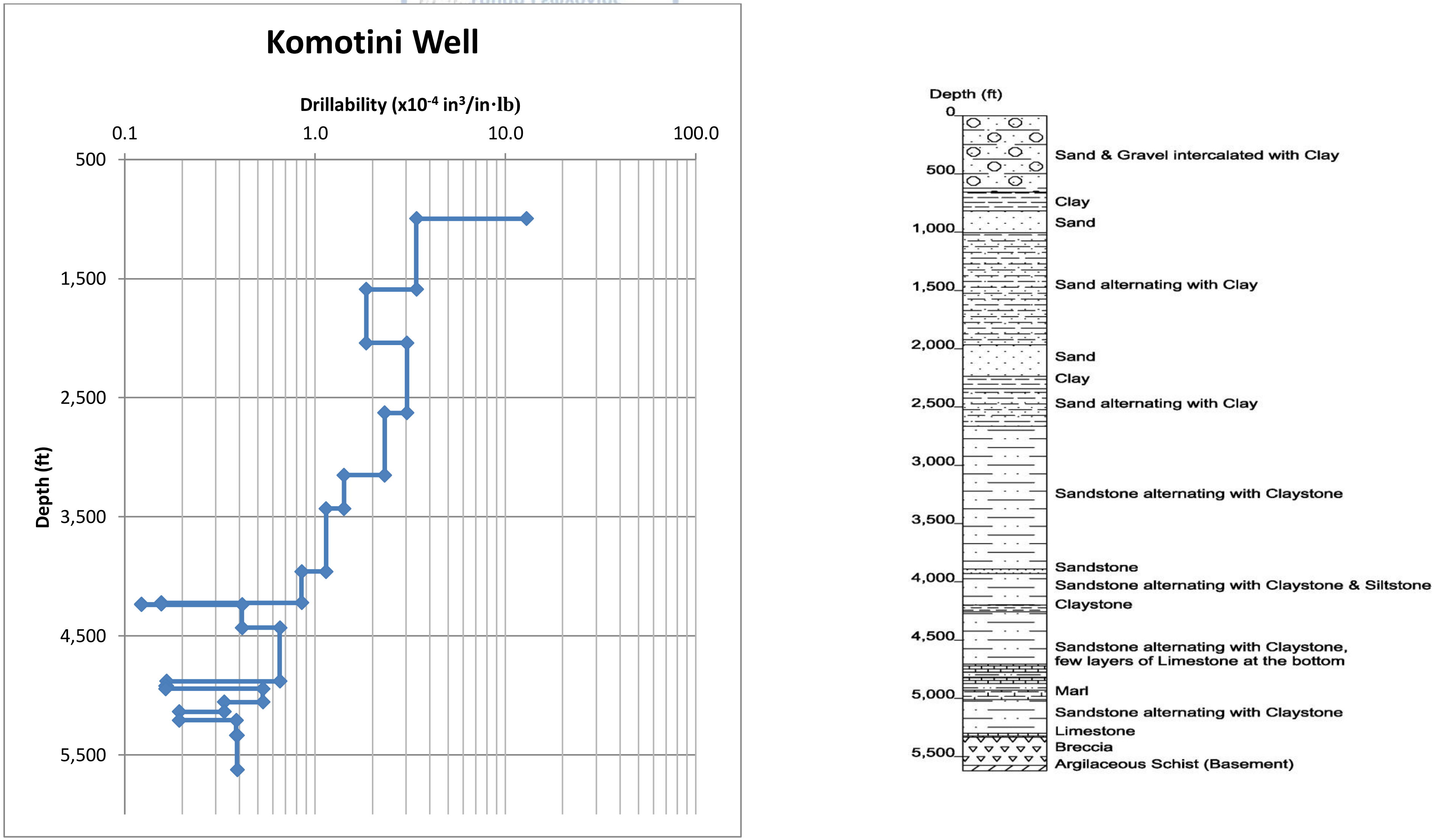

(a) (b)

Figure 4.6: (a) Diagram of Drillability vs. Depth; (b) Lithostratigraphic column for Komotini well

Based on the Figure 4.6, it is obvious that drillability generally declines up to the final depth of the well (5,623 ft), due to the higher compaction of the formations over depth.

In the interval from the surface up to 2,041 ft, drilling was performed by using the same type drill bit (RS) with two different drill bit sizes of 17½" and 12¼" in diameter. Normally, the reduction of the drill bit size from 17½" into 12¼" could cause an increase in drillability, this did not happen. The increase of the weight applied on bit from 9,000 lb to 13,000 lb and of the rotary speed form 80 rpm to 120 rpm contributed to the further decrease of drillability, in the interval between 997 and 1,591 ft. For the same reason, the increase of weight applied on bit at 15,000 lb slightly affects the further decrease in drillability, in the interval from 1,591 to 2,041 ft.

Between 2,041 and 3,432 ft, the drill bit of RS type was replaced by drill bit of RM type with the same diameter of 12¼" causing an increase of drillability in the interval from 2,041 to 2,628 ft. In this interval, the decrease in the weight applied on bit and in the rotary speed may have contributed to the increase of drillability as well. Then, in the interval between 2,628 and 3,432 ft, drilling was conducted by a combination of weight applied on bit and rotary speed ranging from 17,000 to 20,000 lb and from 100 to 110 rpm, respectively. In this interval, drillability constantly decreases because of the compaction of the sandstone alternating with claystone at higher depths.

The first 804 ft of the next interval (3,432 to 4,236 ft) were drilled by changing the drill bit of RM type with X3A (manufactured by Hughes). Regardless of this change, as the weight applied on bit was increasing downwards, a continuous decrease in drillability is observed.

Below the depth of 4,236 ft, drilling was conducted using several drill bits manufactured by Hughes, all with the same size of 8½" in diameter. Normally, the decrease of the drill bit size may contribute to an increase of the drillability, due to the lower volume of formation to be excavated per foot of penetration.

The interval from 4,236 to 4,432 ft was drilled by the X1G drill bit. Although there was a reduction in both the weight applied on bit at 20,000 lb and the rotary speed at 100 rpm, drillability decreased in the next three feet consisting of claystone. In the interval between 4,239 and 4,432 ft, which consists mainly of sandstone alternating with claystone and siltstone, drillability increased again but to a lower value than the one achieved above 4,236 ft.

In the interval from 4,432 to 4,921 ft, consisting of alternations of sandstone and claystone with few layers of limestone at the bottom, the X1G drill bit was replaced by a J22 drill bit. The change in drill bit type in association with the decrease in both WOB and rotary speed contributed to an increase of drillability in the interval between 4,432 and 4,882 ft. Then, in the following interval from 4,882 to 4,921 ft where the weight applied on bit and rotary speed are further decreased, drillability also decreases due to the higher compaction of the formations.

The replacement of the J22 drill bit type to J44 for drilling the next 23 feet, in the interval between 4,921 and 4,944 ft, have led the drillability to remain unchanged. According to Table 3.2, the drill bit of J44 type is suitable for drilling harder formations than J22, thus compensating the higher compaction of deeper formations (sandstone alternating with claystone, marl), since the input energy provided by the drilling parameters remained constant, as in the previous interval.

Between 4,944 and 5,056 ft, drilling was conducted using an X1G drill bit which has replaced the J44 drill bit. The WOB remained constant at 30,000 lb, as in the previous interval, and the rotary speed was increased to 100 rpm, resulting in an increase of drillability. This increase can be also attributed to the presence of soft formation (marl). Then, up to the depth of 5,210 ft, the increase in the compaction of the sandstone alternating with claystone at higher depths has led to a constantly decrease of drillability. In this interval, two different types of drill bits (X1G and J22) were used, operating with WOB and rotary speed ranging from 29,000 to 35,000 lb and from 75 to 100 rpm, respectively.

In the interval from 5,210 to 5,335 ft, where alternations of sandstone with claystone and limestone at the lower part have been observed, the J22 drill bit was replaced by the X1G operating with lower WOB at 29,000 lb and higher rotary speed at 120 rpm. The replacement of the drill bit of insert type (J22) with a milled tooth bit (X1G) which is suitable for drilling softer formations, unexpectedly led to an increase of drillability.

Below the depth of 5,335 ft, there is the breccia and the metamorphic argillaceous schist which constitutes the basement. Drilling was performed by replacing the X1G bit with a J44 bit, maintaining the same WOB at 29,000 lb, as in the previous interval, and with a lower rotary speed at 80 rpm. In spite of all these changes, drillability remained almost unchanged.

4.5 Drillability comparison between Nestos 1 and Nestos 2 wells

The small distance that separates the two wells of Nestos 1 and Nestos 2 allows for the implementation of a comparative analysis of drillability for the intervals of relevant depth drilled by the same drill bit type and size. According to Tables 3.3-3.4, each interval is drilled with approximately the same drilling mud density, in both wells, and therefore the density of drilling mud can be considered as constant for all the drilled intervals of Nestos 1 and Nestos 2 wells. Thus, the evaluation of drillability is based on the assumptions of similar lithostratigraphy and constant drilling mud density. In Figure 4.7, the drillabilities of both wells are presented based on the data of Tables 4.1-4.2.

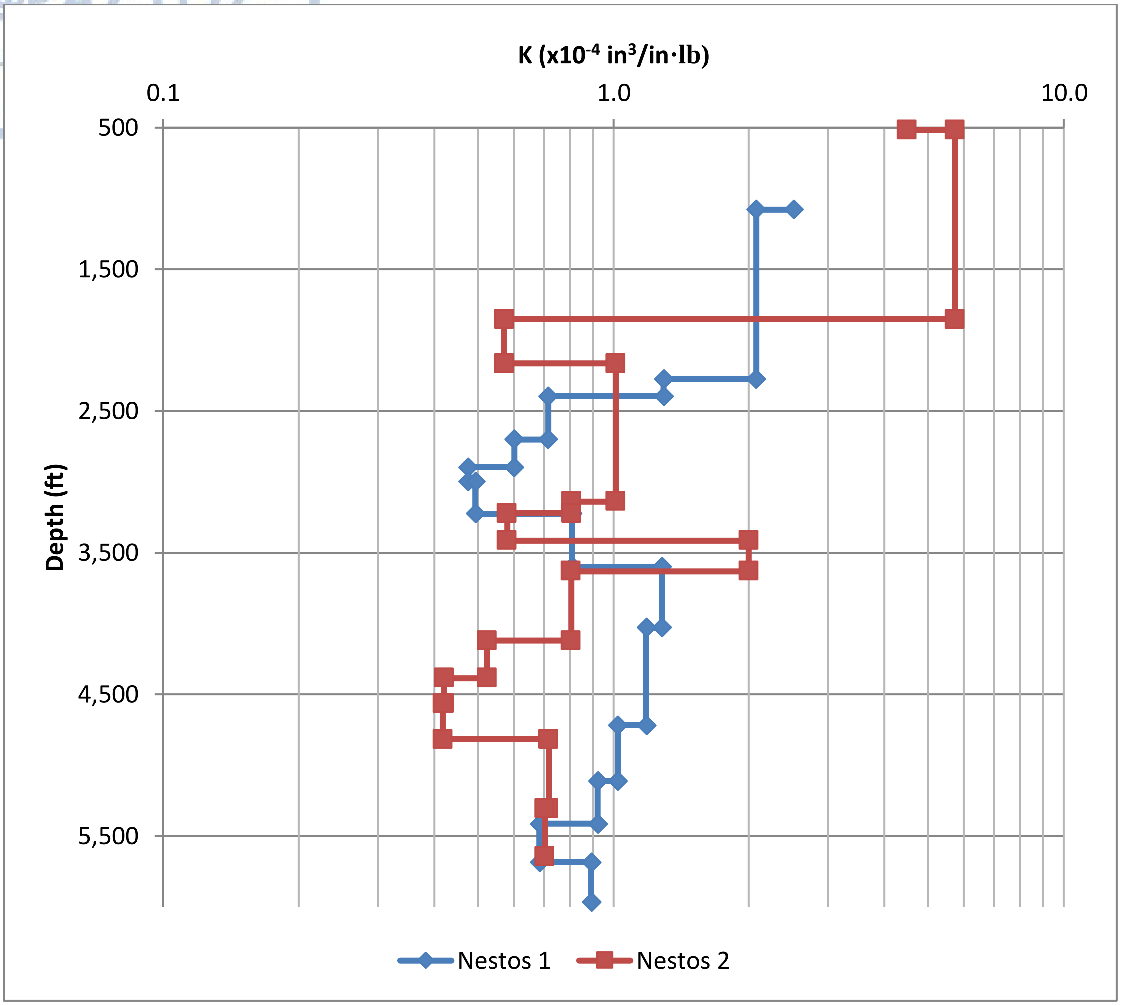

Figure 4.7: Drillability comparison between Nestos 1 and Nestos 2 wells

Both wells are drilled by using two different drill bit sizes of 17½" and 12¼" in diameter with the same type of RS drill bit, except for the interval in Nestos 1 well which is drilled by the 17½" RMTA drill bit, between 2,897 and 2,998 ft, as well as the intervals drilled by the 12 1/4" RM drill bit, from 3,599 to 4,028 ft, and from 4,386 to 4,564 ft, in Nestos 1 and Nestos 2 wells, respectively. Based on the above assumptions, drillability depends only on the drilling parameters used in each interval, specifically on the weight applied on bit and the rotary speed, for a specific drill bit size.

It is obvious that from surface up to 1,854 ft, where the sand alternating with clay and gravel constitute the predominant formations in both wells, drillability of Nestos 2 well is significantly greater than of Nestos 1 well. This is due to the lower input energy applied on the drill bit of Nestos 2 well, by operating with lower WOB (from

14,300 to 22,000 lb) than in Nestos 1 well (24,000-40,000 lb) and rotary speed ranging from 100 to 120 rpm, while in Nestos 1 well remained constant at 100 rpm.

In the interval from 1,854 to 2,395 ft, even though the Nestos 1 well was drilled with a higher WOB and rotary speed than in Nestos 2 well, its drillability is unexpectedly greater due to the extensive presence of glauconite in Nestos 1 well, in contrast to the sand and gravel interbedded with clay observed in Nestos 2 well.

In Nestos 1 well, the interval between 2,395 and 3,225 ft was drilled by lowering the WOB from 40,000 to 29,000 lb and the rotary speed from 130 to 100 rpm whereas, in Nestos 2 well, the drilling of the same interval was conducted with constant WOB at 39,700 lb and a rotary speed varying from 140 to 130 rpm. According to the drilling parameters used, the expected drillability of Nestos 1 well should be less than of Nestos 2 well, but the high heterogeneity of the drilled formations, where limestone and anhydrite beds alternating with sandstone, claystone, marl, and varves lie in both wells, has led to the opposite results.

The fact that the interval from 3,225 to 3,415 ft consists of medium hard formations, such as limestone and sandstone, and soft formation of glauconite which is interbedded with the sandstone, resulted in an increase of drillability in Nestos 1 well. Furthermore, in Nestos 1 well, the increase of drillability was enhanced by the decrease of WOB at 25,000 lb in combination with a slight increase in the rotary speed at 105 rpm (interval 3,225-3,599 ft). In Nestos 2 well, the maintenance of WOB at 39,700 lb and of rotary speed at 130 rpm, as in the last segment of the previous interval, has led to a reduction of drillability, probably due to the higher compaction of the anhydrite and limestone beds alternating with sandstone, claystone, and marl. As a result, the drillability in Nestos 1 well is greater than in Nestos 2 well.

Below the depth of 3,415 ft, drilling of Nestos 2 well was conducted with a lower drill bit size of 12¼" in diameter, resulting in a significant increase of drillability, and thus, into a greater drillability than of Nestos 1 well, in the interval between 3,415 and 3,632 ft. Since the rotary speed remained unchanged at 130 rpm, the lower WOB of 19,800 lb contributed to the further increase of drillability in the Nestos 2 well.

Likewise, below the depth of 3,599 ft, the drill bit size for Nestos 1 well decreased from 17½" to 12¼" leading to a rapid increase of drillability which did not exceed the drillability of Nestos 2 well, in the interval from 3,599 to 3,632 ft.

In the interval between 3,632 and 5,413 ft, drillability of Nestos 1 well is consistently greater than of Nestos 2 well, due to the extensive presence of glauconite which is alternated by sandstone with interbeds of conglomerate and clay, whereas the lithology of Nestos 2 well is mostly characterized by interbeds of medium hard formations, including varves, sandstone, limestone, anhydrite, claystone, etc. In addition, the drilling parameters used for drilling the Nestos 1 well varied (WOB from 24,000 to 33,000 lb, and rotary speed from 95 to 120 rpm), causing a further increase in the drillability value in comparison with the drillability of Nestos 2 well where the WOB ranged from 33,100 to 35,100 lb and the rotary speed from 130 to 140 rpm.

Finally, in the interval from 5,413 to 5,643 ft, the high heterogeneous formation of conglomerate, which is interbedded with sandstone, glauconite, and clay, caused a significant decrease of drillability in Nestos 1 well. Moreover, for the same well, the increase in both WOB and rotary speed at 26,000 lb and 100 rpm, respectively, contributed to the further decrease of drillability. On the other hand, in Nestos 2 well, drillability remained unchanged regardless the reduction of the WOB at 24,300 lb and the maintenance of rotary speed constant at 140 rpm, probably owing to the mechanical properties of the drilled claystone. As a result, both wells seem to have approximately equal drillabilities.

5. Geopressures

During the drilling of a well, many significant geomechanical parameters can be determined by the drilling parameters and the characteristics of the drill bits used, such as formation pore pressure or formation pressure and fracture gradient, which describe the geopressures regime in the region of interest. The lack or disability of estimating the geopressures may cause serious problems such as, lost circulation of drilling fluids, blow outs due to inappropriate control of the internal pressures, instability of the wellbore walls, segments falling and drill string stuck and hence, the drilling cost will be increased.

The estimation of the geopressures in the subsurface is based on the computation of the d-exponent, where its quantity is helpful in estimating the formation pressure (P_f). The knowledge of the geopressures is crucial, as they comprise a significant parameter for most of the aspects of well planning.

5.1 Origin of geopressures

By definition, abnormal pressure is every geopressure that differs from the normal trend of pressure build up over depth in a specific region and at the depth of interest. The pressure can be less than normal, so it is characterized as underpressure, or greater than normal and is characterized as overpressure (Stamataki, 2003).

The underpressured zones contribute in relative small problems in drilling, while the most interesting zones of abnormal pressures are the overpressured zones.

5.1.1 Formation Pressure

The formation pore pressure or formation pressure (P_f) is defined as the pressure applied by the fluids that may be enclosed into the porous space of the formation (usually saline water, oil and/or natural gas). The terms: pore pressure, formation pressure, and formation fluid pressure are identical (Stamataki, 2003).

As a consequence, the formation pressure differs from the overburden pressure. The overburden pressure (σ_v) is the stress that arises from the weight of the layers which overly a zone of interest. In regions where the tectonics is not active, the overburden gradient (relation between the overburden stress and the depth of interest) is approximately 1 psi/ft, while in regions with intense tectonic activity (e.g.

sedimentary basins where compression still exists or there are intensively fractured zones) the overburden gradient varies with depth and an average value of 0.8 psi/ft is considered to be representative. In general, the overburden gradient does not remain constant in different geological regions and increases with depth, due to the compaction of the rock mass.

In porous rocks, the overburden stress (σ_v) is compensated with the rock stress (σ_s) and the formation pore pressure (P_f), so that:

$$\sigma_v = \sigma_s + P_f \tag{5.1}$$

5.1.2 Normal Formation Pressure

The normal formation pressure is the pressure that corresponds to the hydrostatic pressure exerted by a water column (fresh or brine) at the depth of interest. The pressure of a water column (P_D), which represents the vertical continuity of the fluid into the porous network, is given by the following equation (Stamataki, 2003):

$$P_D = \rho \cdot g \cdot D \tag{5.2}$$

or

$$P_D = G_w \cdot D \tag{5.3}$$

where:

ρ: density of water (lb/gal)

g: gravitational acceleration (g=9.807 m/s^2)

D: depth beneath a reference plane (e.g. mean sea level) (ft)

G_w: pressure gradient, the pressure exerted by a water column per unit depth (psi/ft)

If the density (ρ) units are given in lb/gal, then the pressure gradient units will be in psi/ft, according to the following equation:

$$G_w = 0.052 \cdot \rho \tag{5.4}$$

In the equation (5.4), the coefficient 0.052 encloses all the required transformations of units and the numerical value of g.

According to the equation (5.4), the density of fresh water is considered as 8.35 lb/gal (1 gr/cm^3) corresponding to a pressure gradient of 0.433 psi/ft. On the other hand, the density of brine is considered as 8.94 lb/gal (1.073 gr/cm^3) and the equation (5.4) results in a pressure gradient of 0.465 psi/ft. Regardless of the water density, the normal pressure is considered to be the pressure that corresponds to an open hydraulic system which communicates at each point (Stamataki, 2003).

5.1.3 Abnormal Pressure Zones

The term «abnormal pressure zones» is referred to subsurface formations in which the geopressures are much different than the expected, for the relevant depth and the lithology of the formation. These abnormal pressures are, in most cases, greater than the expected ones. The abnormal pressures are present in systems that are characterized by the weakness in hydraulic communication. If the communication was possible, the pressure would be normal. As a result, the abnormal pressure zones are considered as closed hydraulic systems. This fact implies that some mechanism has intruded leading to the interruption of the hydraulic communication. The three most common mechanisms are the following (Perakis, 2006):

- Interference of impervious rock
- Artesian systems
- Faults

5.2 Prediction and Estimation Methods of Geopressures

The methods that contribute in predicting and/or estimating geopressures are distinguished as follows (Stamataki, 2003):

1. Analysis and processing of logging data
2. Analysis and processing of in situ drilling data

5.2.1 Analysis and Processing of Logging Data

The processing of the information derived from loggings conducted in wells that lie in the surrounding area is a widely used procedure for the evaluation of geopressures in a region of interest. The utilization of the results plays a key role in designing and drilling a new well. The processed logging data help in estimating the formation pressure throughout the depth as well as in determining the depth of abnormal pressure zones. The most commonly used logs concern formation parameters that are affected by formation pressures such as, the interval transit time of acoustic waves (sonic log), the density of rocks (density log) and electrical conductivity, or its inverse, electrical resistivity (resistivity log) (Perakis, 2006).

5.2.2 Analysis and Processing of In Situ Drilling Data

The experienced drilling personnel can assess any possible "response" that comes from the well during drilling. Hence, the well "speaks" to the drilling personnel through the variations of drilling parameters, especially the penetration rate. However, it is considered that the bottom hole is efficiently cleaned by the drilling mud in order to set a base for the better understanding of how much a drilling parameter has been eventually changed.

The penetration rate depends on lithology, drilling technical parameters (weight on bit, rotary speed, characteristic properties of drilling fluid, etc.) and variations of pressures of the formations being drilled. If the drilling parameters remain constant, then the variations on penetration rate would be related to the lithology and the formation pressures. Sudden and intense variations on penetration rate (Figure 5.1A) imply changes in the lithology, fact that could be confirmed by the analysis of the cuttings carried up to the surface. On the other hand, penetration rate varies (Figure 5.1B) due to changes in formation pressures (Stamataki, 2003).

The aim of a drilling engineer is to determine the formation pressures as a result of the observed variations in the penetration rate. A drilling engineer uses these variations as indications for making his estimations more qualitative, but simultaneously, he needs to co-estimate other facts as well, as, for instance, his experience, in order to provide more accurate answers (Stamataki, 2003).

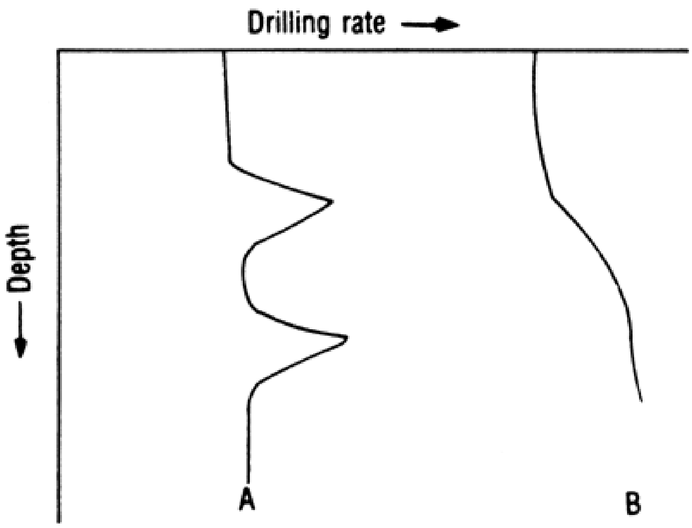

Figure 5.1: Variation of penetration rate due to changes in lithology (A) and changes of formation pressures (B) (Stamataki, 2003).

5.2.3 Penetration Rate and d-exponent Method

The penetration rate is affected by the difference between the pressure exerted by the drilling mud and the formation pressure at the depth of interest (Garnier & van Lingen, 1959). Vidrine and Benit (1968) showed that in situ pressure differences which range from 0-500 psi tend to have a significant influence on penetration rate. Jorden and Shirley (1966) have developed a valuable mathematical model for estimating the penetration rate, known as "d-exponent" model, where the penetration rate is estimated by the following equation:

$$R = 60N \cdot \left(\frac{12W}{10^3 \cdot D_b}\right)^d \tag{5.5}$$

where:

R: penetration rate (ft/hr)

N: rotary speed (rpm or rev./min)

W: weight on bit (lb/1000)

D_b: bit diameter (in)

d: d-exponent

If the rotary speed and the weight applied on bit in a certain formation remain constant, then the value of d-exponent will be only affected by the variations in penetration rate, assuming that the mud density does not change as well. From the equation (5.5), the numeric value of d-exponent is mathematically expressed as follows:

$$d = \frac{\log\left(\frac{R}{60N}\right)}{\log\left(\frac{12W}{10^3 \cdot D_b}\right)} \tag{5.6}$$

The above equation (5.6) applies for a specific bit and for constant values of rotary speed and weight applied on bit.

The illustration of d-exponent over depth results in diagrams similar to those of loggings, where the significant deviation from the expected normal values indicates the transition into zones of abnormal pressure, under the assumption that no changes in the drilling mud density occur. In this case, the difference between the pressure exerted by the drilling fluid and the formation pressure decreases due to the increase of formation pressure. Hence, the d-exponent is a valuable means for evaluating formation pressure only when the drilling fluid density remains constant, because the d-exponent values increase linearly with depth in zones with a constant pressure gradient, while the penetration into zones of abnormal pressure will lead to deviated values of d-exponent from linearity (Perakis, 2006).

Therefore, the deviation of the d-exponent from normal values might be either due to an increase of formation pressure, with constant drilling mud density, or due to an increase of drilling mud density, when penetrating zones of the normal pressure gradient. In both cases, there is a decrease in differential pressure (Stamataki, 2003). During drilling, the density of drilling mud does not remain constant causing problems in recognizing the abnormal variations of formation pressures. For that reason, Rehm and McClendon (1971) defined the modified (or corrected) d-exponent to account for changes in drilling mud density. According to their model, each value of d-exponent is multiplied by a coefficient defined as the ratio of drilling mud density (ρ_n), which is equivalent to the normal pressure gradient of the formations in the region of interest, divided by the drilling mud density (ρ) that is actually used at each interval of interest:

$$d_{mod} = d \cdot \frac{\rho_n}{\rho} \tag{5.7}$$

where:

d_{mod}: the modified d-exponent

d: the d-exponent as computed by the equation (5.6)

ρ_n: the equivalent drilling mud density corresponding to the normal pressure gradient of the formations in the region of interest (lb/gal)

ρ: the actual drilling mud density (lb/gal)

In general, the region of interest is characterized by a value of normal pressure gradient. In most cases, the normal pressure gradient is assigned to be 0.465 psi/ft corresponding to the pressure gradient of brine water.

Zamora (1972) proposed an empirical method in determining the formation pressure from the drilling data. This method is based on the d_{mod}-exponent that is computed by equation (5.7) and is presented in a semi-logarithmic graph. In such a graph, a linear trendline is drafted which corresponds to the normal values of d_{mod-n} (regime of normal pressure gradient) at the depth of interest can be computed. According to the values of d_{mod-n} and d_{mod}, where the last is determined by the semi-logarithmic graph, the formation pressure at the depth of interest can be determined as follows:

$$P_f = \text{normal } P_f \cdot \frac{d_{mod-n}}{d_{mod}} \tag{5.8}$$

where:

P_f: the formation pressure gradient (psi/ft)

normal P_f: the normal pressure gradient of the region (psi/ft)

d_{mod-n}: the modified exponent that is computed by the normal trend of the formations under normal compaction

d_{mod}: the modified exponent that is computed by the drilling data

5.3 Estimation of geopressures

The estimation of geopressures for the three wells under study is based on the indirect method of d-exponent.

5.3.1 Computation of d and d_{mod} exponents and formation pressure

The drilling data used for the determination of d, d_{mod}, and the formation pressure gradient (P_f) are presented in the following sections. The resulting values of d and d_{mod} exponents as well as the formation pressure gradient (P_f) for each interval are also computed by the equations of (5.6), (5.7) and (5.8) which were described above and are shown in the following Tables.

For the determination of d, d_{mod}, and formation pressure gradient (P_f) only the drilling data related to intervals of normal drilling were taken into account. Hence, coring and other drilling operations such as reaming, re-drilling or cementing were excluded. In addition, the determination of d_{mod}-exponent is based on the value of 8.94 lb/gal (brine density) as the density that corresponds to the normal pressure gradient of the formations in the region.

5.3.2 Computation of d and d_{mod} exponents and formation pressure for Nestos 1 well

The computations of d and d_{mod} exponents for Nestos 1 well are presented in the following Table 5.1.

Table 5.1: Computation of d and d_{mod} exponents for Nestos 1 well

Drilling Data							Computations	
# Interval	Depth (ft)	Bit Diameter-D_b (in)	Penetration Rate-R (ft/hr)	Weight on Bit-W ($x10^3$ lb)	Rotary Speed-N (rpm)	Mud Density-ρ (lb/gal)	d[1]	d_{mod}[2]
1	1,079	17½	34.8	24	100	9.93	1.26	1.13
2	2,273	17½	47.0	40	100	10.18	1.35	1.18
3	2,395	17½	35.2	40	120	10.26	1.48	1.29
4	2,700	17½	21.1	40	130	10.26	1.64	1.43
5	2,897	17½	12.7	31	120	10.60	1.64	1.39
6	2,998	17½	7.8	29	100	10.60	1.69	1.43
7	3,225	17½	8.1	29	100	10.68	1.68	1.41
8	3,599	17½	12.3	25	105	10.68	1.54	1.29
9	4,028	12¼	41.5	33	120	10.60	1.50	1.27

Table 5.1: Computation of d and d_{mod} exponents for Nestos 1 well (continued)

Drilling Data							Computations	
# Interval	Depth (ft)	Bit Diameter-D_b (in)	Penetration Rate-R (ft/hr)	Weight on Bit-W ($x10^3$ lb)	Rotary Speed-N (rpm)	Mud Density-ρ (lb/gal)	d[1]	d_{mod}[2]
10	4,717	12¼	32.8	31	110	10.26	1.52	1.32
11	5,111	12¼	24.3	26	110	11.02	1.53	1.25
12	5,413	12¼	17.3	24	95	10.35	1.55	1.34
13	5,685	12¼	14.8	26	100	10.77	1.64	1.37
14	5,964	12¼	17.4	26	90	11.18	1.57	1.26

[1] d is computed by (5.6) equation

[2] d_{mod} is computed by (5.7) equation

The diagram of d_{mod}-depth which arises from the above computations is presented in Figure 5.2. Due to the difference in magnitude between depth and exponent of d_{mod}, the values of d_{mod} are plotted in logarithmic scale. Thus, the diagram of d_{mod} over depth is a semi-logarithmic diagram.

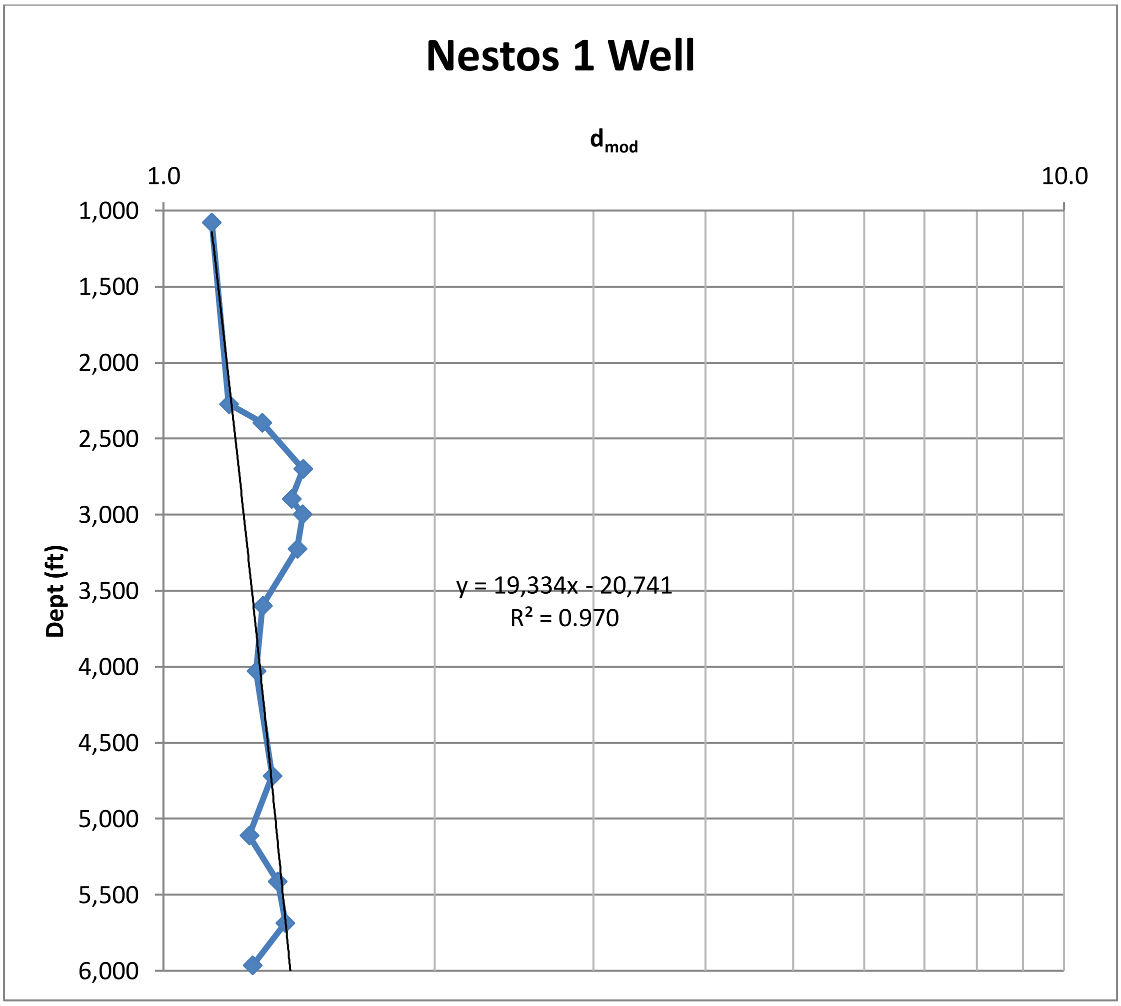

Figure 5.2: Diagram of d_{mod} over Depth for Nestos 1 well

In the above Figure 5.2, the values of d_{mod} between 2,273 and 3,599 ft do not show a specific increasing trend, and thus, have been excluded from the determination of the linear trendline corresponding to the formations under normal compaction (probably due to field measurement errors). Moreover, the values of d_{mod} above 2,273 ft and below 3,599 ft are fluctuated around the linear trendline with small deviations, indicating the absence of zones with abnormal pressures. As a result, the linear equation for the expected $d_{mod\text{-}n}$ values is y=19,334·x-20,741, where y is the depth of interest and x is the value of $d_{mod\text{-}n}$ at this depth.

The formation pressure gradient (P_f) at several depths is computed by using the exponents of d_{mod}, $d_{mod\text{-}n}$ and the normal pressure gradient (normal P_f), according to equation (5.8). The values of d_{mod} are calculated by equation (5.7), whereas the computation of $d_{mod\text{-}n}$ is based on solving the equation of the linear trendline (Figure 5.2). Furthermore, the normal pressure gradient is taken as equal to the pressure gradient of brine (0.465 psi/ft). Thus, Table 5.2 shows formation pressure gradients and formation pressures for Nestos 1 well.

Table 5.2: Computation of formation pressure gradients and formation pressures for Nestos 1 well

Depth (ft)	d_{mod}	d_{mod-n}	Formation Pressure Gradient-P_f (psi/ft)	Formation Pressure (psi)
1,079	1.13	1.13	0.464	500
2,273	1.18	1.19	0.468	1,065
2,395	1.29	1.20	0.433	1,036
2,700	1.43	1.21	0.395	1,065
2,897	1.39	1.22	0.410	1,187
2,998	1.43	1.23	0.400	1,200
3,225	1.41	1.24	0.409	1,320
3,599	1.29	1.26	0.454	1,635
4,028	1.27	1.28	0.470	1,892
4,717	1.32	1.32	0.464	2,187
5,111	1.25	1.34	0.499	2,552
5,413	1.34	1.35	0.470	2,543
5,685	1.37	1.37	0.465	2,646
5,964	1.26	1.38	0.511	3,049

According to the data of Table 5.2, the following diagram of formation pressure over depth can be plotted (Figure 5.3).

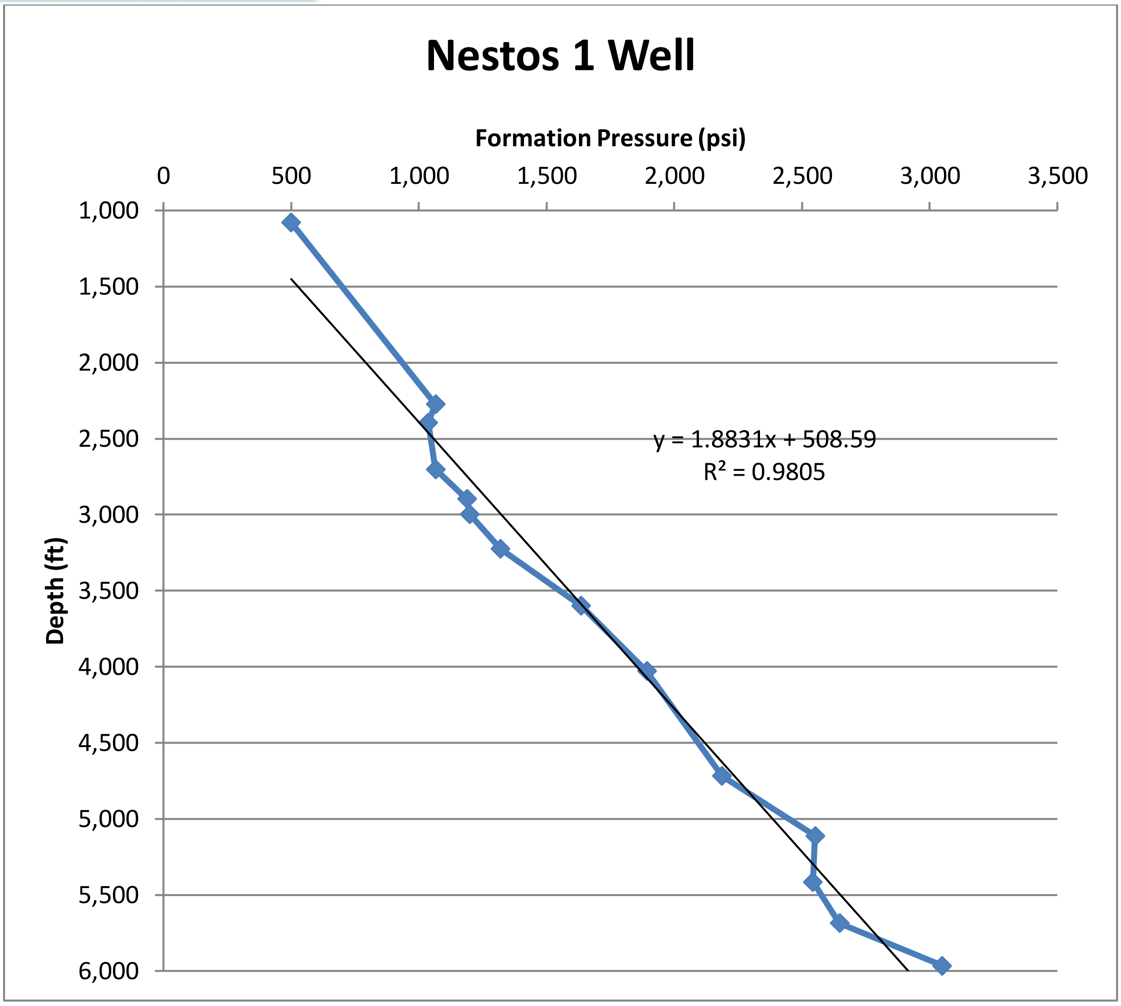

Figure 5.3: Diagram of formation pressure over depth for Nestos 1 well

In the above Figure 5.3, the linear relation between formation pressure and depth is very obvious. Near surface penetration rates achieved are usually high, due to formation weathering and low overburden pressure, which result in the decrease of the d_{mod} values. Hence, formation pressure above the 2,273 ft is overestimated. In addition, the interval from 2,273 to 3,599 ft consists of sandstone and clay interbedded with limestone, sand with conglomerate and alternations of limestone, anhydrite, glauconite and varves. These alternations directly reduce the rate of penetration, and in turn, the value of d_{mod} is increased. For this reason, the formation pressure in this interval is underestimated. Even though there are small deviations around the linear trendline, the fact that the formation pressure generally follows the linearity of the trendline indicates the absence of abnormal pressure zones.

5.3.3 Computation of d and d_{mod} exponents and formation pressure for Nestos 2 well

The computations of d and d_{mod} exponents for Nestos 2 well are presented in the following Table 5.3.

Table 5.3: Computation of d and d_{mod} exponents for Nestos 2 well

Drilling Data							Computations	
# Intervals	Depth (ft)	Bit Diameter-D_b (in)	Penetration Rate-R (ft/hr)	Weight on Bit-W ($x10^3$ lb)	Rotary Speed-N (rpm)	Mud Density-ρ (lb/gal)	d[1]	d_{mod}[2]
1	515	17½	36.8	14.3	100	10.60	1.10	0.93
1a	1,854	17½	86.6	22.0	120	10.43	1.05	0.90
2	2,165	17½	14.1	33.1	130	10.43	1.67	1.43
3	3,140	17½	32.2	39.7	140	10.26	1.54	1.35
4	3,222	17½	23.8	39.7	130	10.10	1.61	1.42
6	3,415	17½	17.1	39.7	130	10.01	1.70	1.52
7	3,632	12¼	42.0	19.8	130	10.01	1.33	1.18
8	4,121	12¼	28.3	33.1	130	10.01	1.64	1.46
9	4,386	12¼	18.4	33.1	130	10.01	1.76	1.58
10	4,564	12¼	14.8	33.1	130	10.26	1.83	1.59
11	4,816	12¼	16.8	35.3	140	10.52	1.85	1.57
12	5,305	12¼	27.2	33.1	140	10.52	1.67	1.42
13	5,643	12¼	19.5	24.3	140	10.68	1.62	1.36

[1] d is computed by (5.6) equation

[2] d_{mod} is computed by (5.7) equation

The semi-logarithmic diagram of d_{mod} over depth is constructed in accordance with the above computations, as presented in Figure 5.4.

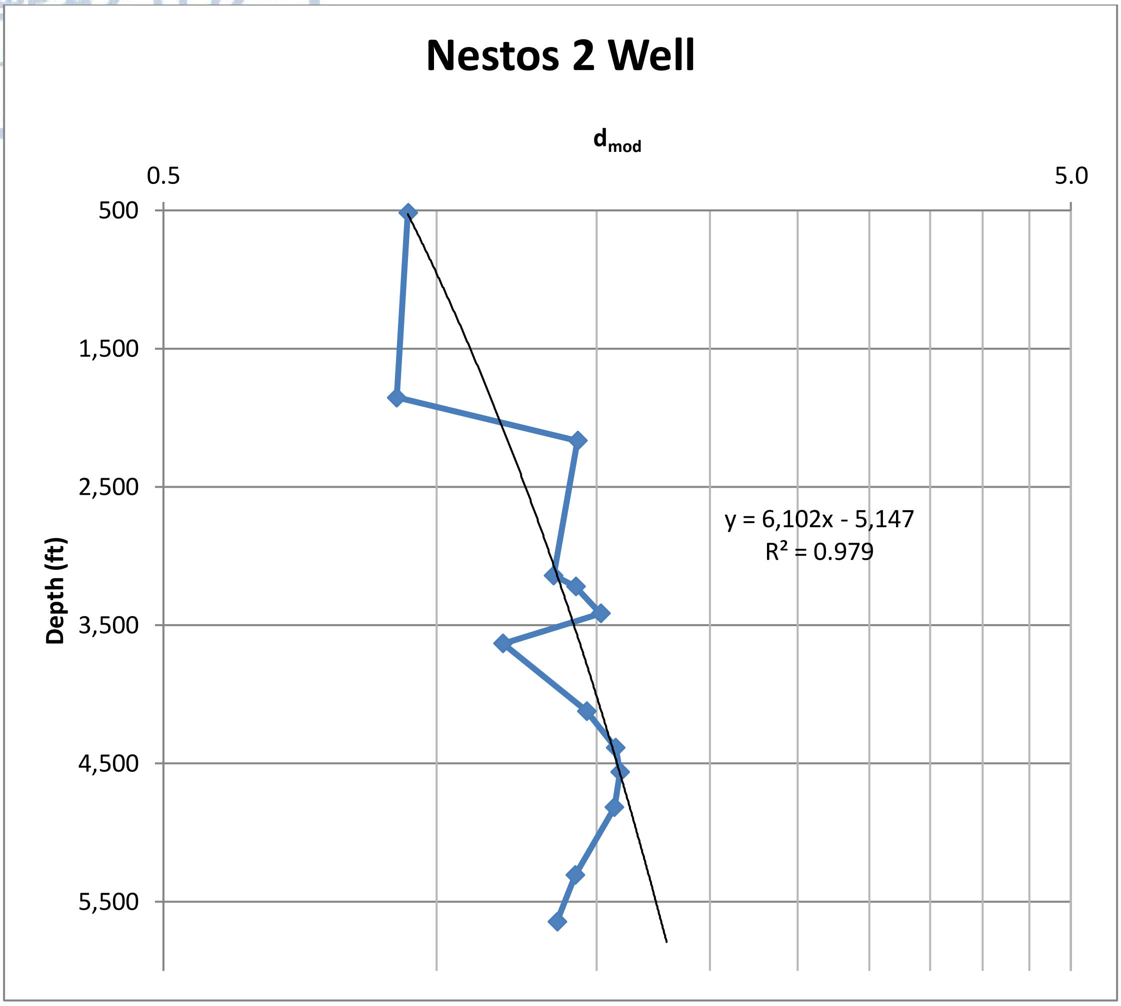

Figure 5.4: Diagram of d_{mod} over depth for Nestos 2 well

Figure 5.4 shows that the values of d_{mod} generally increase over depth, although there are some intervals where the d_{mod} values do not change as expected. Near surface there are two deviated values of d_{mod} from the linear trendline, one local minimum and one local maximum, at depths of 1,854 ft and 2,165 ft, respectively. Above the 1,854 ft, the rate of penetration is high, due to low formation stress state, causing a slightly decrease in the value of d_{mod}, while below this depth up to 2,165 ft the heterogeneity of formations, sand, and gravel interbedded with clay, led to a reduce of the rate of penetration, and thus, to an increase of d_{mod}. Moreover, in the interval between 3,415 and 3,632 ft the beds of anhydrite and limestone alternating with sandstone, claystone, and marl led to the values of d_{mod} deviating around the linear trendline as well. Furthermore, below the depth of 4,816 ft, the value of d_{mod} unexpectedly decreases over depth, probably owing to the alternations of formations with different mechanical characteristics, such as varves with interbeds of sandstone, claystone, siltstone and sandy marl. All these deviations from the linearity of the normal values of d_{mod} do not actually indicate the existence of abnormal pressure zones. As a result, the linear equation for the expected d_{mod-n} values is y=6,102·x-5,147, where y is the depth of interest and x is the value of d_{mod-n} at this depth.

As mentioned above, the computation of the formation pressure gradient (P_f) at several depths is based on d_{mod}, d_{mod-n} exponents as well as on the normal pressure gradient (normal P_f) which is assigned to be 0.465 psi/ft (pressure gradient of brine), according to equation (5.8). Table 5.4 shows formation pressure gradients and formation pressures for Nestos 2 well.

Table 5.4: Computation of formation pressure gradients and formation pressures for Nestos 2 well

Depth (ft)	d_{mod}	d_{mod-n}	Formation Pressure Gradient-P_f (psi/ft)	Formation Pressure (psi)
515	0.93	0.93	0.464	239
1,854	0.90	1.15	0.590	1,094
2,165	1.43	1.20	0.390	844
3,140	1.35	1.36	0.469	1,474
3,222	1.42	1.37	0.448	1,443
3,415	1.52	1.40	0.430	1,469
3,632	1.18	1.44	0.565	2,053
4,121	1.46	1.52	0.483	1,989
4,386	1.58	1.56	0.461	2,023
4,564	1.59	1.59	0.465	2,121
4,816	1.57	1.63	0.484	2,329
5,305	1.42	1.71	0.560	2,972
5,643	1.36	1.77	0.606	3,418

According to the above Table 5.4, the following diagram of formation pressure over depth is presented (Figure 5.5).

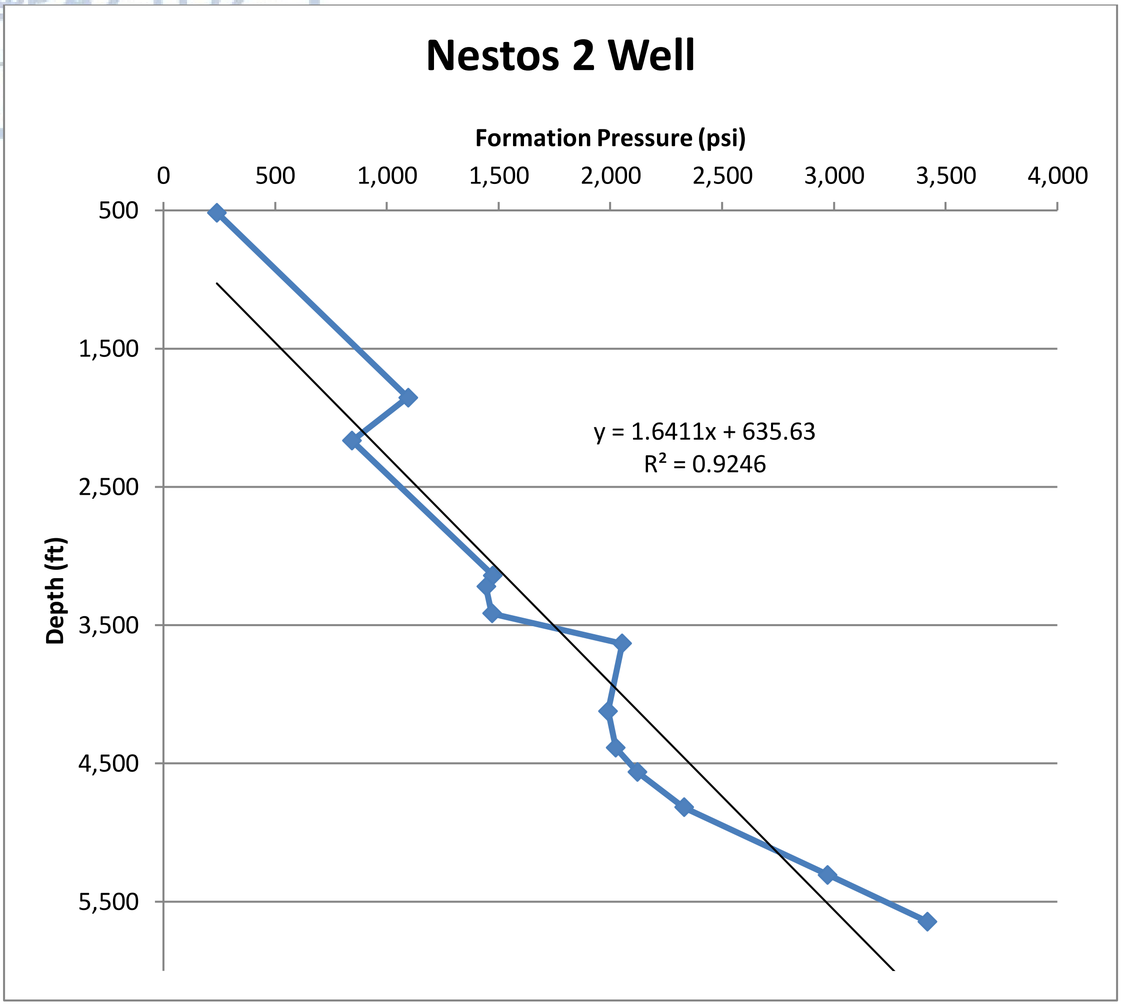

Figure 5.5: Diagram of formation pressure over depth for Nestos 2 well

In Figure 5.5, the formation pressure generally increases linearly over depth. The overestimated values of formation pressure, above the depth of 2,165 ft, are the result of high values of penetration rate that have been achieved during drilling (or low values of d_{mod}) due to the low overburden load. The interval from 2,165 to 3,140 ft is the only interval where the actual formation pressure is well estimated relative to the linear trendline. Below the depth of 3,140 ft, the value of formation pressure is over- or underestimated in comparison with the expected value derived by the linear equation, resulting in small deviations. This fact suggests the absence of abnormal pressure zones for the whole length of Nestos 2 well.

5.3.4 Computation of d and dmod exponents and formation pressure for Komotini well

The computations of d and d_{mod} exponents for Komotini well are presented in the following Table 5.5.

Table 5.5: Computation of d and d_{mod} exponents for Komotini well

Drilling Data							Computations	
# Interval	Depth (ft)	Bit Diameter-D_b (in)	Penetration Rate-R (ft/hr)	Weight on Bit-W ($x10^3$ lb)	Rotary Speed-N (rpm)	Mud Density-ρ (lb/gal)	d[1]	d_{mod}[2]
1	997	17½	52.1	9	80	10.01	0.89	0.79
2	1,591	12¼	44.2	13	120	9.85	1.17	1.06
3	2,041	12¼	28.1	15	120	9.93	1.32	1.19
4	2,628	12¼	36.0	13	110	9.85	1.20	1.09
5	3,150	12¼	34.4	17	110	9.68	1.27	1.18
6	3,432	12¼	22.9	20	100	9.68	1.41	1.30
7	3,960	12¼	24.6	22	120	9.76	1.48	1.36
8	4,222	12¼	21.1	25	120	9.76	1.58	1.45
8a	4,236	12¼	4.4	29	120	9.85	2.07	1.88
9	4,239	8½	2.9	20	100	9.85	2.14	1.94
10	4,432	8½	17.4	30	120	9.85	1.90	1.73
11	4,882	8½	15.8	24	85	10.01	1.71	1.53
12	4,921	8½	3.9	26	75	9.93	2.15	1.93
13	4,944	8½	3.7	30	65	10.01	2.19	1.96
14	5,056	8½	18.6	30	100	10.10	1.82	1.61
14a	5,138	8½	11.2	29	100	9.93	1.96	1.76
12a	5,210	8½	6.0	35	75	10.01	2.21	1.97
15	5,335	8½	15.6	29	120	9.93	1.91	1.72
13a	5,623	8½	10.5	29	80	10.10	1.91	1.69

[1] d is computed by (5.6) equation

[2] d_{mod} is computed by (5.7) equation

According to the values of d_{mod} from the above Table 5.5 plotted in a logarithmic scale, the semi-logarithmic diagram of d_{mod} over depth is constructed, as it is demonstrated in Figure 5.6.

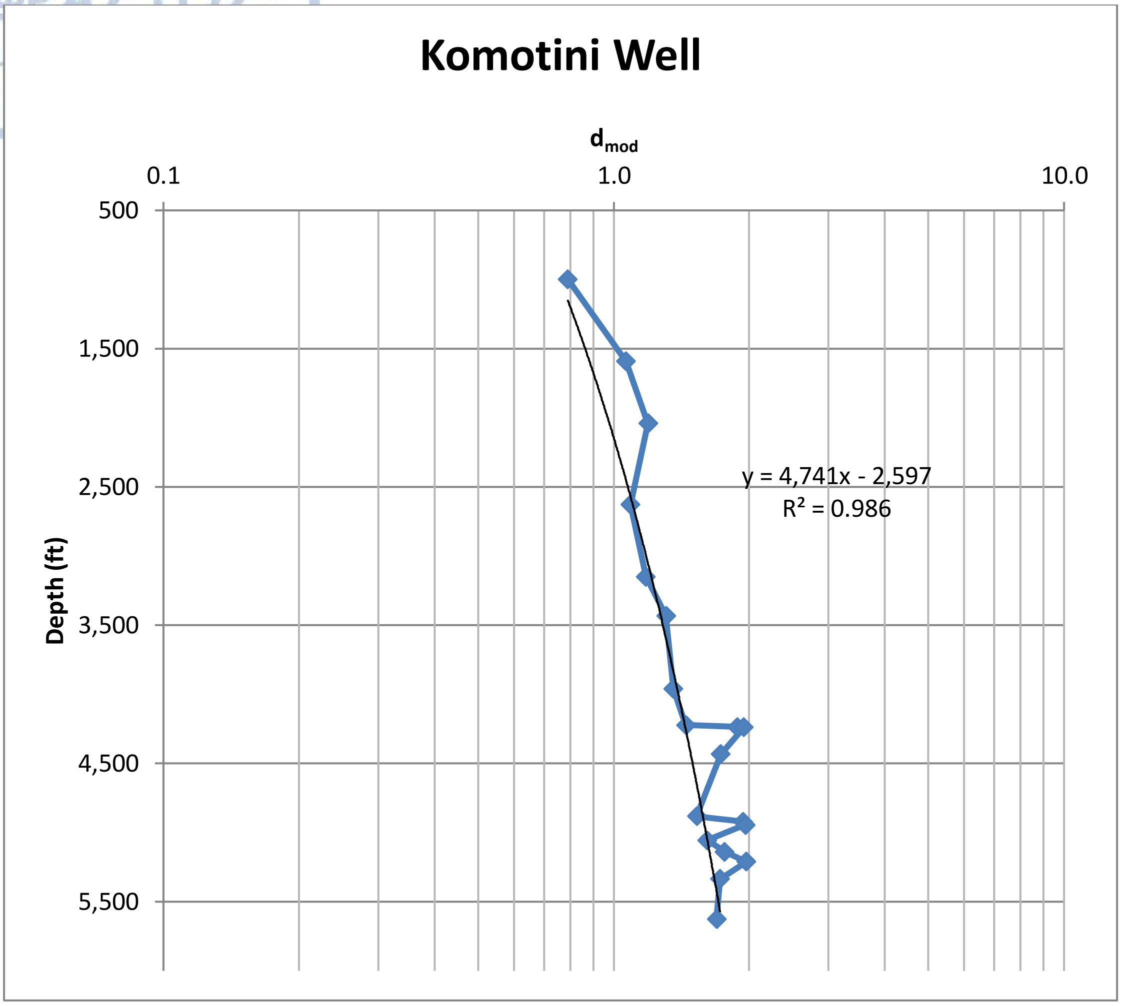

Figure 5.6: Diagram of d_{mod} over depth for Komotini well

In Figure 5.6, the values of d_{mod} increase over depth approaching, in most cases, the linearity of the equation y=4,741·x-2,597, where y corresponds to the depth of interest and x corresponds to the value of d_{mod} at this depth. In the interval between 997 and 3,150 ft, the d_{mod} values are overestimated due to the higher achieved penetration rates and the low-stress state of the alternations of sand with clay. As for the interval from 3,150 ft to 4,222 ft, the d_{mod} values increase smoothly in accordance with the linear trendline. Below the depth of 4,222 ft, the value of d_{mod} starts to deviate from linearity, but the fact that its magnitude is low indicates the presence of normal pressure zones.

It should be noted that changes of bit type directly affect the value of d_{mod}. This is the reason for the three peaks at depths of 4,239 ft, where the X3A bit was replaced by

X1G bit, 4,944 ft, where the J22 bit was replaced by J44 bit, and 5,210 ft, where the X1G bit was replaced by J22 bit.

The values of d_{mod} and d_{mod-n}, which derived from the linear equation in Figure 5.6, are the basis for the computation of the formation pressure gradient (P_f), according to equation (5.8). In addition, the value of normal pressure gradient (normal P_f) is taken as 0.465 psi/ft corresponding to the pressure gradient of brine. From the above, the following Table 5.6 shows formation pressure gradients and formation pressures for Komotini well.

Table 5.6: Computation of formation pressure gradients and formation pressures for Komotini well

Depth (ft)	d_{mod}	d_{mod-n}	Formation Pressure Gradient-P_f (psi/ft)	Formation Pressure (psi)
997	0.79	0.77	0.455	453
1,591	1.06	0.89	0.391	621
2,041	1.19	0.99	0.385	785
2,628	1.09	1.11	0.472	1,240
3,150	1.18	1.21	0.478	1,506
3,432	1.30	1.27	0.452	1,551
3,960	1.36	1.38	0.472	1,869
4,222	1.45	1.43	0.460	1,942
4,236	1.88	1.43	0.354	1,499
4,239	1.94	1.43	0.343	1,453
4,432	1.73	1.47	0.396	1,757
4,882	1.53	1.56	0.476	2,322
4,921	1.93	1.57	0.378	1,861
4,944	1.96	1.58	0.374	1,851
5,056	1.61	1.60	0.461	2,329
5,138	1.76	1.62	0.426	2,190
5,210	1.97	1.63	0.385	2,005
5,335	1.72	1.66	0.447	2,385
5,623	1.69	1.71	0.472	2,652

The diagram of formation pressure over depth is presented, in Figure 5.7.

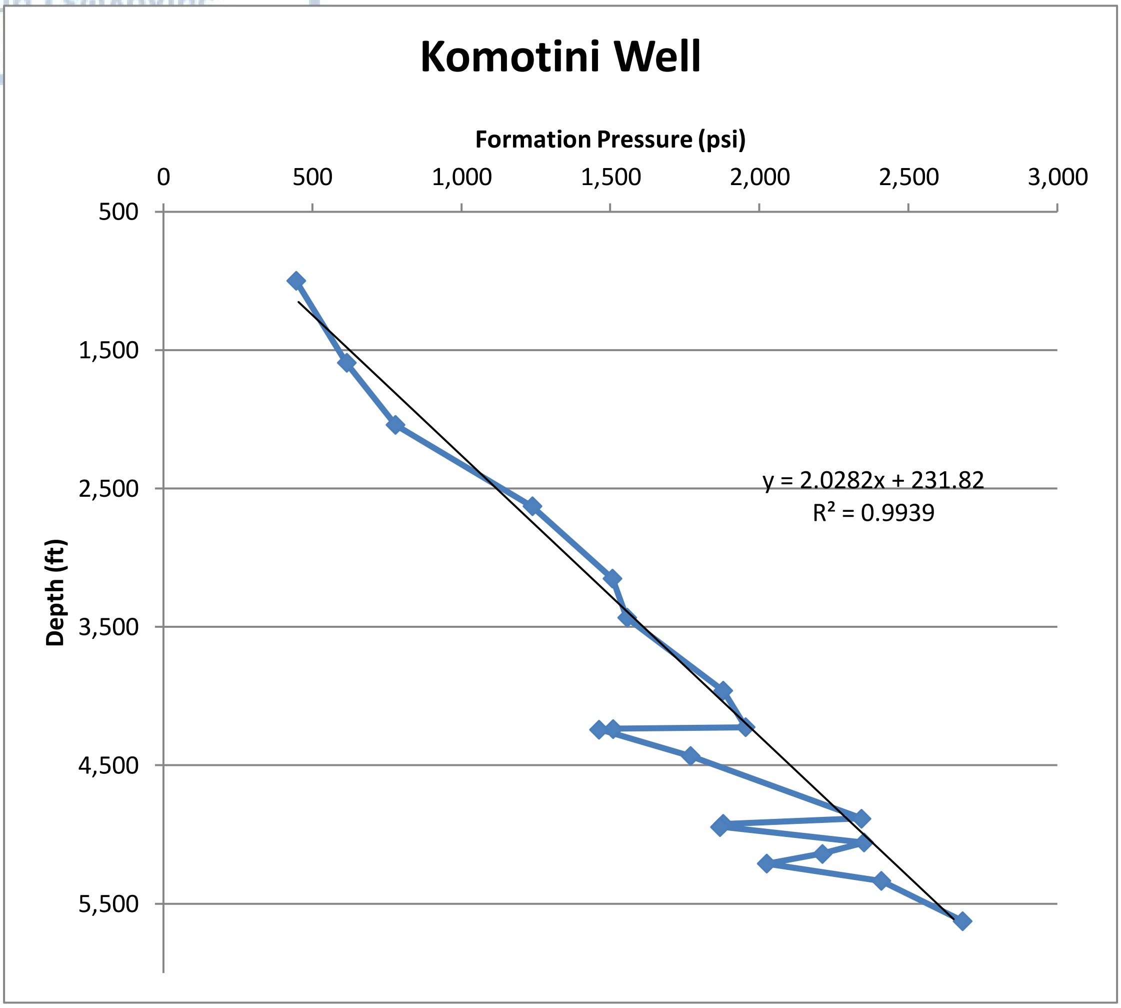

Figure 5.7: Diagram of formation pressure over depth for Komotini well

Figure 5.7 shows that the formation pressure values increase smoothly over depth up to the depth of 4,222 ft. The computation of formation pressure is based on the d_{mod} and d_{mod-n} values which are highly affected by the lithology being drilled, the drilling parameters and the bit types used. Below the depth of 4,222 ft, the interval which consists of medium hard formations, such as alternations of sandstone and claystone with few layers of limestone and marl, was drilled by several bit types that directly affect the penetration rate, and in turn, the values of d_{mod} and d_{mod-n}. Hence, the formation pressure is underestimated compared to the linear trendline, but the magnitude of underestimation does not justify the occurrence of abnormal pressure zones.

5.4 Differential Pressure

The differential pressure is defined as the difference between the pressure exerted by the drilling mud (P_m) and the formation pressure (P_f) at a specific depth (Stamataki, 2003):

$$\Delta P = P_m - P_f \tag{5.9}$$

The drilling mud pressure is determined by (5.3) equation, as follows:

$$P_m = G_m \cdot D \tag{5.10}$$

where:

G_m: drilling mud pressure gradient, which is the pressure exerted by the mud column per unit depth (psi/ft)

D: depth beneath a reference plane (e.g. mean sea level) (ft)

The pressure gradient of drilling mud, G_m, is actually equivalent to the product ρ·g, where ρ is the density of mud (lb/gal) and g is the constant of gravitational acceleration (g=9.807 m/s^2). According to (5.3) equation, if the drilling mud density (ρ) is expressed in lb/gal and the drilling mud pressure gradient is expressed in psi/ft, then:

$$G_m = 0.052 \cdot \rho \tag{5.11}$$

In equation (5.11), the coefficient 0.052 encloses all the required transformations of units and the numerical value of g, as in the case of equation (5.4).

As mentioned in Chapter 4, the differential pressure (ΔP) is directly associated with the penetration rate. The greater the differential pressure the lesser the penetration rate. If the differential pressure value is high, then this means that the drilling mud pressure is much higher than the formation pressure. The penetration rate generally increases for negative differential pressure ($P_m < P_f$). However, when the formation pressure exceeds by far the drilling mud pressure, there is a high danger of the wellbore walls to collapse and of an influx of the formation pore fluids into the wellbore during drilling (kick). Thus, the drilling personnel must maintain the well conditions overbalanced so as the drilling mud pressure to be higher or equal to the formation pressure for the whole length of the well.

5.4.1 Comparison of differential pressure and penetration rate for Nestos 1 well

Table 5.7 shows the differential pressure, the drilling mud pressure as well as the drilling mud pressure gradient in each interval for Nestos 1 well, according to the equations (5.9), (5.10) and (5.11), respectively.

Table 5.7: Computation of differential pressure for Nestos 1 well

# Interval	Depth-D	Penetration Rate-R	Drilling mud density-ρ		Mud Pressure Gradient-G_m	Mud Pressure-P_m	Formation Pressure	Differential Pressure-ΔP
	ft	ft/hr	kg/dm³	lb/gal	psi/ft	psi	psi	psi
1	1,079	34.8	1.19	9.93	0.516	557	500	57
2	2,273	47.0	1.22	10.18	0.529	1,204	1,065	139
3	2,395	35.2	1.23	10.26	0.534	1,278	1,036	242
4	2,700	21.1	1.23	10.26	0.534	1,441	1,065	376
5	2,897	12.7	1.27	10.60	0.551	1,596	1,187	409
6	2,998	7.8	1.27	10.60	0.551	1,652	1,200	453
7	3,225	8.1	1.28	10.68	0.555	1,791	1,320	471
8	3,599	12.3	1.28	10.68	0.555	1,999	1,635	364
9	4,028	41.5	1.27	10.60	0.551	2,220	1,892	328
10	4,717	32.8	1.23	10.26	0.534	2,518	2,187	331
11	5,111	24.3	1.32	11.02	0.573	2,928	2,552	376
12	5,413	17.3	1.24	10.35	0.538	2,913	2,543	370
13	5,685	14.8	1.29	10.77	0.560	3,183	2,646	536
14	5,964	17.4	1.34	11.18	0.582	3,468	3,049	419

According to the data shown in Table 5.7, the diagrams of penetration rate and differential pressure over depth (Figure 5.8a and 5.8b, respectively) are constructed. By juxtaposing Figures 5.8a and 5.8b, the relation between penetration rate and the differential pressure is determined.

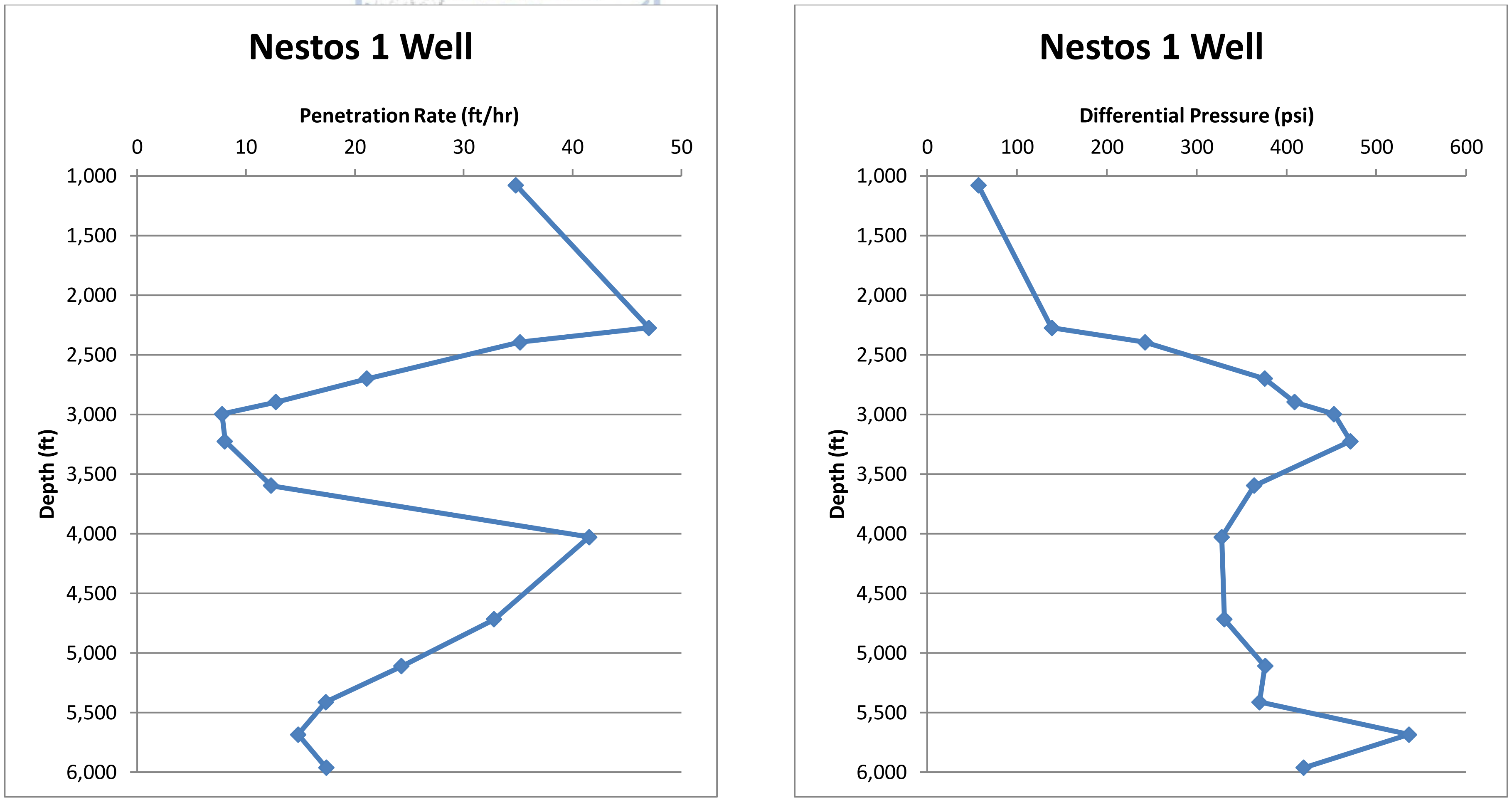

(a) **(b)**

Figure 5.8: (a) Penetration rate over depth; (b) Differential pressure over depth for Nestos 1 well

The juxtaposition of diagrams (a) and (b) in Figure 5.8 provides the following observations:

- From the surface up to 2,273 ft, both the penetration rate (R) and differential pressure (ΔP) increase, due to the low overburden pressure and the soft formation of glauconite.
- In the interval between 2,273 and 2,998 ft, the penetration rate (R) constantly decreases whereas the differential pressure (ΔP) increases, confirming their theoretical correlation.
- The interval from 2,998 to 3,225 ft consists of limestone and anhydrite interbedded with sandstone and varves as well as glauconite. The heterogeneity itself directly affects the response of penetration rate (R) and differential pressure (ΔP), where both increase.
- The penetration rate (R) also increases further, while the differential pressure (ΔP) decreases smoothly, in the interval from 3,225 to 4,028 ft. Furthermore, the reduction of the bit size, from 17½" to 12¼", contributes to the significant increase of the penetration rate (R) in the last interval from 3,599 to 4,028 ft.
- Between 4,028 and 5,685 ft, the penetration rate (R) constantly reduces, due to the higher compaction of the alternations of sandstone and glauconite interbedded with conglomerate and clay. At the same interval, the differential pressure (ΔP) generally follows an almost constant to a slightly increasing trend, except one interval (5,111-5,413 ft) where its value decreases with depth.
- Below the depth of 5,685 ft, the penetration rate (R) presents again an increase of its value, whereas the differential pressure (ΔP) decreases, as expected.

5.4.2 Comparison of differential pressure and penetration rate for Nestos 2 well

The computation of differential pressure, the drilling mud pressure, and the drilling mud pressure gradient, in each interval for Nestos 2 well, is based on the equations (5.9), (5.10) and (5.11), respectively (Table 5.8).

Table 5.8: Computation of differential pressure for Nestos 2 well

# Interval	Depth-D	Penetration Rate-R	Drilling Mud Density-ρ		Mud Pressure Gradient-G_m	Mud Pressure-P_m	Formation Pressure	Differential Pressure-ΔP
	ft	ft/hr	kg/dm³	lb/gal	psi/ft	psi	psi	psi
1	515	36.8	1.27	10.60	0.551	284	239	45
1a	1,854	86.6	1.25	10.43	0.542	1,005	1,094	-89
2	2,165	14.1	1.25	10.43	0.542	1,175	844	331
3	3,140	32.2	1.23	10.26	0.534	1,676	1,474	202
4	3,222	23.8	1.21	10.10	0.525	1,692	1,443	248
6	3,415	17.1	1.20	10.01	0.521	1,779	1,469	309
7	3,632	42.0	1.20	10.01	0.521	1,891	2,053	-162
8	4,121	28.3	1.20	10.01	0.521	2,146	1,989	157
9	4,386	18.4	1.20	10.01	0.521	2,284	2,023	261
10	4,564	14.8	1.23	10.26	0.534	2,436	2,121	315
11	4,816	16.8	1.26	10.52	0.547	2,633	2,329	304
12	5,305	27.2	1.26	10.52	0.547	2,901	2,972	-71
13	5,643	19.5	1.28	10.68	0.555	3,134	3,418	-284

The Figures 5.9a and 5.9b present the variation of penetration rate and differential pressure over depth, respectively, based on the data of Table 5.8. Figures 5.9 are juxtaposed in order to obtain information about the correlation between penetration rate and differential pressure.

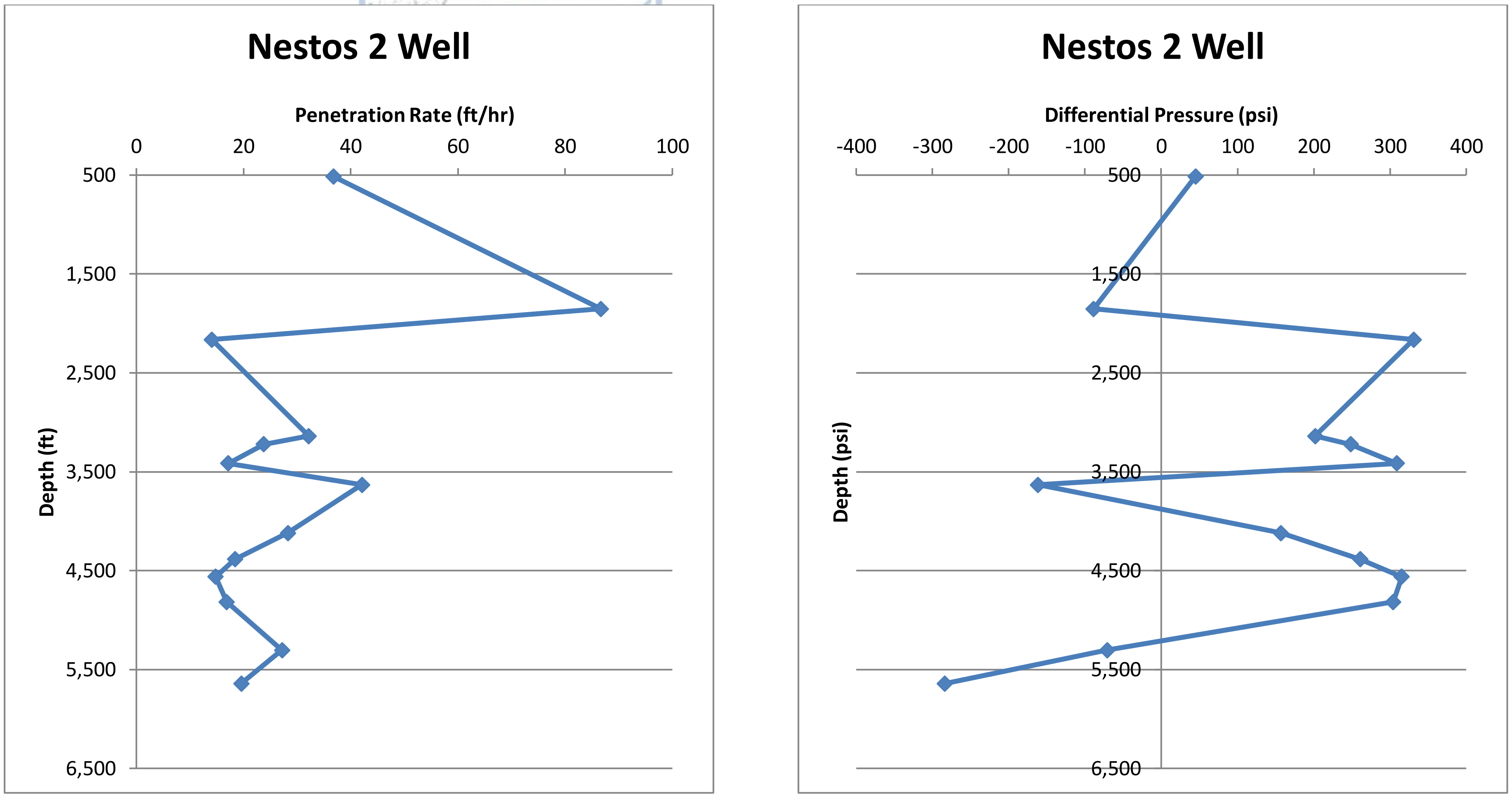

(a) **(b)**

Figure 5.9: (a) Penetration rate over depth; (b) Differential pressure over depth for Nestos 2 well

The diagrams (a) and (b) in Figure 5.9 contribute in the evaluation of the response of penetration rate and differential pressure, as follows:

- It is obvious that from the surface up to 5,305 ft the penetration rate (R) and differential pressure (ΔP) are well-correlated (inversely proportional), according to theory.
- Near the surface and up to 1,854 ft, the soft formations of sand and gravel with clay intercalations lie under low overburden pressure, contribute in the significant increase of the penetration rate (R) with depth.
- From 3,140 to 3,415 ft, the penetration rate (R) progressively decreases over depth due to the higher compaction of the formations, while the differential pressure (ΔP) increases.
- A sudden increase in penetration rate (R) accompanied with an excessive decrease in differential pressure (ΔP) occur in the interval between 3,415 and 3,632 ft, as a result of the lowering in the bit size from 17½" to 12¼".
- Below the depth of 3,632 and up to 4,564 ft, the penetration rate (R) again starts to decrease, owing to the higher compaction of the sandstone and claystone interbedded with clay at lower depths. As for the differential pressure (ΔP), its response is the expected by reaching a local maximum value at 4,564 ft.
- The high heterogeneity of the formations drilled, such as varves with interbeds of sandstone, claystone, siltstone and sandy marl, leads to the increase of the penetration rate (R), in the interval lies from 4,564 to 5,305 ft. In addition, the differential pressure (ΔP) decreases, as expected.
- In the intervals from 515 to 1,854 ft, from 3,415 to 3,632 ft and below 4,816 ft, the differential pressure (ΔP) is negative indicating underbalanced drilling conditions because of the use of inappropriate drilling mud density. Such conditions put the well into great risk.
- Below the depth of 5,305 ft, the penetration rate (R) and differential pressure (ΔP) surprisingly show the same response, as they both decrease, probably due to the increase of drilling mud density.

5.4.3 Comparison of differential pressure and penetration rate for Komotini well

The differential pressure, the drilling mud pressure and the drilling mud pressure gradient for each interval of Komotini well are computed by the equations (5.9), (5.10) and (5.11), respectively, and are shown in Table 5.9.

Table 5.9: Computation of Differential Pressure for Komotini well

# Interval	Depth-D	Penetration Rate-R	Drilling mud density-ρ		Mud Pressure Gradient-G_m	Mud Pressure-P_m	Formation Pressure-P_f	Differential Pressure-ΔP
	ft	ft/hr	kg/dm³	lb/gal	psi/ft	psi	psi	psi
1	997	52.1	1.20	10.01	0.521	519	445	75
2	1,591	44.2	1.18	9.85	0.512	815	614	201
3	2,041	28.1	1.19	9.93	0.516	1,054	779	275
4	2,628	36.0	1.18	9.85	0.512	1,346	1,237	109
5	3,150	34.4	1.16	9.68	0.503	1,585	1,508	78
6	3,432	22.9	1.16	9.68	0.503	1,728	1,555	172
7	3,960	24.6	1.17	9.76	0.508	2,011	1,878	132
8	4,222	21.1	1.17	9.76	0.508	2,144	1,954	190
8a	4,236	4.4	1.18	9.85	0.512	2,169	1,508	661
9	4,239	2.9	1.18	9.85	0.512	2,171	1,462	708
10	4,432	17.4	1.18	9.85	0.512	2,270	1,770	500
11	4,882	15.8	1.20	10.01	0.521	2,542	2,343	200
12	4,921	3.9	1.19	9.93	0.516	2,541	1,878	664
13	4,944	3.7	1.20	10.01	0.521	2,575	1,867	707
14	5,056	18.6	1.21	10.10	0.525	2,655	2,351	304
14a	5,138	11.2	1.19	9.93	0.516	2,653	2,211	443
12a	5,210	6.0	1.20	10.01	0.521	2,713	2,025	688
15	5,335	15.6	1.19	9.93	0.516	2,755	2,409	346
13a	5,623	10.5	1.21	10.10	0.525	2,953	2,682	271

According to the above computations shown in Table 5.9, the diagrams of penetration rate and differential pressure over depth (Figure 5.10a and 5.10 b, respectively) can be constructed. By juxtaposing the diagram in Figure 5.10, the variation of both, penetration rate and differential pressure, is analyzed.

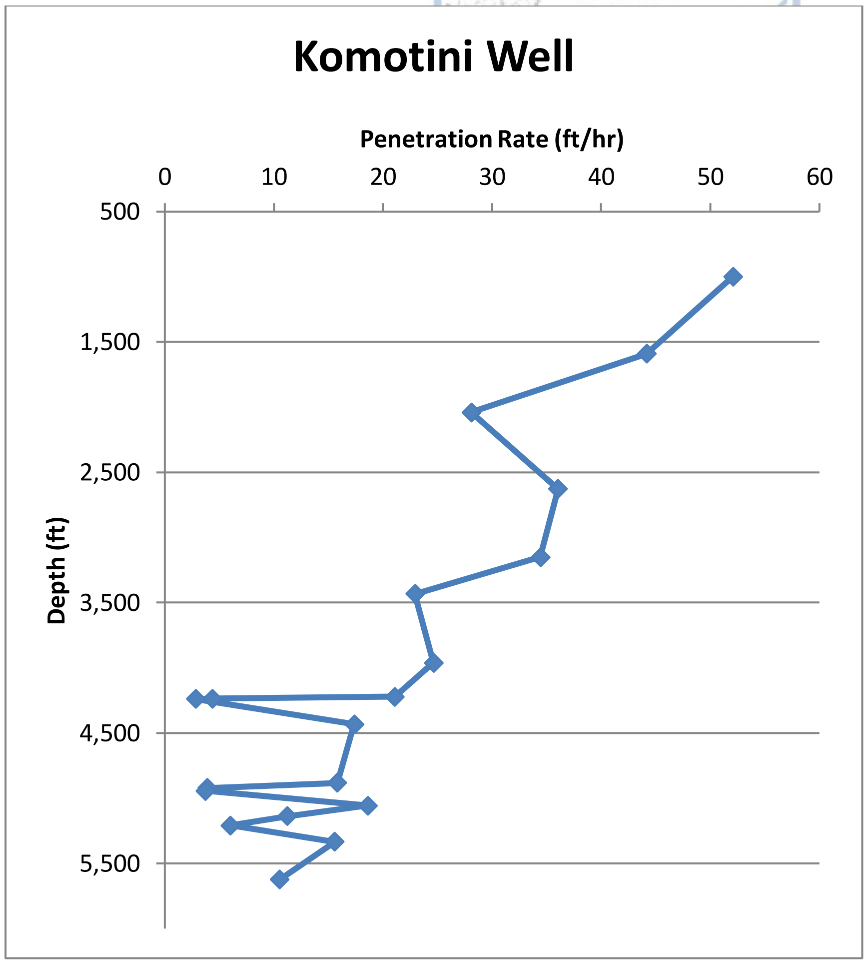

(a)

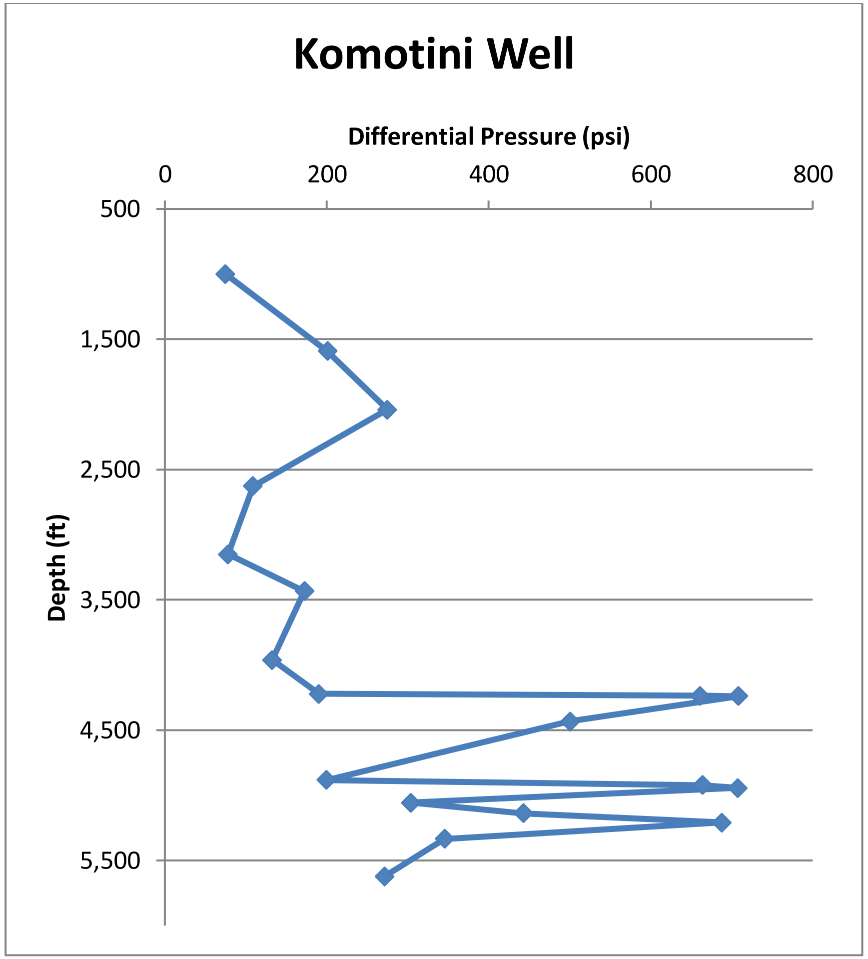

(b)

Figure 5.10: (a) Penetration rate over depth; (b) Differential pressure over depth for Komotini well

The diagrams of the penetration rate and differential pressure over depth, which are shown in Figure 5.10, are juxtaposed in order to identify their correlation:

- In general, the penetration rate (R) changes inversely with differential pressure (ΔP) over depth.
- From the surface up to 2,041 ft, the responses of penetration rate (R) and differential pressure (ΔP) are the expected, where the first normally decreases with depth, due to the higher compaction of soft formations, such as sand and gravel alternating with clay, and the last increases over depth.
- In the interval from 2,041 to 2,628 ft, the penetration rate (R) increases over depth, owing to the change of bit type form RS to RM. As a result, the drilling of soft and unconsolidated alternations of sand with clay is more effective. In addition, the differential pressure (ΔP) follows the expected decrease.
- The responses of penetration rate (R) and differential pressure (ΔP) show that both slightly decrease between 2,628 and 3,150 ft. This is probably due to the slight reduction in both drilling mud density and formation pressure gradient as well as the transition from loose sediments (sand alternating with clay) to more consolidated alternations of sandstone and claystone.
- The replacing of the current RM bit by X3A bit causes a slight increase of penetration rate (R) and a corresponding decrease of differential pressure (ΔP) in drilling through the alternations of sandstone with claystone, in the interval from 3,432 to 3,960 ft.
- Between 3,960 and 4,236 ft, the penetration rate (R) continues to decrease due to the higher compaction of the sandstone alternating with claystone and siltstone, while the differential pressure (ΔP) increases, as expected.
- Below the depth of 4,236 ft, several bit types were used in drilling that directly affects the behavior of penetration rate (R) and differential pressure (ΔP), which nevertheless, are well-correlated, according to theory, in most intervals.
- Surprisingly both parameters present the same decreasing response in the interval from 4,432 to 4,882 ft, caused by the heterogeneity of the alternations of sandstone with claystone along with few layers of limestone at the bottom of this interval.

- The breccia below the depth of 5,335 ft, is characterized as a very heterogeneous formation, causing the decrease, in both, penetration rate (R) and differential pressure (ΔP).

6. Well Cost

The estimation and analysis of the well cost constitutes the final stage of the well design. It is obvious that well cost depends on the technical characteristics of the well and in many cases will affect the decision making about drilling of a proposed well.

6.1 Cost per foot

The criterion for bit selection is based on cost per foot (C), which can be described by the following equation (Rabia, 1985):

$$C = \frac{B + (T_t + t_r)C_R}{F} \tag{6.1}$$

where:

C: drilling cost for each bit being examined ($/ft)

B: drill bit cost ($)

C_R: rig cost per hour ($/hr)

t_r: rotating time (hr)

T_t: tripping time (hr)

F: footage or length of section drilled (ft)

In equation (6.1), it can be seen that the cost per foot or cost/ft depends on five variables and for a given bit cost (B), and hole section (F), cost per foot will be highly sensitive to changes in rig cost per hour (C_R), tripping time (T_t) and rotating time (t_r). Assuming that all the other variables remain constant, the rotating time (t_r) is directly proportional to cost per foot. As for the trip time, it includes the total of the “dead” times required to:

1. Run the drill string in the wellbore at the depth where the drilling starts for the current bit.

2. Add drill pipes on the drill string to deepen the wellbore from the starting depth till the end of the current bit run.
3. Pull the drill string out of the wellbore in order to change the bit.

Tripping time is normally estimated from the drilling records and implies the total time for running in and pulling out of the wellbore a specific drill bit for every interval to be drilled. In addition, it is usually expressed in hr/1,000 ft. Unfortunately, tripping time for the three wells under study is not available.

In such a case, where there is a lack of drilling data, tripping time can be estimated by considering an average time of 1.5 min for adding each new drill pipe on the drill string. The same time is also considered for removing a drill pipe from the drill string as well. Furthermore, the estimation of “dead” times can be conducted based on the data of the following Table 6.1, where the average values of tripping times depending on wellbore diameter are given. Moreover, the interpolation method can be also used for estimating the tripping time of the intermediate depths.

Table 6.1: Estimation of the average tripping time in hours (Stamataki, 2003)

Bit Pull Out Depth (ft)	Wellbore Diameter-D (in)		
	D<8¾	8¾<D<9⅞	D>9⅞
2,000	1.50	3.00	4.50
4,000	2.50	4.20	5.75
6,000	3.50	5.40	7.00
8,000	4.70	6.50	8.00
10,000	5.80	7.25	9.00
12,000	7.00	8.25	10.25
14,000	8.25	9.25	11.50
16,000	9.75	10.25	12.50
18,000	11.00	11.25	13.75
20,000	11.80	12.25	15.00

The valuable method of cost per foot allows for the analysis of the results in order to choose the most appropriate and economical drill bit for each interval, and thus the one, with the lowest value of C ($/ft). On the basis of this method, alternative scenarios can be assessed about the use of different rigs, other drill bit types as well as different drilling mud environments.

In this study tripping time (T_t) is estimated as described above for all the three wells. In addition, the hourly rig cost (C_R) is taken as 900 \$/hr, since the average daily rig cost is considered to be 20,000 \$/day for onshore rig and 120,000 \$/day for offshore rig. In addition, the following Table 6.2 presents the cost (B) of the drill bits used in the three wells under study:

Table 6.2: Drill bit cost (B) for the three wells under study (Adam, Maleas & Misirlis, 1978)

Drill Bit		Amounts in U.S. Dollars		
Size (in)	**Type**	**Nestos 1**	**Nestos 2**	**Komotini**
17½	RS	13,860	11,880	1,980
17½	RMTA	19,800	-	-
12¼	RS	6,930	10,780	1,540
12¼	RM	7,700	13,850	2,310
12¼	X3A	-	-	2,960
8½	X1G	-	-	2,352
8½	J22	-	-	2,229
8½	J44	-	-	2,500

6.1.1 Cost Evaluation for Nestos 2 Well

The cost per foot (C) for each interval of Nestos 1 well is computed via the equation (6.1) according to the drill bit cost (B), the rotating time (t_r), the tripping time (T_t) and the footage (F) which are presented in the following Table 6.3:

Table 6.3: Computation of cost per foot for Nestos 1 well

# Interval	Depth (ft)	D (in)	Type	B (\$)	t_r (hr)	T_t (hr)	F (ft)	C (\$/ft)
1	1,079	17 ½	RS	13,860	31.00	2.43	1,079	40.71
2	2,274	17½	RS	13,860	25.40	4.67	1,194	34.27
3	2,395	17½	RS	13,860	3.45	4.75	121	174.95
4	2,700	17½	RS	13,860	14.45	4.94	305	102.61
5	2,897	17½	RS	13,860	15.45	5.06	197	164.18
6	2,999	17½	RMTA	19,800	13.05	5.12	102	355.50
7	3,225	17½	RS	13,860	28.00	5.27	226	193.48

Table 6.4: Computation of cost per foot for Nestos 1 well (continued)

# Interval	Depth (ft)	D (in)	Type	B ($)	t_r (hr)	T_t (hr)	F (ft)	C ($/ft)
8	3,599	17½	RS	13,860	30.35	5.50	374	123.32
9	4,029	12¼	RM	7,700	10.35	5.77	430	51.67
10	4,718	12¼	RS	6,930	21.00	6.20	689	45.59
11	5,112	12¼	RS	6,930	16.20	6.44	394	69.37
12	5,413	12¼	RS	6,930	17.40	6.63	302	94.62
13	5,686	12¼	RS	6,930	18.40	6.80	272	108.75
14	5,964	12¼	RS	6,930	16.05	6.98	279	99.17

Based on the above results, the variation of cost per foot (C) over depth for Nestos 1 well is presented below, in Figure 6.1.

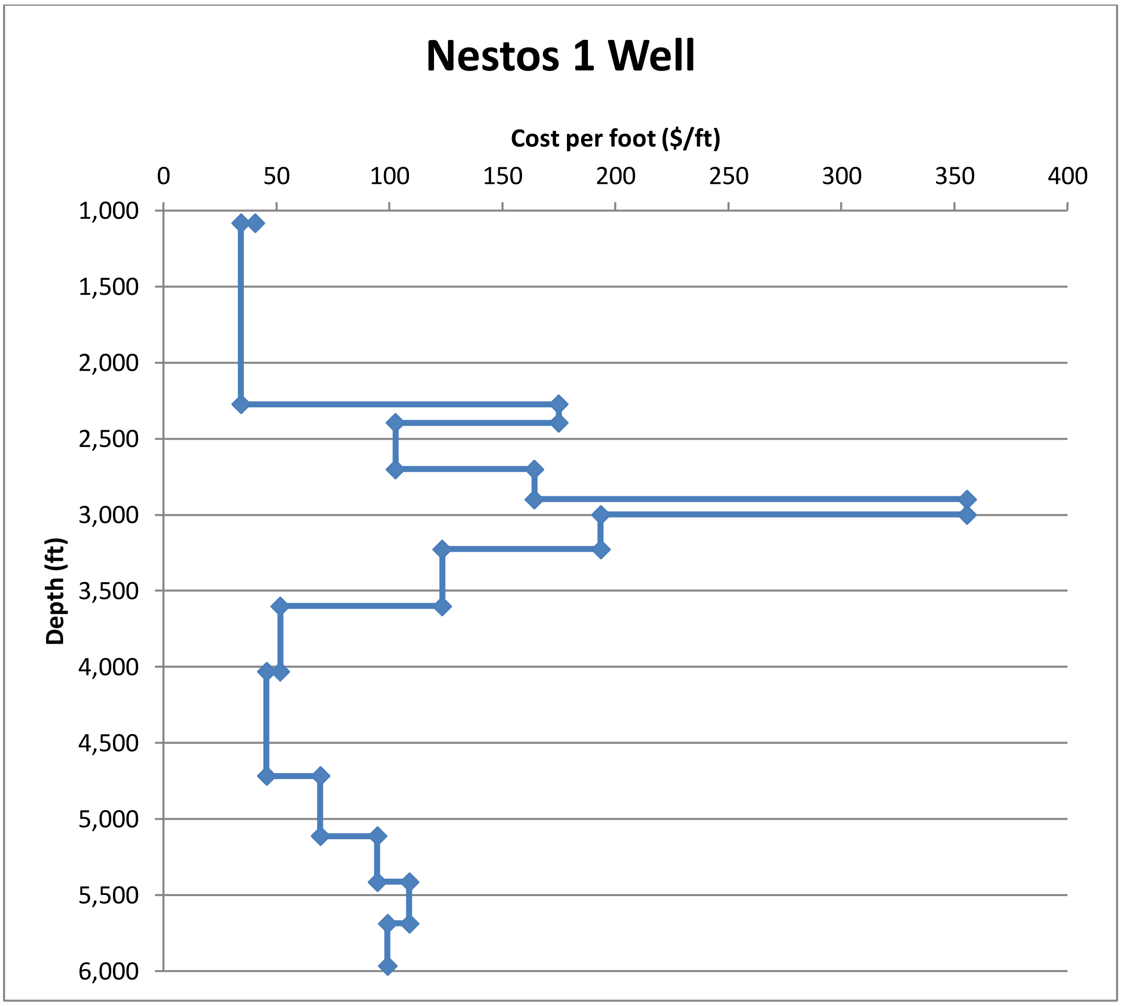

Figure 6.1: Diagram of Cost per foot over depth for Nestos 1 well

The evaluation of cost per foot for each interval of Nestos 1 well is outlined below, according to Figure 6.1.

The interval from the surface up to 2,897 ft is drilled by an RS drill bit of 17½" in diameter, and thus, the drill bit cost is constant. Regardless of the increase in tripping time at 4.67 hr, in the interval from 1,079 to 2,274 ft, the cost per foot slightly decreases due to the reduction of the rotating time at 25.4 hr, since the length of this interval approaches the length of the previous interval (from the surface up to 1,079 ft). Despite the extreme low rotating time at 3.45 hr accompanied by the expected increase in tripping time at 4.75 hr, the cost per foot significantly increases owing to the small length of footage (121 ft), in the interval from 2,274 to 2,395 ft. Then, the increase in both rotating time and tripping time at 14.45 hr and 4.94 hr, respectively, should lead to an increase of cost per foot in the interval between 2,395 and 2,700 ft. However, the much higher footage achieved (over 2.5 times than in the previous interval) contributes to the decrease of cost per foot.

There is a constant increase in cost per foot in the interval from 2,700 to 2,999 ft caused by the increase in both rotating time and tripping time, which vary from 13.05 to 15.45 hr and from 5.06 to 5.12 hr, respectively, as well as by the continuous decrease of footage achieved (102-197 ft). In addition, the replacement of the current drill bit of RS type with an RMTA bit, which is more expensive, enhances further the increase of cost per foot in the last section of this interval.

A decreasing trend of cost per foot is obvious between 2,999 and 4,718 ft, where both rotating time and tripping time vary from 10.35 to 30.35 hr and from 5.27 to 6.20 hr, respectively. The replacing of the RMTA drill bit with an RS drill bit for the next 600 ft is the main reason for this decrease in cost per foot. Furthermore, the constant decrease of footage, ranging from 226 to 689 ft, slightly enhances the decrease of cost per foot. Additionally, the lowering of the drill bit size from 17½" to 12¼" below the depth of 3,599 ft contributes to the further decrease in cost per foot. Moreover, the application of the two drill bit types of RM and RS with 12¼" in diameter lead to a further reduction of cost per foot, in the interval between 3,599 and 4,718 ft.

In the interval from 4,718 to 5,686 ft, the fact that both rotating time and tripping time increase, ranging from 16.2 to 18.4 hr and from 6.44 to 6.8 hr, respectively, while the footage decreases, varying between 272 and 394 ft, yields into a continuously increase of cost per foot.

Finally, in the interval between 5,686 and 5,965 ft, the cost per foot decreases due to the lower rotating time at 16.05 hr and the higher footage achieved of 279 ft compared to the previous interval.

6.1.2 Cost Evaluation for Nestos 2 Well

The following Table 6.4 presents the drill bit cost (B), the rotating time (t_r), the tripping time (T_t) and the footage (F) which constitute the basis for the computation of cost per foot (C) via equation (6.1).

Table 6.5: Computation of cost per foot for Nestos 2 well

# Interval	Depth (ft)	D (in)	Type	B ($)	t_r (hr)	T_t (hr)	F (ft)	C ($/ft)
1	515	17½	RS	11,880	14.00	1.16	515	49.55
1a	1,854	17½	RS	11,880	15.45	4.17	1339	22.07
2	2,165	17½	RS	11,880	22.15	4.60	312	115.37
3	3,140	17½	RS	11,880	30.30	5.21	974	44.99
4	3,222	17½	RS	11,880	3.45	5.26	82	240.45
6	3,415	17½	RS	11,880	11.30	5.38	194	138.95
7	3,632	12¼	RS	10,780	5.15	5.52	217	94.13
8	4,121	12¼	RS	10,780	17.30	5.83	489	64.63
9	4,386	12¼	RS	10,780	14.45	5.99	266	109.79
10	4,564	12¼	RM	13,850	12.00	6.10	177	170.14
11	4,816	12¼	RS	10,780	15.00	6.26	253	118.41
12	5,305	12¼	RS	10,780	18.00	6.57	489	67.28
13	5,643	12¼	RS	10,780	17.30	6.78	338	96.02

According to the data of Table 6.3, the changes of cost per foot (C) in each drilled interval of Nestos 2 well are demonstrated in the following Figure 6.2.

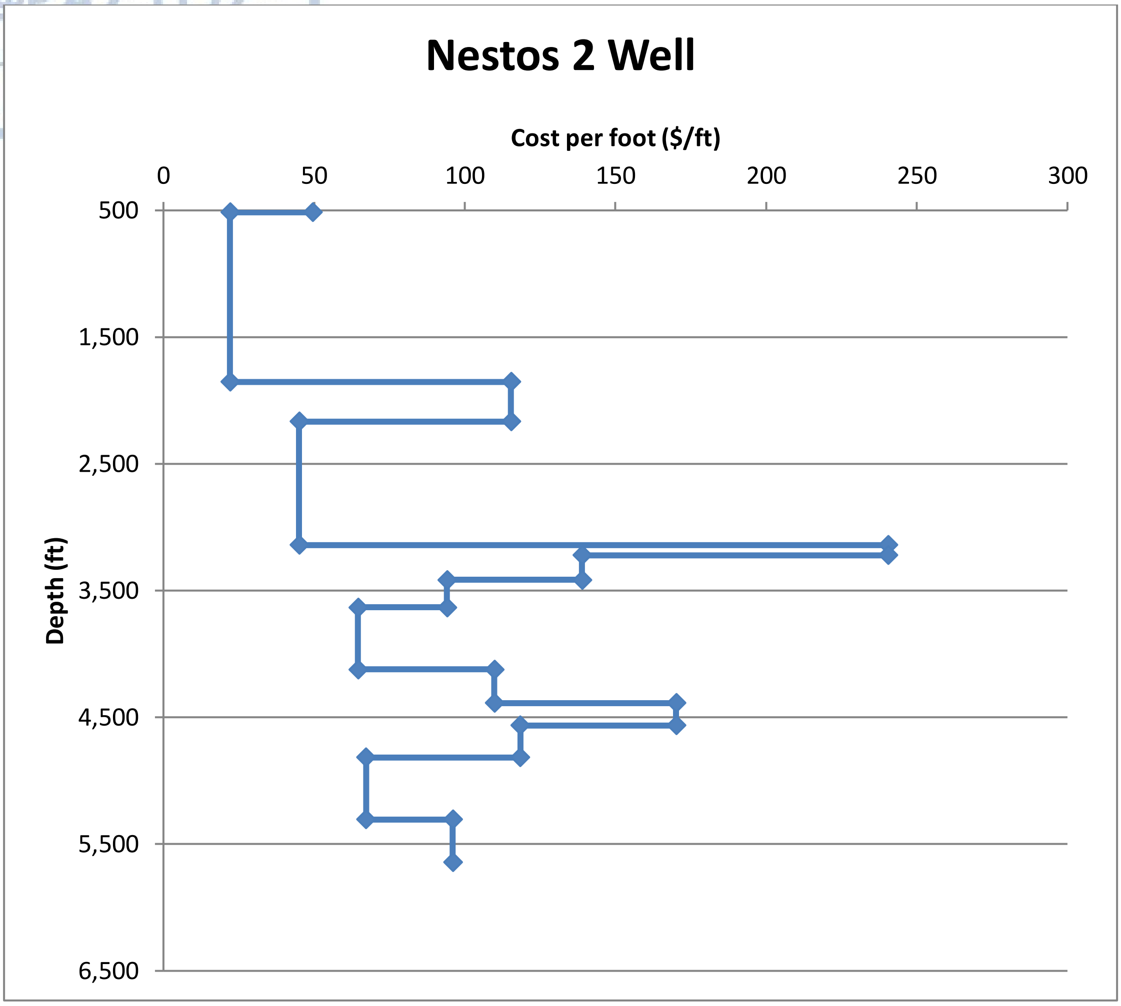

Figure 6.2: Diagram of Cost per foot over depth for Nestos 2 well

Figure 6.2 shows the cost per foot (C) over depth for Nestos 2 well providing the ability to evaluate its changes.

From surface up to 3,415 ft, drilling was conducted with an RS drill bit of 17½" in diameter, resulting in a constant drill bit cost. Despite the increase in both rotating time and tripping time at 15.45 hr and at 4.17, respectively, the cost per foot decreases over depth due to the high increase of footage achieved (1,339 ft), in the interval between 515 and 1,854 ft. The small footage of 312 ft achieved in the next interval (1,854-2,165 ft) causes again an increase in cost per foot, while there is also a further increase in both rotating time and tripping time at 22.15 hr and at 4.6 hr, respectively. Then, in the interval from 2,165 to 3,140 ft, the cost per foot decreases again due to the increase of the footage achieved (974 ft), whereas there is also an increase in both rotating time at 30.3 hr and tripping time at 5.21 hr. Moreover, the reduction of footage at 82 ft, which is drilled by low rotating time at 3.45 hr and slightly increased tripping time at 5.26 hr, leads to the significant increase in cost per foot in the interval between 3,140 and 3,222 ft (higher decrease in footage than rotating time). In addition, in the last interval drilled with the 17½" RS drill bit (3,222 to 3,415 ft) the cost per foot decreases due to the higher increase of footage achieved (194 ft) compared to rotating time (11.3 hr), while the effect of tripping time (5.38 hr) on cost per foot is here negligible.

Below the depth of 3,415 ft, drilling was performed by a drill bit of 12¼" in diameter which greatly affects the value of cost per foot contributing into its decrease, since now the drill bit cost is lower than the intervals above.

An obvious decreasing trend of cost per foot is presented in the interval from 3,415 to 4,121 ft which are drilled by a 12¼" RS drill bit. The increase of footage at 217 ft along with the decrease of rotating time at 5.15 hr and the slight increase of tripping time at 5.52 hr contribute to the decrease in cost per foot, in the interval between 3,415 and 3,632 ft. As for the next interval (3,632-4,121 ft), the extent of the increase in both footage and rotating time, where the first is 489 ft and the last is 17.3 hr, causes a further decrease of cost per foot. In this interval, the increase in tripping time at 5.83 hr did not invert the imminent decreasing trend of cost per foot as well.

Then, the cost per foot constantly increases in the interval from 4,121 to 4,564 ft on account of the continuous decrease in both footage and rotating time, which varies from 177 to 266 ft and 12 to 14.45 hr, respectively. The increase in cost per foot is slightly affected by the increase in tripping time which ranges within 5.99 and 6.1 hr. Additionally, the replacement of the RS drill bit with an RM bit leads to the further increase of cost per foot owing to the higher drill bit cost, in the last interval from 4,386 to 4,564 ft.

Afterward, below the depth of 4,564 ft, the RM drill bit was replaced by an RS drill bit leading to a decrease in drill bit cost. The cost per foot constantly decreases in the interval from 4,564 to 5,305 ft due to the increase in footage achieved which ranges from 253 to 489 ft and to the decrease in drill bit cos. At the same time, the increase in both rotating time and tripping time, which vary from 15 to 18 hr and from 6.26 to 6.57 hr, respectively, is low, and thus, their effect on cost per foot is low, too.

Lastly, the higher decrease of footage at 338 ft in comparison to the slight decrease of rotating time at 17.3 hr and the slight increase of tripping time at 6.78 hr, resulting in the decrease of cost per foot, in the interval between 5,305 and 5,643 ft.

6.1.3 Cost Evaluation for Komotini Well

Table 6.5 contains all the required data, including the drill bit cost (B), the rotating time (t_r), the tripping time (T_t) and the footage (F), which constitute the basis for the computation of cost per foot (C), according to equation (6.1).

Table 6.6: Computation of cost per foot for Komotini well

# Interval	Depth (ft)	D (in)	Type	B ($)	t_r (hr)	T_t (hr)	F (ft)	C ($/ft)
1	997	17½	RS	1,980	19.15	2.24	997	21.29
2	1,591	12¼	RS	1,540	13.45	3.58	594	28.40
3	2,041	12¼	RS	1,540	16.00	4.53	449	44.53
4	2,628	12¼	RM	2,310	16.30	4.89	587	36.41
5	3,150	12¼	RM	2,310	15.15	5.22	522	39.57
6	3,432	12¼	RM	2,310	12.30	5.39	282	64.63
7	3,960	12¼	X3A	2,960	21.45	5.72	528	50.27
8	4,222	12¼	X3A	2,960	12.45	5.89	262	70.87
8a	4,236	12¼	X3A	2,960	3.00	5.90	13	769.89
9	4,239	8½	X1G	2,352	1.15	5.90	3	2,650.65
10	4,432	8½	X1G	2,352	11.15	6.02	194	91.98
11	4,882	8½	J22	2,229	28.45	6.30	449	81.22
12	4,921	8½	J22	2,229	10.15	6.33	39	509.45
13	4,944	8½	J44	2,500	6.15	6.34	23	598.33
14	5,056	8½	X1G	2,352	6.00	6.41	112	121.21
14a	5,138	8½	X1G	2,352	7.30	6.46	82	179.67
12a	5,210	8½	J22	2,229	12.00	6.51	72	303.20
15	5,335	8½	X1G	2,352	8.00	6.58	125	124.15
13a	5,623	8½	J44	2,500	27.45	6.76	289	115.32

In Figure 6.3, the cost per foot (C) for each drilled interval of Komotini well is plotted against depth in order to evaluate its variations.

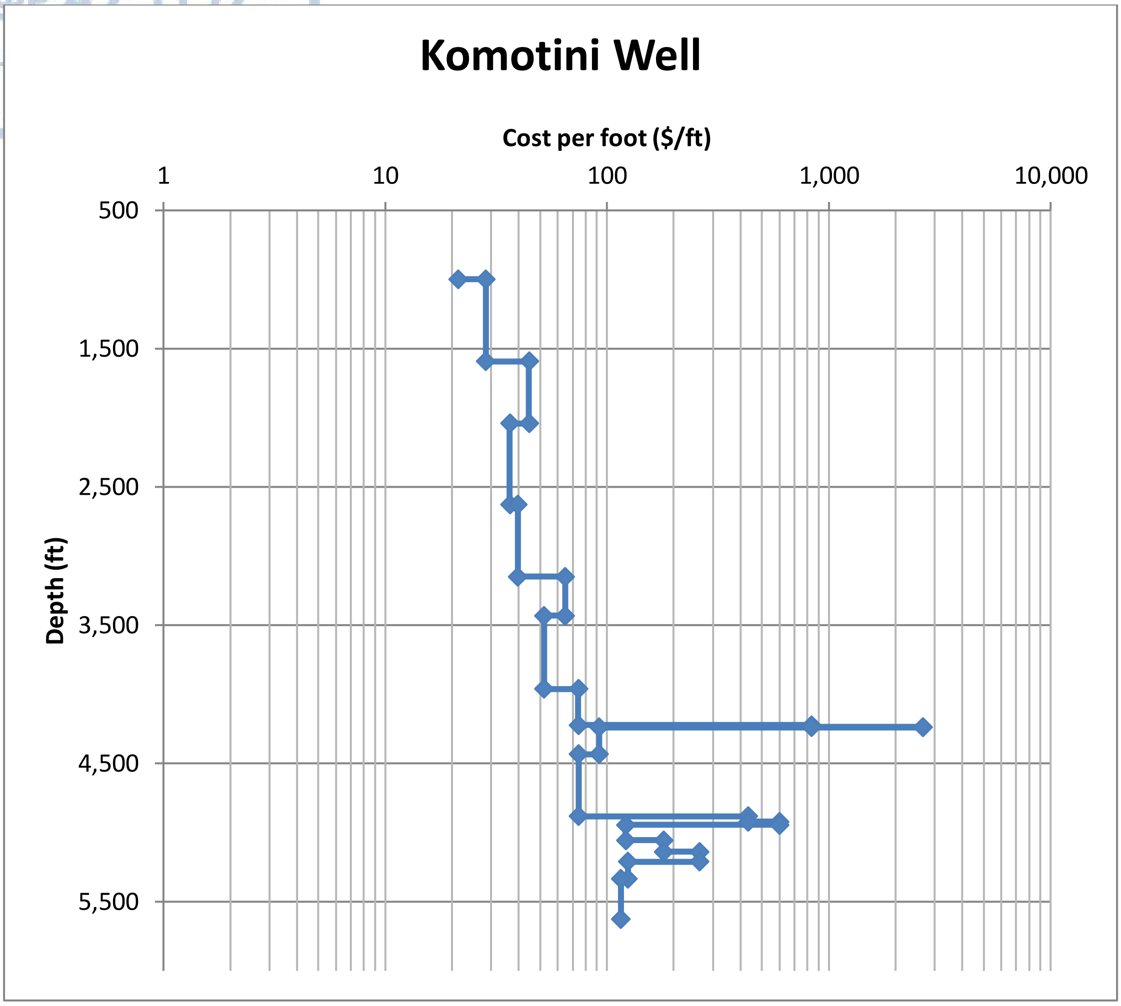

Figure 6.3: Diagram of Cost per foot over depth for Komotini well

According to Figure 6.3, the evaluation of the changes in cost per foot (C) over depth is given below:

In general, the cost per foot constantly increases from the surface up to 4,239 ft. However, there are two intervals where the cost per foot appears to decrease temporarily (from 2,041 to 3,150 ft and from 3,432 to 3,960 ft). It should be noticed that besides the three different drill bit sizes of 17½", 12¼" and 8½", there was also a variety of drill bit types, including RS, RM, X3A and X1G used in the drilling of the Komotini well.

Despite the decrease in drill bit size from 17½" to 12¼", leading to a reduction of drill bit cost, the cost per foot increases in the interval from 997 to 1,591 ft, due to the higher decrease of footage achieved (594 ft) compared to drill bit cost and rotating time at 1,540 $ and 13.45 hr, respectively. In the same interval, the tripping time increased at 3.58 hr. Then, the increase in both rotating time and tripping time at 16 hr and 4.53 hr, respectively, accompanied by the decrease of footage at 449 ft contribute to the further increase of cost per foot in the interval from 1,591 to 2,041 ft. Afterwards, the change of the drill bit type from RS to RM, which is suitable for drilling medium hard formations, results in decrease of cost per foot in the next interval from 2,041 to 2,628 ft, regardless the increase in drill bit cost (2,310 $), rotating time (16.3 hr), tripping time (4.89 hr) and footage (587 ft). Then, an increasing trend of cost per foot is presented in the interval from 2,628 to 3,432 ft, owing to the greater decrease of footage which ranges within 282 and 522 ft than of rotating time which varies from 12.3 to 15.15 hr, while the tripping time continues to slightly increase downwards (5.22-5.39 hr).

By replacing the current RM drill bit with the imported by Hughes X3A drill bit, the cost per foot decreases in the interval which lies from 3,432 to 3,960, due to the lower drill bit cost at 2,096 $ and the higher drill bit performance in comparison with the previous interval, since the footage of 528 ft is drilled in 21.45 hr (rotating time) with 5.72 hr of tripping time. In the interval between 3,960 and 4,236 ft, the continuous decrease in both rotating time and footage lead to an increase of cost per foot, as the reduction in rotating time is less than the reduction in the footage, where both vary from 3 to 12.45 hr and from 13 to 262 ft, respectively. Furthermore, the increase of tripping time (5.89-5.9 hr) slightly affects the increase in cost per foot.

Below the depth of 4,236 ft, drilling was performed with a lower drill bit size of 8½" in diameter and by using different drill bit types, such as the milled tooth bit of X1G and the insert bits of J22 and J44, all manufactured by Hughes.

Despite the fact that the 8½" X1G drill bit has a lower bit cost at 2,352 $, the extreme low footage of 3 ft in the next interval causes the excessive increase in cost per foot. Then, the rapid decrease in cost per foot in the interval from 4,239 to 4,432 ft is mainly caused by the great increase in footage at 194 ft, regardless the increase in both rotating time and tripping time at 11.15 hr and 6.02 hr, respectively.

In the interval from 4,432 to 4,882 ft, the use of the J22 drill bit which costs 2,299 $, instead of the X1G drill bit, further reduces the cost per foot due to the greater increase in footage at 449 ft than in rotating time at 28.45 hr and in tripping time at

6.3 hr, except for the lower drill bit cost. Moreover, the cost per foot significantly increases in the next interval which lies between 4,882 and 4,921 ft, as a result of the decrease in footage at 39 ft which is greater than the increase in rotating time at 10.15, whereas the effect of tripping time (6.33 hr) on cost per foot is low.

In addition, the J22 drill bit was replaced by J44 drill bit in the interval from 4,921 to 4,944 ft, which is suitable for drilling harder formations, and thus, more expensive (2,500 $), thus contributing to a further increase in cost per foot. The increase in cost per foot is also enhanced by the reduction of footage achieved (23 ft), while the effect of both rotating time (6.15 hr) and tripping time (6.34 hr) on cost per foot is practically low.

Then, the interval from 4,944 to 5,056 ft was drilled by an X1G drill bit which replaced the J44 drill bit, yielding into a serious decrease of cost per foot. The cost per foot also increases in the next interval between 5,056 and 5,138 ft, due to the combination of the decrease in footage at 82 ft and the increase in both rotating time and tripping time at 7.3 hr and 6.46 hr, respectively.

In the interval from 5,138 to 5,210 ft, the further decrease in footage at 72 ft accompanied by the further increase in both rotating time and tripping time at 12 hr and 6.51 hr, respectively, lead to the significant increase in cost per foot, even though a change in drill bit type took place, where the J22 drill bit is cheaper than X1G drill bit. Additionally, the next interval between 5,210 and 5,335 ft was drilled by using the X1G drill bit which replaced again the J22 drill bit, resulting in the significant decrease in cost per foot due to the increase of footage at 125 ft along with the decrease of rotating time at 8 hr, whereas both the drill bit cost and tripping time slightly increase at 2,352 $ and 6.58 hr, respectively.

Finally, the last footage of 289 ft was drilled in 27.45 hr (rotating time) with a slight increase in tripping time at 6.76 hr. The more expensive J44 drill bit which replaced the previously used X1G drill bit has caused a slight decrease in cost per foot due to the greater increase of footage achieved in comparison to the other three parameters.

6.2 Cost comparison for Nestos 1 and Nestos 2 wells

The small distance that separates the neighboring wells of Nestos 1 and Nestos 2 provides the ability to make an evaluation between the drilled intervals in both wells, on the basis of cost per foot. Under the assumption of similar lithostratigraphic columns and of constant drilling mud density which is approximately the same in both wells, Figure 6.4 is constructed based on the data of Tables 6.3-6.4, illustrating side by side the variations of cost per foot over depth for Nestos 1 and Nestos 2 wells.

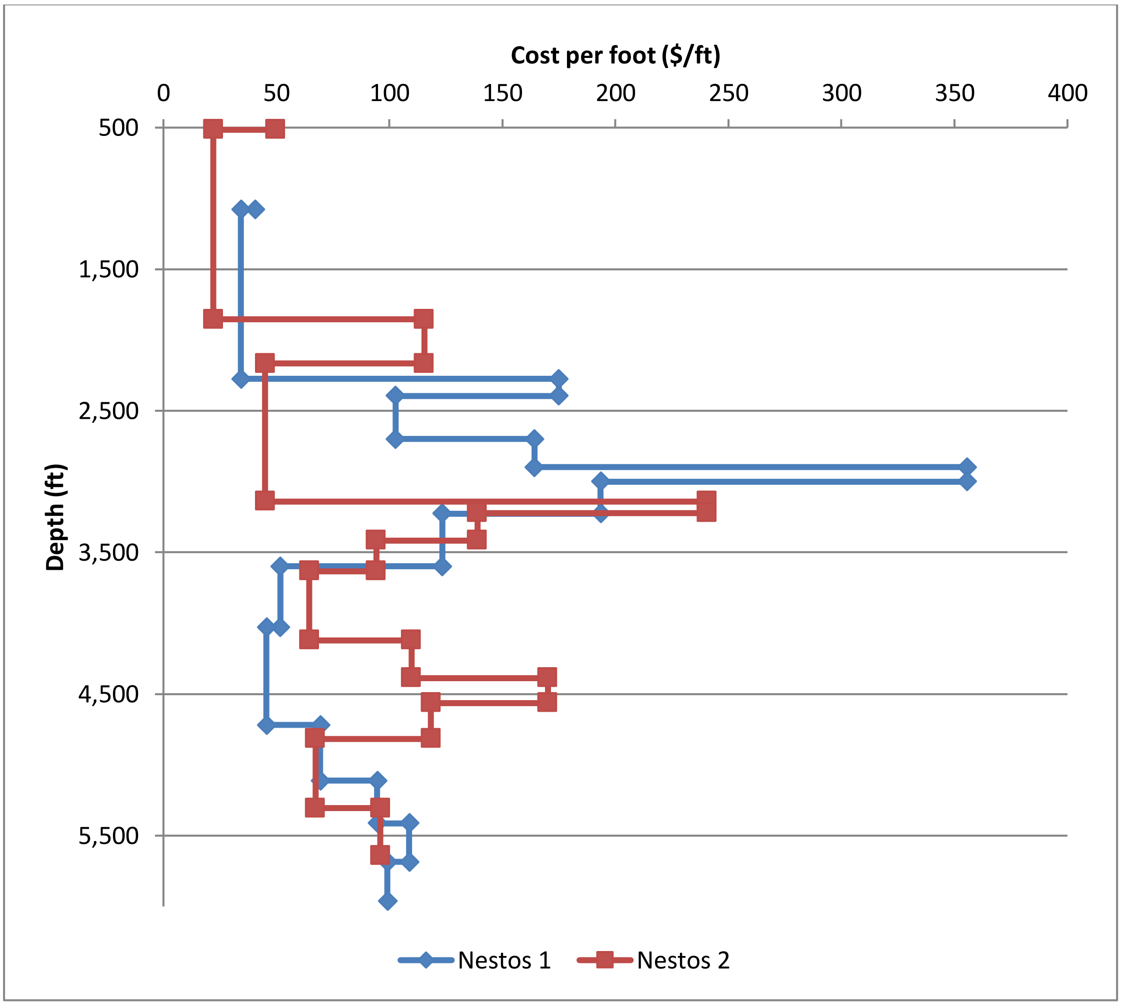

Figure 6.4: Cost per foot comparison between Nestos 1 and Nestos 2 wells

All the intervals of Nestos 1 and Nestos 2 wells were drilled by drill bits of a diameter greater than 9⅞". As a result, the estimated tripping time in both wells is identical for a specific interval. Consequently, the comparison of cost per foot between these wells does not take into account the tripping time.

According to Figure 6.4, it is obvious that the cost per foot in Nestos 2 well is generally less than Nestos 1 well for the interval ranging from surface up to 3,599 ft, except for four intervals, as less expensive drill bits of 17½" in diameter were used in Nestos 2 well operated at lower rotating times than in Nestos 1 well. Additionally, in Nestos 2 well, greater footage was achieved in this interval contributing to further reduction of cost per foot in comparison to Nestos 1 well.

As mentioned above, there are four intervals in Nestos 2 well with a higher cost per foot than in Nestos 1 well. The first two lie from the surface up to 515 ft and from 1,854 to 2,165, respectively, whereas the other two intervals are successive, between 3,140 and 3,415 ft. Despite the differences in drill bit cost and rotating time in these intervals, the parameter that greatly affects cost per foot in Nestos 2 well is mostly the footage which is significantly less than the footage achieved in Nestos 1 well, at the same depth intervals.

There is a zone, from 3,599 to 4,816 ft, where the cost per foot in Nestos 2 well is constantly greater than in Nestos 1 well, mainly owing to the difference between the costs of the drill bits used in these wells. Below the depth of 3,599 ft, the drill bit size decreases from 17½" to 12¼" in diameter, leading to a significant reduction in cost per foot for Nestos 1 well. On the other hand, the same change in drill bit size took place when drilling the Nestos 2 well beneath the 3,632 ft, but the decrease in cost per foot is not as high as in the case of Nestos 1 well since now the cost of the drill bits is only slightly reduced. Moreover, the difference in cost per foot among the wells of Nestos 1 and Nestos2 is also enhanced by the fact that in Nestos 2 well the zone is separated into four intervals ranging from 253 to 489 ft which have been penetrated within 12 to 17.3 hr, where drilling of this zone in the Nestos 1 well is subdivided into just two intervals of 430 ft and 689 ft with rotating times at 10.35 hr and 21 hr, respectively.

Below the depth of 4,816 ft, the cost per foot for both wells seems to be approximately equal, even though there is an extreme difference in cost of the 12¼" RS drill bits which were used in these wells. In Nestos 1 well, the footage of the three consecutive intervals, between 4,718 and 5,686 ft, constantly decreases downwards at 394 ft, 302 ft, and 272 ft, respectively, leading to a continuous increase in cost per foot, and thus, the difference in the cost of the drill bits used for these wells is compensated. In addition, the great footage at 489 ft between 4,816 and 5,305 ft in combination with the decrease in footage at 338 ft for the last interval, from 5,305 to

5,643 ft, of the Nestos 2 well, contribute to the significant decrease and increase in cost per foot, respectively, approaching the values of cost per foot for the corresponding intervals of Nestos 1 well. Moreover, the rotating time varies from 16.2 to 18.4 hr and from 17.3 to 18 hr for Nestos 1 and Nestos 2 wells, respectively, indicating its low effect on cost per foot for the intervals beneath 4,816 ft.

7. Conclusions and Future Research

7.1 Conclusions

According to the analysis and processing of the drilling data that took place in the context of this study, valuable conclusions emerge about the technical and economic performance of drill bits. These conclusions are presented below:

- Drillability generally decreases over depth when using a specific drill bit type and size that operates with approximately constant drilling mud density due to the exposure of deeper formations in higher compaction and stress state in comparison to formations which lie in lower depths. Additionally, formations that lie near the surface often consist of loose sediments requiring lower specific energy to be drilled, and thus, being more drillable, than formations which lie in higher depths where their sediments are more compacted, resulting to higher values of specific energy or presenting lower drillability.
- According to the d-exponent method used for estimating the formation pore pressure in the wells of Nestos 1, Nestos 2 and Komotini, no zone of abnormal pressure was observed. Regarding Nestos 1 and Nestos 2 wells, this is due to the fact that only a portion of drilling data was available, from the surface up to a certain depth.
- Small deviations of d_{mod}-exponent around the linear trendline, corresponding to the normal values of $d_{mod\text{-}n}$-exponent, are mostly related to change in lithology or to the replacement of the drill bit type with another.
- In Nestos 2 well, there were four intervals (515-1,854 ft, 3,415-3,632 ft, and the two last successive intervals from 4,816 to 5,643 ft) where drilling was conducted underbalanced ($P_m < P_f$) exposing the wellbore safety in high risk.
- The differential pressure (ΔP) is inversely proportional to the penetration rate (R) for the most intervals in the three wells under study.
- The use of a specific drill bit type and size (constant drill bit cost) which operates under constant drilling mud density and with no significant changes in the values of weight applied on bit (WOB) and rotary speed (N), usually leads to a constant increase in tripping time (t_r) over depth due to the higher compaction of the formations. As a result, cost per foot is expected to increase constantly over depth,

as it can be clearly seen in the plots of cost per foot over depth, especially in the wells of Nestos 1 and Komotini.

- In Komotini well, it is obvious that cost per foot is increased downwards, approaching linearity, whereas in the Nestos 1 well the linear increasing trend of cost per foot is interrupted by a small decrease achieved between 2,999 and 4,718 ft. As for Nestos 2 well, there is no apparent increasing or decreasing trend, implying that its lithology is more complex in comparison to the other wells.
- Cost per foot (C) is highly affected by changes in rotating time (t_r) and footage (F) drilled, and thus, by the penetration rate (R_P) achieved in each interval when using a drill bit of specific type and size (constant drill bit cost), since the estimated tripping time (T_t) increases linearly with depth.
- The lowering of drill bit size causes a significant increase of drillability since now the volume of rock that is required to be excavated is less than before. In addition, cost per foot rapidly decreases with drill bit size due to the use of cheaper drill bits compared to the ones used in the intervals above.
- Assuming that drilling mud properties remain constant, the heterogeneous and weathered formations near surface directly affect the penetration rate which, in turn, leads to unexpected values of drillability, cost per foot as well as formation pore pressure at the depth of interest, far away from the expected values. As a consequence, the relation between differential pressure and penetration rate is significantly affected as well. Hence, the more homogeneous the formation to be drilled, the smoother the response of this formation regarding the parameters mentioned above.

Based on the comparative analysis between the neighboring wells of Nestos 1 and Nestos 2 the following results arise:

- There is an interval between 3,599 and 5,413 ft where the drillability of Nestos 1 well is constantly greater compared to the drillability of Nestos 2 well, even though drilling in both wells was conducted using two types of drill bits (RS and RM) and of the same size of 12¼" in diameter. The difference in drillability is mainly due to the presence of glauconite (friable mineral) which is alternated by sandstone in the Nestos 1 well, whereas the lithology of Nestos 2 well is more complex consisting of sandstone, conglomerate, and claystone interbedded with clay which followed by varves with interbeds of sandstone, claystone, siltstone and sandy marl in the lower part, in the upper and lower part, respectively. Consequently, higher penetration rates were achieved in the Nestos 1 well in comparison to Nestos 2 well.

- The same response, as in the case of drillability, is shown as well on the plot of cost per foot over depth in the interval ranging from 3,599 to 4,816 ft, but now the relation is inversed where the cost per foot of Nestos 1 well is constantly less than cost per foot in Nestos 2 well. This is due to the less rotating time achieved and the use of cheaper drill bits in Nestos 1 well than in Nestos 2 well.
- In the interval from 4,816 to 5,413 ft, the cost per foot in both wells is approximately equal. Even though higher footage was achieved in Nestos 2 well compared to Nestos 1 well, resulting in the reduction of cost per foot for Nestos 2 well, the high difference of drill bit cost between the neighboring wells compensated cost reduction.

7.2 Future Research

Future research regarding the technical and economic performance of the drill bits used in the three wells would take into account the variations in drilling mud density, even if they are too small. Considering appropriate equivalent mud density and other parameters of the hydraulic program, the effect of both drilling mud density and jet velocity on penetration rate could be evaluated and drillability, cost per foot, formation pore pressure and differential pressure at the depth of interest, could then be more accurately determined.

Additionally, several delays that caused serious problems in the drilling process, such as the delay in the arrival of the Hughes' drill bits to the site of Komotini well, should be considered for the computation of tripping time in an effort of a more precise economic evaluation of the drill bits based on cost per foot.

8. Bibliography

1. Adam A., Maleas, A. & Misirlis, D. (1978) *Comparison of Exploratory Wells of Nestos 1, Nestos 2, & Komotoni 1.* Diploma Thesis, School of Mining and Metallurgical Engineering, National Technical University of Athens.
2. Adams, N. J. (1985) *Drilling Engineering-A Complete Well Planning Approach.* Tulsa, Oklahoma USA, PennWell Publishing Company.
3. Beijing Faster Drilling Tools Limited (2017) *API 14 1/2 Kingdream New Steel Tooth Bit/Milled Tooth Bit/Rotary Rock Bits/Oil Drilling Bits*. Available from: http://www.fasterdrilling.com/en/products/triconebit/
4. Black, A. D., Bland, R. G., Curry, D. A., Ledgerwood L. W., Robertson H. A., Judzis, A., Prasad, U. & Grant, T. (2008) Optimization of Deep Drilling Performance with Improvements in Drill Bit and Drilling Fluid Design. *IADC/SPE Drilling Conference*. 4-6 March, Orlando, Florida. Available from: doi:10.2118/112731-MS
5. Bourgoyne Jr., A. T., Millheim, K.K., Chenevert M. E. & Young Jr., F. S. (1991) *Applied Drilling Engineering.* TX, Richardson.
6. Centala, P. K., Burley, M. M., Burnett, T., Ford, R. J. & Sinesi J. P. (2006) Unlocking Two-Cone-Bit Potential: Technology, People, and Planning Make It Possible and the Lessons Learned. *IADC/SPE Drilling Conference*. 21-23 February, Miami, Florida, USA. Available from: doi: 10.2118/99017-MS
7. Ersoy, A. (2003) Automatic Drilling Control Based on Minimum Drilling Specific Energy Using PDC and WC Bits. *Mining Technology: Transactions of the Institutions of Mining and Metallurgy: Section A.* 112 (2), 86-96. Available from: doi: 10.1179/037178403225001629
8. Garnier, A. J. & van Lingen, N. H. (1959) Phenomena Affected Drilling Rates at Depth. *Society of Petroleum Engineers*. 216, 232-239. Available from: https://www.onepetro.org/general/SPE-1097-G
9. Horizontal Technology, Inc. (2018) *TCI Bits.* Available from: http://www.horizontaltech.com/horizontal-drill-bits-tci.php
10. Hu, Q. & Qingyou, L. (2006) A New Disc One-Cone Bit. *International Oil & Gas Conference and Exhibition in China.* 5-7 December, Beijing, China. Available from: doi: 10.2118/102381-MS

11. Institute of Geology and Mineral Exploration (1982) *Chrisoupolis Sheet*. 47, 1:50,000. Athens, Publication Department of Geological Maps of I.G.M.E..
12. Jorden, J. R. & Shirley, O. J. (1966) Application of Drilling Performance Data to Overpressure Detection. *Journal of Petroleum Technology*. 18 (11), 1,387-1,394. Available from: doi: 10.2118/1407-PA
13. Kelessidis, V. C. (2010) Prediction of Rock Drillability for Exploration Drilling for Minerals and Hydrocarbons-how close are we? *Technical Chronicles Scientific Journal of Technical Chamber of Greece*. 1, 201-218. Available from: http://portal.tee.gr/portal/page/portal/PUBLICATIONS/SCIENTIFIC_PUBLICATIONS/2010/1o_teuxos2010/B-06.pdf
14. Kelessidis, V. C. (2012) *NEAR SURFACE AND SPECIAL WELLS: Sampling wells for mining, geotechnical and environmental research-Water wells-Geothermal wells-Special wells (scientific-faults)*. Thessaloniki, Greece. Tziolas Publications.
15. Koulidis, A. (2014) *Drillability Comparison of Limestones and Sandstones for Hydrocarbon Wells with the Assistance of Payzone Software*. Diploma Thesis, School of Mineral Resources Engineering, Technical University of Crete. Available from: http://purl.tuc.gr/dl/dias/F15E892D-7885-4AF4-B0A1-8563E96FE6CD
16. McGehee, D. H., Dahlem, J. S., Gieck, J. C., Kost, B., Lafuze, D., Reinsvold, C. H. & Steinke, S. C. (1992) The IADC Roller Bit Classification System. *IADC/SPE Drilling Conference*. 18-21 February, New Orleans, Louisiana. Available from: doi: 10.2118/23937-MS
17. Mellor, M. (1972) Normalization of Specific Energy Values. *International Journal of Rock Mechanics and Mining Sciences & Geomechanics Abstracts*. 9 (5), 661-663. Available from: doi: 10.1016/0148-9062(72)90016-2
18. Mensa-Wilmot, G., Soza, R. & Hudson, K. (2003) Advanced Cutting Structure Improves PDC Bit Performance in Hard Rock Drilling Environments. *SPE Annual Technical Conference and Exhibition*. 5-8 October, Denver, Colorado. Available from: doi: 10.2118/84354-MS
19. Mitchell, F. R. & Miska, Z. S. (2011) *Fundamentals of Drilling Engineering*. TX, Richardson.
20. Moore, P. L. (1986) *Drilling Practices Manual. Second Edition*. Tulsa, Oklahoma USA, PennWell Publishing Company.

21. Perakis, G. (2006) *Assessment of Geomechanical Parameters-Formation Drillability & Drill Bits in Hydrocarbon Wells.* Diploma Thesis, School of Mining and Metallurgical Engineering, National Technical University of Athens.
22. Rabia, H. (1982) Specific Energy as a Criterion for Drill Performance Prediction. *International Journal of Rock Mechanics and Mining Sciences & Geomechanics Abstracts.* 19 (1), 39-42. Available from: doi: 10.1016/0148-9062(82)90709-4
23. Rabia, H. (1985) *Oilwell Drilling Engineering- Principles and Practice.* London, Graham & Trotman Limited.
24. Rabia, H. (1985) A Unified Prediction Model for Percussive and Rotary Drilling. *Mining Science and Technology.* 2 (3), 207-216. Available from: doi: 10.1016/S0167-9031(85)90149-5
25. Rabia, H. (2002) *Well Engineering & Construction.* London, Entrac Consulting Limited. Available from: https://allbookserve.org/downloads/rabia_well_engineering.pdf
26. Radtke, P. R., Riedel, R. & Hanaway, J. (2004) Thermally Stable Polycrystalline Diamond Cutters for Drill Bits. *Annual and Technical Conference and Exhibition of the Society of Petroleum Engineers*. 26-29 September, Houston, Texas. Available from: doi: 10.2118/90845-MS
27. Rehm, B. & McClendon, R. (1971) Measurement of Formation Pressure from Drilling Data. *Fall Meeting of the Society of Petroleum Engineers of AIME*, 3-6 October, New Orleans, Louisiana. Available from: doi: 10.2118/3601-MS
28. Stamataki, S. (2003) *Drilling Technology.* Athens, Greece. NTUA Press Publications.
29. Teale, R. (1965) The Concept of Specific Energy in Rock Drilling. *International Journal of Rock Mechanics and Mining Sciences.* 2 (1), 57-73. Available from: doi: 10.1016/0148-9062(65)90022-7
30. Torquato Drilling Accessories. (2011) *Torquato Drag Bits.* Available from: http://www.torquato.com/dragbits.html
31. Vidrine, D. J. & Benit, E. J. (1968) Field Verification of the Effect of the Differential Pressure on Drilling Rate. *Society of Petroleum Engineers*. 20 (7), 676-682. Available from: doi: 10.2118/1859-PA
32. Walker, D. R. & Shaw M. C. (1954) A Physical Explanation of the Empirical Laws of Comminution. *Mining Engineering.* 6, 313-320.

33. Wamsley, W. H. & Smith R. F. (2007) Introduction to Roller-Cone and Polycrystalline Diamond Drill Bits. In: Lake, L. (ed.) *Petroleum Engineering Handbook*. 2. Texas, USA. Richardson. Chapter 5.
34. Winters, W. J. & Doiron H. H. (1987) The 1987 IADC Fixed Cutter Bit Classification System. *IADC/SPE Drilling Conference*. 15-18 March, New Orleans, Louisiana. Available from: doi: 10.2118/16142-MS
35. Zamora, M. (1972) Slide-rule Correlation Aids 'd' Exponent Use. *Oil and Gas Journal*. 70 (51), 73-75.